SYNTHESIS AND CATALYTIC APPLICATIONS OF PHOSPHINITE COMPLEXES OF NICKEL

Aziza Adilkhanova
Bachelor of Science in Chemistry

Submitted in fulfillment of the requirements for the degree of

Master of Science In Chemistry

School of Sciences and Humanities
Department of Chemistry
Nazarbayev University

53 Kabanbay Batyr Avenue,
Nur-Sultan, Kazakhstan,
010000

Supervisor: Andrey Y. Khalimon

April 2021

Abstract

A series of imino- and aminophosphinite pincer complexes of nickel(II) (POCN)NiR (where R = Alk, O^{t}Bu, SPh, OAc, OTf, etc.) were synthesized and characterized. The prepared compounds were subjected to comparative studies of their catalytic activity in deoxygenative hydroboration of carboxamides. Using 5 mol% of nickel(II) pre-catalysts, primary and secondary amides were converted to the corresponding N-borylamine products within 24 hours at 60-80°C, presenting rare examples of catalytic systems for mild deoxygenative reduction of amides to secondary and primary amines. On the other hand, in contrast with the previously reported systems, the reduction of tertiary amides resulted in no or very low conversion of the substrates. The highest catalytic activities were observed for complexes substituted with alkyl and *tert*-butoxy ligands. Such reactivity was found consistent with the rates of the pre-catalysts activation with HBPin to generate the POCN Ni(II) hydride derivatives, which were suggested as active hydroboration catalysts. Mechanistic studies by means of stoichiometric and control experiments support formation of the Ni(II) hydride species and for primary amides additionally suggest the presence of an amide pre-activation step *via* dehydrogenative coupling with HBPin to produce N-borylamides. Based on mechanistic studies, deoxygenative reduction of both primary and secondary carboxamides was proposed to proceed *via* intermediate formation of the imine derivatives, such as RC(H)=N(Bpin) and RC(H)=NR, respectively, which further undergo addition of HBPin to produce the corresponding N-borylamine products.

Acknowledgements

First and foremost, I would like to express my sincere gratitude to my research supervisor Dr. Andrey Y. Khalimon for his support and patience during my MSc study. Advice and comments given by Dr. Khalimon have been a great help in my thesis research. Without his guidance and persistent help this MSc thesis would not have been possible. Thank you so much for supporting and assisting me at every stage of the project.

I would like to offer my special thanks to Anton Dmitrienko (Brock University), Prof. Melanie Pilkington (Brock University) for collecting X-ray diffraction data. I am also grateful for the assistance given by our former research group members Aishabibi Kassymbek (Brock University) and Medet Segizbayev (Brock University) and their help with the syntheses of several alkyl nickel pincer complexes.

I would like to express my appreciation to the CHEM 692 course coordinator - Dr. Darkhan Utepbergenov and thesis reviewers – Dr. Vsevolod Peshkov and Dr. Mannix Balanay for their time and valuable feedback on my thesis.

I am extremely grateful to every member of Khalimon's research group, especially Dr. Ozgur Oztopcu, Dr. Kristina Gudun, Valeriya Frolova and Raikhan Zakarina for their continuous support and help throughout my work and studies.

Finally, my deepest appreciation goes to my family, especially my mother for always supporting me during these years of my education and my sister for always being there for me as a friend.

Table of Contents

List of Abbreviations & Symbols

DMF	*N*,*N*-dimethylformamide
PMHS	Polymethylhydrosiloxane
$PhSiH_3$	phenylsilane
TMDS	1,1,3,3-tetra-methyldisolxane
BDSB	1,2-bis(dimethylsilyl)benzene
NHC	N-heterocyclic carbene
OAc	Acetate
[Ph-HEMIM][OTf]	1-(2-hydroxy-2-phenylethyl)-3-methylimidazolium triflate
NMR	Nuclear Magnetic Resonance
UV	Ultraviolet
GC	Gas Chromatography
Dpephos	bis[(2-diphenylphosphino)phenyl]ether
PPh_3	Triphenylphosphine
$LiBHEt_3$	lithium triethylborohydride
Acac	Acetylacetonate
$PhMeSiH_2$	methylphenylsilane
$PhMe_2SiH$	Dimethylphenylsilane
Et_3SiH	Triethylsilane
TMEDA	Tetramethylethylenediamine
Ph_2SiH_2	Diphenylsilane
Dme	1,2-dimethoxyethane
Dipp	Diisopropylphenyl
Dmp	Dimethylphenyl
To^M	tris(4,4-dimethyl-2-oxazolinyl)phenylborate
HBPin	Pinacolborane
THF	tetrahydrofuran
CH_3CN	acetonitrile
C_6D_6	deuterated benzene
NEt_3	Triethylamine
$^iPr_2PCl$	Chlorodiisopropylphosphine
L-Selectride	lithium tri-*sec*-butylborohydride
OTf	Triflate

List of Schemes

List of Figures

List of Tables

1 Introduction

Catalytic reduction of carbonyl compounds is one of the fundamental transformations in modern synthetic organic chemistry relevant to production of both commodity and specialty chemicals [1-3]. Whereas catalytic reduction of aldehydes and ketones is known to proceed quite easily, and many catalytic systems have been reported to mediate these transformations efficiently and selectively [4], the reduction of deactivated carbonyl substrates, such as esters and carboxamides presents a significantly more challenging task [5]. Such transformations typically require rather sophisticated catalytic systems and/or rather harsh reaction conditions (such as high temperatures and long reaction times, etc.) [6-8] due to significantly decreased electrophilicity of the ester and amide carbonyl carbon compared to simple aldehydes and ketones (Scheme 1). Nonetheless, such transformations are of great importance to modern organic synthesis. In particular, catalytic deoxygenative reduction of readily available carboxamides provides a direct access to a diversity of amines (Scheme 2) [9], which serve as building blocks of many natural products, biologically active compounds, organic functional materials, pharmaceutically relevant compounds and agrochemicals [10-11].

Scheme 1. Amide resonance structure.

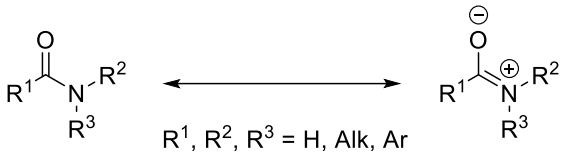

Scheme 2. Catalytic deoxygenative reduction of carboxamides to amines (C-O bond cleavage).

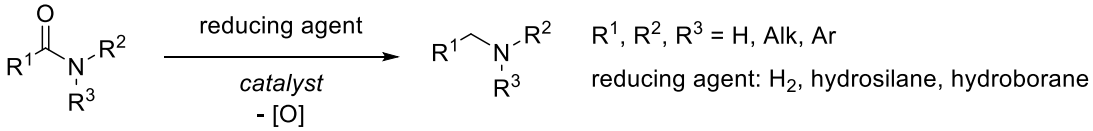

Most commonly used conventional methods for preparation of amines include alkylations of primary and secondary amines with alcohols and hydrocarbyl halides [12], stoichiometric reduction of imines [13], amides [14], nitriles [15] and nitro compounds [16] as well as reductive amination of aldehydes and ketones with hydride reagents (such as $NaBH_4$, $NaBH(CN)_3$, etc.) [17]. Despite their wide applications, these methods typically show low functional group tolerance, produce large amounts of salt waste are difficult to control. In contrast, catalytic reductions offer an improved functional group tolerance and allow for waste minimization and, hence, catalytic deoxygenative reduction of readily available carboxamides (Scheme 2) to the corresponding amines is considered as an appealing alternative to stoichiometric methods mentioned above.

Most of the reported catalytic systems allowing for efficient and selective deoxygenative reduction of carboxamides to the corresponding amines are based on low-abundant and expensive precious metals (heavy late transition metals, such as ruthenium [8, 12, 18-24], rhodium [12, 25-27] iridium [12, 28-33] and platinum [34-36]. Even though these metals show high efficiency in reduction of aldehydes, ketones and even esters, deoxygenative reduction of carboxamides mediated by such systems often shown poor selectivities and requires elevated temperatures and long reaction times.

Generally, the development of more efficient and selective homogeneous catalytic systems using more economical and less toxic non-precious metals has become a hot topic in the field of organometallic chemistry and catalysis in the past decades [37]. A series of non-precious metal catalysts have been disclosed for mild, efficient and selective catalytic reduction (hydrogenation, hydroboration and hydrosilylation) of aldehydes, ketones and even esters [38-42]. In contrast, non-precious metal catalyzed deoxygenative reduction of carboxamides is comparatively underdeveloped and mostly limited to deoxygenative hydrosilylation reactions [43-44].

The reported examples include deoxygenative hydrosilylation by comparatively inexpensive iron [39], manganese [38], cobalt [45], nickel [41, 46], titanium [47-48], molybdenum [49-50], copper [51] and zinc pre-catalysts [52-55]. Still, for the majority of such reactions high catalyst loadings (up to 20 mol%), long reaction times (up to 72 hours), and increased temperatures (up to 155°C) are required. Moreover, many of the reported systems for hydrosilylation of carbamides show poor selectivities in the C-O (Scheme 2) *vs.* C-N bond cleavage (Scheme 3), which results in formation of complex mixtures of amine products with aldehydes and/or alcohols.

Scheme 3. Catalytic hydrosilylative C-N bond cleavage in carboxamides.

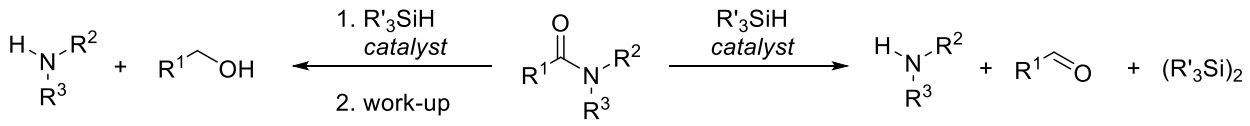

R^1, R^2, R^3 = H, Alk, Ar

Significantly less examples of homogeneous catalytic systems have been shown for deoxygenative hydrogenation of carboxamides, despite the most atom economical nature of such processes. Most of these reactions concern secondary and primary carboxamides, which undergo Lewis acid-assisted reductive dehydration of amides to either imines or nitriles (respectively), followed by their hydrogenation to amines. The reactions typically require large amounts of strong Lewis acids and rather high hydrogen pressures (up to 100 bar) [56-57] and temperatures (up to 220 °C) [56, 58-60].

Compared to hydrosilylation, relatively little is also reported on deoxygenative hydroboration of carboxamides to amines, and only a few examples of such catalytic systems (mostly concerning magnesium and lanthanide-based complexes) have been disclosed in the literature [61-63]. Apart from preparation of amines, deoxygenative hydroboration of secondary and primary amides provides a direct access to N-boryl substituted amine derivatives, which due to the presence of labile B-N bonds can be potentially used directly in the synthesis of more complex N-containing organic molecules.

Figure 1. Pincer type complexes(a), (^{iPr}POCN^{Ar})NiMe complex (b) and proposed modification of POCN pincer ligands and their Ni complexes (c).

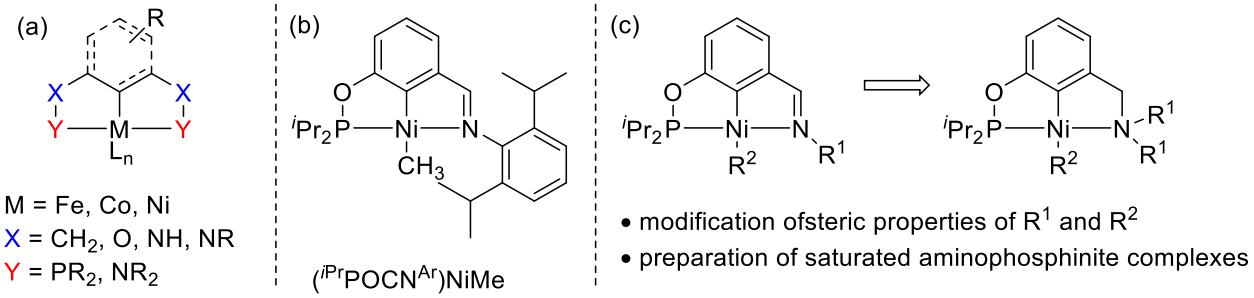

Our research group has been interested in the development of base metal (Mn, Fe, Co and Ni) complexes for efficient, mild and selective reduction of carbonyl compounds [14, 64]. One of the most popular class of ligands to design base metal complexes are pincer type ligands (akin to in complexes depicted in Figure 1a). Such tridentate ligands provide necessary stability of the complexes due to chelating effect and could be easily tuned by modification of the steric and electronic properties of the bridgehead and side-arm donors to achieve necessary reactivity [65]. As part of ongoing research program, the Khalimon group has recently demonstrated the first example of a nickel catalyst, namely an iminophosphinite pincer complex (^{iPr}POCN^{Ar})NiMe (Figure1), active in hydroborative conversion of carboxamides to amines [64]. This complex represents the first example of a d-block element catalyst for deoxygenative hydroboration of carboxamides and the reported preliminary studies indicated its high catalytic activity in hydroboration of DMF, *N*-phenylpropanamide and acetamide at 60 °C [64]. However, the detailed studies of this catalytic system and investigation of the scope of the amide substrates were hampered by the instability of (^{iPr}POCN^{Ar})NiMe, which resulted in poor reproducibility of the obtained results. Therefore, this thesis work aims to tune the properties of POCN pincer type ligands and the related nickel complexes in order to design the most stable but at the same time highly active catalytic system for efficient, selective and mild (<100 °C) deoxygenative hydroboration of carboxamides to amines (Figure 1). Thus, the first part of this thesis is devoted to the synthesis and characterization of a series of modified iminophsosphinite Ni(II) derivatives

as well as the related aminophosphinite nickel complexes. In the second part, the obtained complexes were subjected to comparative studies of their catalytic activities in deoxygenative hydroboration of model carboxamide substrates, such as benzamide, *N*-alkyl and *N*-arylbenzamides as well as *N*,*N*-dialkylbenzamides. Finally, the mechanism of the amide hydroboration reactions mediated by POCN nickel complexes was studied by means of NMR analysis and a series of control experiments, which are discussed in details in the last part of this thesis.

The following literature review section describes deoxygenative hydrosilylation and hydroboration of amides to amines catalyzed by base metal complexes.

2 Literature review

This literature review focuses on deoxygenative reduction of amides to the corresponding amines catalyzed by non-precious metals (so called base metals, such as Fe, Mn, Co, Ni) using hydrosilylation and hydroboration approaches. Deoxygentaive hydrogenation is not considered since the reactions are typically performed under forcing conditions (high pressure and temperatures) and do not show sufficient selectivities [56-60, 66-68].

2.1 Hydrosilylation of amides

2.1.1 Iron-catalyzed deoxygenative hydrosilylation of amides

Deoxygenative hydrosilylation of secondary and tertiary amides catalyzed by non-precious metal was first reported in 2009 [69]. Beller and co-workers used inexpensive iron carbonyl complex $Fe_3(CO)_{12}$ as a catalyst and PMHS (polymethylhydrosiloxane) as a hydrogen source (Scheme 4). The scope of amides mostly consisted of tertiary amides showing good to excellent yields (50-98%) with only one example of secondary amide, resulting in only 25% yield. However, *N*-methylbenzamide was converted to the corresponding amine with 99% yield when reducing agent was changed to $PhSiH_3$. The reactions were activated thermally at 100 °C and were conducted for 24 h.

Scheme 4. $Fe_3(CO)_{12}$-catalyzed hydrosilylation of tertiary and secondary amides

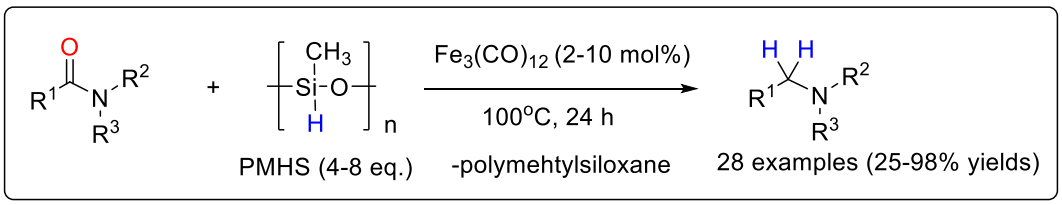

Substrate	Yield	Substrate	Yield
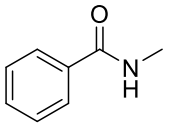	25% (99% when using $PhSiH_3$)	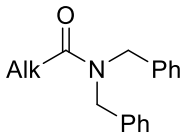	Alk= CH_3 (89%) ^{t}Bu (98%) CH_2CH_2Ph (63%)
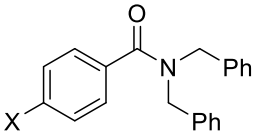	X= H (89%) CH_3 (93%) OCH_3 (93%) CF_3 (84%) Cl; Br; I (95;92;83%) $COOCH_3$ (58%)	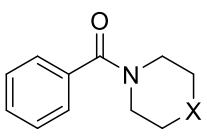	X= CH_2 (94%) O (80%)
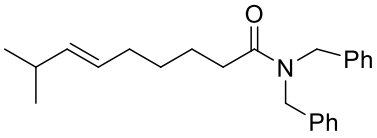	76%	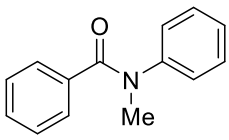	81%

The same year, Nagashima *et al.* demonstrated the results of hydrosilylation of tertiary amides catalyzed by iron carbonyl complexes $Fe(CO)_5$ and $Fe_3(CO)_{12}$ using TMDS (1,1,3,3-tetramethyldisolxane) [70]. The reactions were initiated either photochemically (400 W high-pressure mercury lamp) or thermally at 100 °C. Similarly, to Beller's report the reactions required rather high catalysts loadings (10 mol%) and long reaction times. The improved conditions were reported for deoxygenative hydrosilylation of amides with BDSB (1,2-bis(dimethylsilyl)benzene) using a heptanuclear iron-carbonyl cluster $[Fe_3(CO)_{11}(\mu\text{-}H)]_2Fe(DMF)_4$ as pre-catalyst, which was prepared by treatment of $Fe(CO)_5$ with DMF [71]. This system allowed to decrease the reaction times to 0.5-3 h at 100 °C using as low catalyst loading as 0.5 mol% (for iron) (Scheme 5).

Scheme 5. Deoxygenative hydrosilylation of secondary and tertiary amides with 1,2-bis(dimethylsilyl)benzene catalyzed by $[Fe_3(CO)_{11}(\mu\text{-}H)]_2Fe(DMF)_4$.

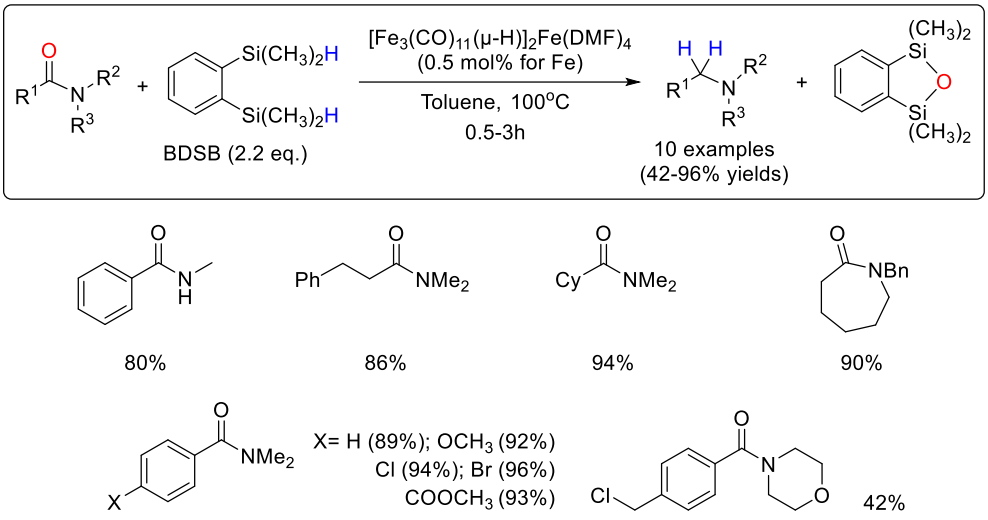

These findings inspired others and in 2011 Sortais *et al.* disclosed the first example of a solvent-free deoxygenative reduction of tertiary amides (as well as one example of a secondary amide) using a well-defined iron cyclopentadienyl N-heterocyclic carbene (NHC) complex $[CpFe(CO)_2(IMes)]I$ as catalyst and $PhSiH_3$ as reducing agent [72]. The hydrosilylation was performed under visible light irradiation at 100 °C for 24 h (Scheme 6). The scope of substrates mostly consisted of tertiary amides with good to excellent yields (73-98%). Deoxygenative hydrosilylation of primary amides was also attempted but did not result in the formation of the corresponding amines. Instead, silane-assisted dehydration of primary amides to nitriles was observed. As an example of such dehydration process, 4-bromobenzamide could be converted to 4-bromobenzonitrile with 65% isolated yield.

Scheme 6. Deoxygenative hydrosilylation of amides catalyzed by [CpFe(CO)$_2$(IMes)]I.

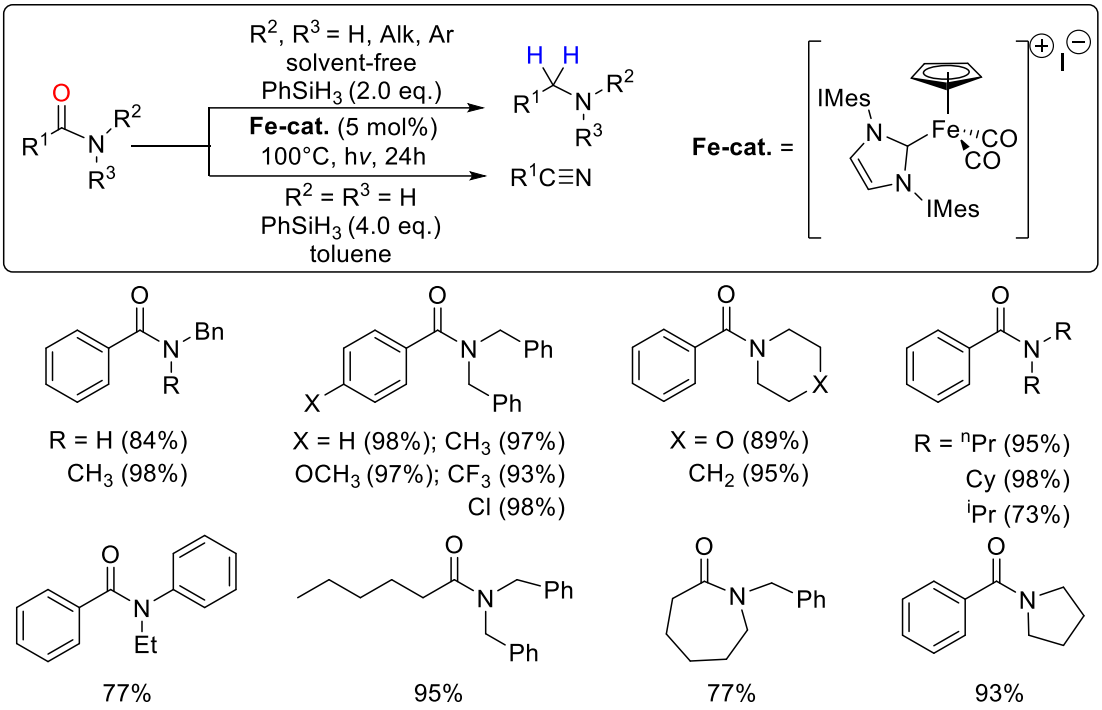

In comparison to iron carbonyl systems discussed above, deoxygenative hydrosilylation of tertiary amides with PMHS was achieved at 65°C using Fe-NHC complex, formed *in situ* from Fe(OAc)$_2$ (1 mol%) by treatment with [Ph-HEMIM][OTf] (1-(2-hydroxy-2-phenylethyl)-3-methylimidazolium triflate) (1.1 mol%), *n*BuLi (2.2 mol%) and LiCl (1 mol%) (Scheme 7) [73]. Inte-

Scheme 7. Fe/[Ph-HEMIM]-catalyzed hydrosilylation of tertiary amides to amines.

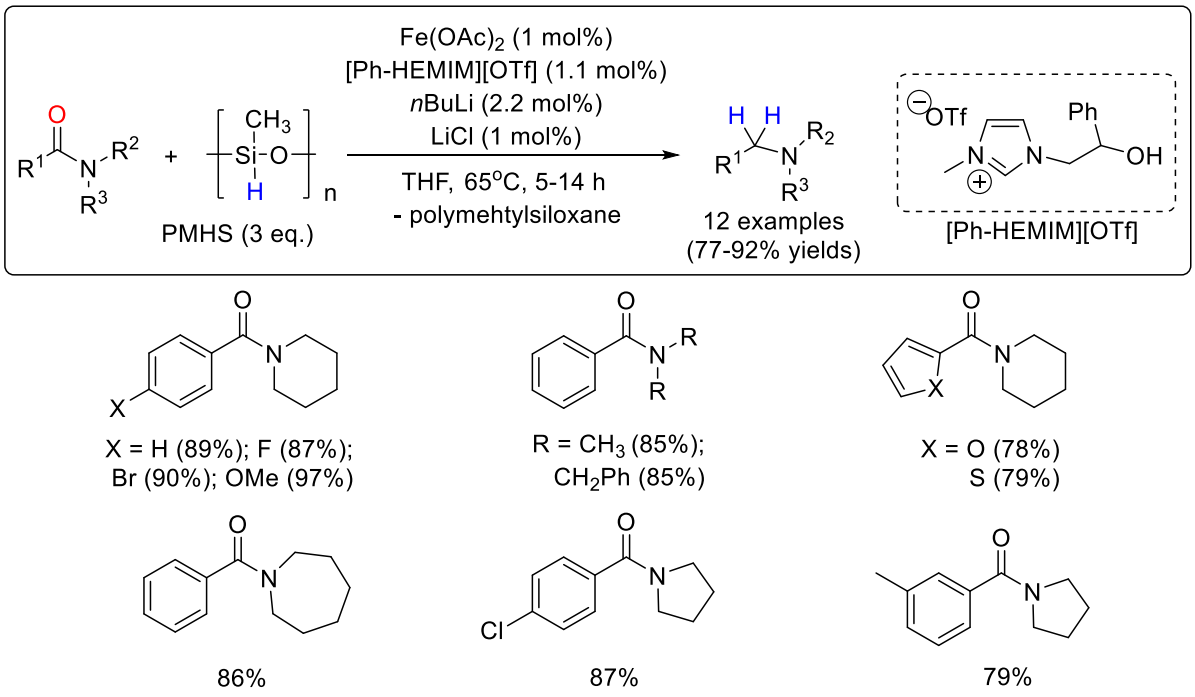

Figure 2. Examples of non-carbonyl iron pre-catalysts for deoxygenative hydrosilylation of carboxamides.

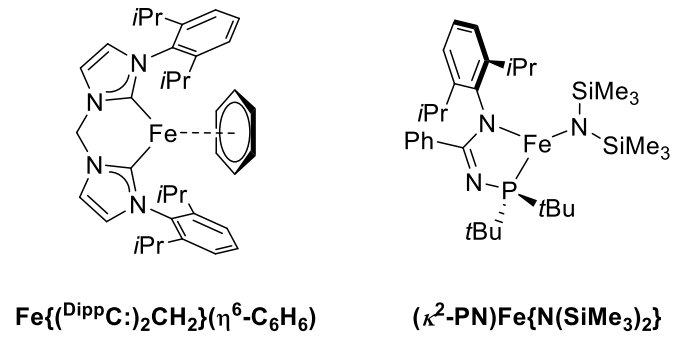

$Fe\{(^{Dipp}C:)_2CH_2\}(\eta^6\text{-}C_6H_6)$ $(\kappa^2\text{-}PN)Fe\{N(SiMe_3)_2\}$

restingly, the reduction of *N*,*N*-dimethylbenzamide in the absence of LiCl apart from the desired amine resulted in formation of by-products of C-N bond cleavage reaction (benzaldehyde and benzyl alcohol). Notably, under the same conditions, the reduction of aliphatic, secondary and primary amides to their corresponding amines was unsuccessful.

To date, several other iron-based catalytic systems for relatively mild (70–75 °C) deoxygenative hydrosilylation of carboxamides have been developed (for examples, see Figure 2), but the reactions are mostly limited to tertiary amide substrates [74-75]. Only a few examples of Fe-catalyzed hydrosilylation of secondary amides to the corresponding secondary amines have been reported [69, 71-72]. Deoxygenative hydrosilylation of primary amides to amines is even more challenging task, primarily due to their relatively easy dehydration to nitriles under hydrosilylation conditions [76]. Such $(EtO)_2MeSiH$-assisted dehydration of $RC(O)NH_2$ to RCN catalyzed by $[Et_3NH][HFe_3(CO)_{11}]$ (7.5 mol%), followed by double hydrosilylation of the produced nitriles with $(EtO)_2MeSiH$ using $Fe(OAc)_2$ / 3,4,7,8-tetramethyl-1,10-phenantroline pre-catalyst (10/20 mol%, respectively) was used by Beller *et al.* (Scheme 8) as a detour strategy for conversion of primary amides to the corresponding primary amines.

Scheme 8. Fe-catalyzed dehydration-hydrosilylation strategy to reduce primary amides.

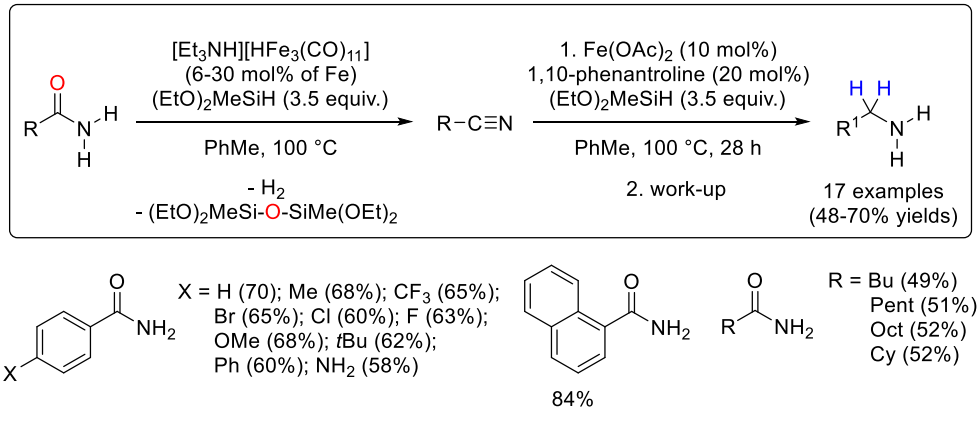

2.1.2 Cobalt-catalyzed deoxygenative hydrosilylation of amides

In comparison to iron-based catalytic systems, cobalt-catalyzed deoxygenative hydrosilylation of amides is less common. In 2013, first cobalt-catalyzed system was employed for reductive hydrosilylation of tertiary amides [77]. The cobalt carbonyl complex $Co_2(CO)_8$ (0.5 mol%) was used under thermal (100 °C, 3-16 h) or photo-assisted (350 nm, 15 h, room temperature) conditions with TMDS (tetramethyldisiloxane) or PMHS (polymethylhydrosiloxane) as reducing agents (both 2.2 equivalents). As a model substrate *N*,*N*-dimethylbenzamide was converted to the corresponding amine for conditions optimization purposes. Under UV light, the desired product was obtained with >97% conversion as determined by GC and ^{1}H-NMR. The scope for the reduction of a variety of substrates was performed under thermal activation (Scheme 9). In some cases, when $PhSiH_3$ was used as a hydrogen source instead of PMHS, the yields of the products were increased. Steric hindrance may seem to have an influence on both silane reagent and substituents of the substrate. Thus, *N*,*N*-di-*n*-propylbenzamide was reduced with 58% yield, whereas more bulky *N*,*N*-dicyclohexylbenzamide showed only 10% conversion.

The reactivity of $Co_2(CO)_8$ for hydrosilylation of tertiary amides [77] is somewhat similar to iron carbonyl complexes $Fe(CO)_5$ and $Fe_3(CO)_{12}$ published by Beller [69] and Nagashima [70], respectively. Nonetheless, $Co_2(CO)_8$-catalyzed transformations required lower catalyst loadings (0.5-1.0 mol% *vs.* 6-30 mol% for iron carbonyls) and shorter reaction times (3-16 h *vs.* 9-24 h for iron carbonyls) which makes it more advantageous compared to iron carbonyl systems.

Scheme 9. $Co_2(CO)_8$-catalyzed hydrosilylation of tertiary amides.

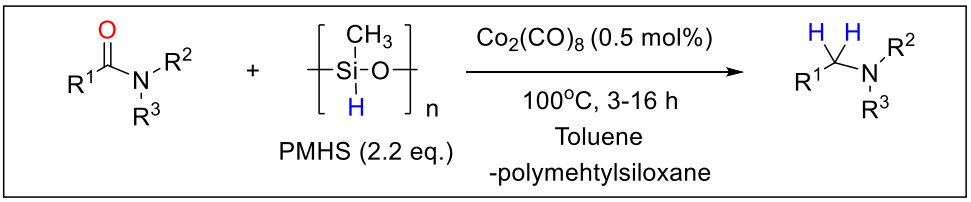

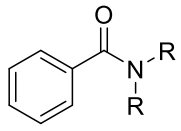

R = Me (>98%); *n*-Pr (58%); *i*-Pr (86%[a]); Cy (10%, 50%[a]); Ph (6%, 70%[a])

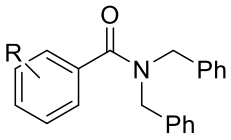

R = H (90%); *m*-Me (86%); *o*-Me (16%, 98%[a]); *p*-OMe (98%); *p*-CF_3 (94%); *p*-Br (93); *p*-Cl (93%[a])

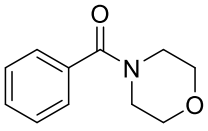

65%

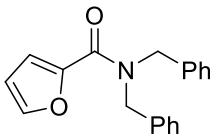

92%

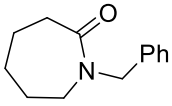

73%

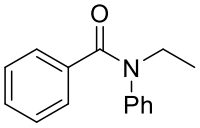

33%, 82%[a]

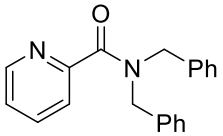

60%

[a] 1 mol% of $Co_2(CO)_8$ was used with amide (1 mmol) and $PhSiH_3$ (1 mmol) instead of PMHS

A wide range of aliphatic, aromatic, and cyclic tertiary amides was reduced to the corresponding amines using the cobalt pre-catalyst system reported previously by our group (Table 1) [14]. Commercially available cobalt chloride, acetate and acetylacetonate salts ligated with either bis[(2-diphenylphosphino)phenyl] ether (DPEphos) or even PPh_3 were used under mild conditions. Using different combinations of cobalt salts and PPh_3/dpephos ligands six catalytic systems were developed (A-F) (Table 1). Catalytic system A, where 5 mol% of (dpephos)$CoCl_2$ was used, required an external activation with $LiBHEt_3$ (10 mol%) for the generation of catalytically active Co(I) hydride in order to perform hydrosilylation of tertiary amides with high yields (91-99%). The systems that do not require $LiBHEt_3$ (such as those, using $Co(acac)_2$ and $Co(OAc)_2$) were activated by the reaction with $PhSiH_3$. The most efficient system was found to be $Co(acac)_2$(dpephos) (5 mol% of Co and 5.5 mol% of dpephos) with $PhSiH_3$ (1.5 equivalents) resulting in high yields of the amine products (90-99%) within 3-24 h at room temperature. Moreover, under more forcing conditions (60-100°C, 24-72h) this system was also successfully applied in deoxygenative hydrosilylation of secondary amides, such as *N*-methylbenzamide and *N*-phenylpropanamide, and more importantly, primary amides, such as acetamide and propenamide, without the formation of the corresponding nitriles.

One of the important factors affecting the reactivity of $Co(acac)_2$/dpephos seems to be a steric hindrance in the silane reagent. Thus, substitution of $PhSiH_3$ with more sterically demanding $PhMeSiH_2$, $PhMe_2SiH$ and Et_3SiH in the reduction of DMF resulted in lower yields or no conversion to the desired product. Interestingly, the steric hindrance of the substrate does not seem to affect the reactivity. Despite the large bite angle of dpephos ligand (102.2°), reduction with $PhSiH_3$ resulted in similar conversions for both *N*,*N*-diisopropylbenzamide and 4-benzoylmorpholine (>99% at 60 °C in 5 h).

Recently, deoxygenative hydrosilylation of tertiary amides with 2 equivalents of $PhSiH_3$ catalyzed by cobalt-based pre-catalyst (κ^2-P,N)Co{$N(SiMe_3)_2$} at 75°C was reported by Sydora, Stradiotto, Turculet *et al.* (Scheme 10) [75]. Thus, the formation of 61% of *N*,*N*-dibenzylbenzamine and 83% of *N*,*N*-diisopropylbenzamine were detected by GC. Co{$N(SiMe_3)_2$} was also tested in the reduction of tertiary amides under analogous conditions. However, this pre-catalyst was found to be less reactive in comparison to its *N*-phosphinoamidinate derivative, resulting in 43% and 47% conversions of *N*,*N*-dibenzylbenzamide and *N*,*N*-diisopropylbenzamide, respectively.

Table 1. Deoxygenative hydrosilylation of amides catalyzed by (dpephos)CoX_2/($LiBHEt_3$) (X = Cl, OAc, acac).

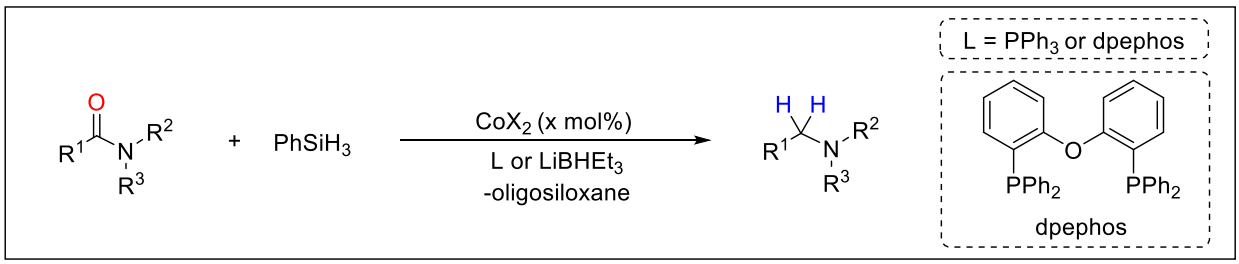

A (dpephos)$CoCl_2$ / $LiBHEt_3$ (5/10 mol%) **B** $Co(acac)_2$ / dpephos (5/5.5 mol%) **C** $Co(OAc)_2$ / dpephos (5/5.5 mol%) **D** $Co(acac)_2$ / PPh_3 (5/10 mol%) **E** $Co(OAc)_2$ / dpephos (0.5/0.55 mol%) **F** $Co(OAc)_2$ / PPh_3 (5/10 mol%)

#	Substrate	Cat. system	T, ^{0}C/t, h	Yield, %	#	Substrate	Cat. system	T, ^{0}C/t, h	Yield, %
1	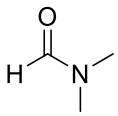	A-F	60/5	>99	5	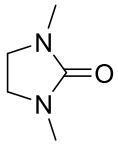	A	60/5	28
		A-C, F	25/5	>99			A	65/16	44[a]
		D	25/24	79			B	100/24	15
2	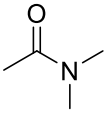	A	60/5	>99	6	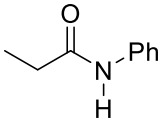	B	60/60	>99[b]
		B	25/17	>99					
		E	60/5	82	7	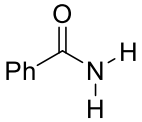	B	100/24	83[c]
		E	60/24	94					
3	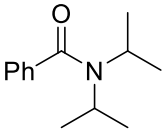	A	60/5	>99	8	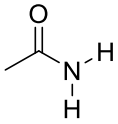	B	75/24	45
		B	25/17	>99			B	75/48	73
		B	65/5	>99	9	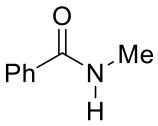	B	75/24	89[b]
		E	60/24	72			B	75/48	>99[b]
4	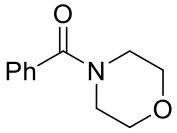	A	60/5	>99	10	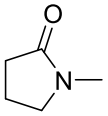	A	60/5	>99
		B	25/17	87			B	25/17	>99
		B	60/5	85			E	60/24	61[d]

[a] 3 equiv. of $PhMeSiH_2$ was used, 32% conversion at 65^{o}C in 5h; [b] Amine and silylamines were produced in a mixture, overall yield for the mixture; [c] Determined by GC-MS after hydrolysis with 20% NaOH (aq.); [d] 45% conversion at 60^{o}C in 5h.

Scheme 10. Deoxygenative hydrosilylation of *N*,*N*-dibenzylbenzamide and *N*,*N*-diisopropylbenzamide catalyzed by (κ^2-P,N)Co{N(SiMe$_3$)$_2$}.

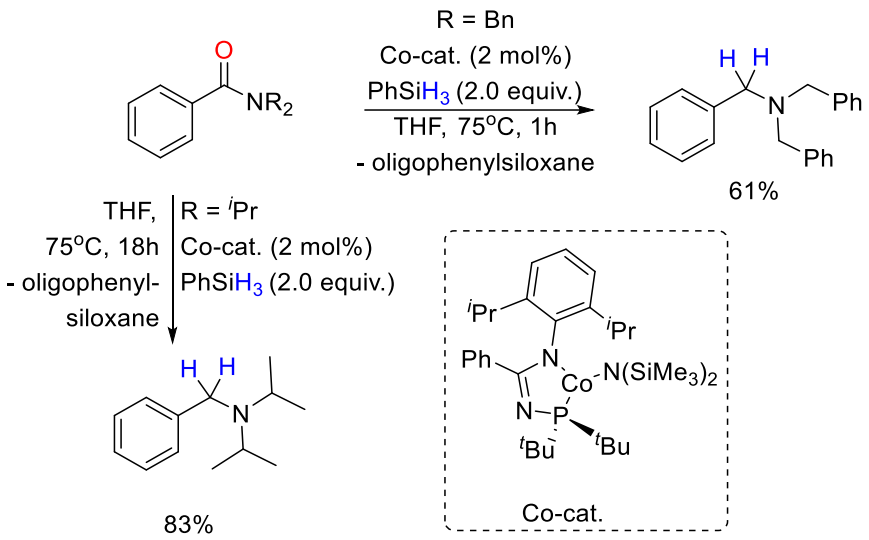

2.1.3 Nickel-catalyzed deoxygenative hydrosilylation of amides

Examples of deoxygenative hydrosilylation of amides catalyzed by Ni-based systems are scarce. In 2014, Sekar and Mamillapalli published hydrosilylative reduction of α-keto amides with 4 equivalents of Ph_2SiH_2 as reducing agent using a catalytic system which composed of $Ni(OAc)_2$ (5 mol%), TMEDA (10 mol%) and KO^{t}Bu (10 mol%) (Scheme 11) [78].

Scheme 11. Hydrosilylation of α-keto amides catalyzed by $Ni(OAc)_2$/TMEDA/KO^{t}Bu.

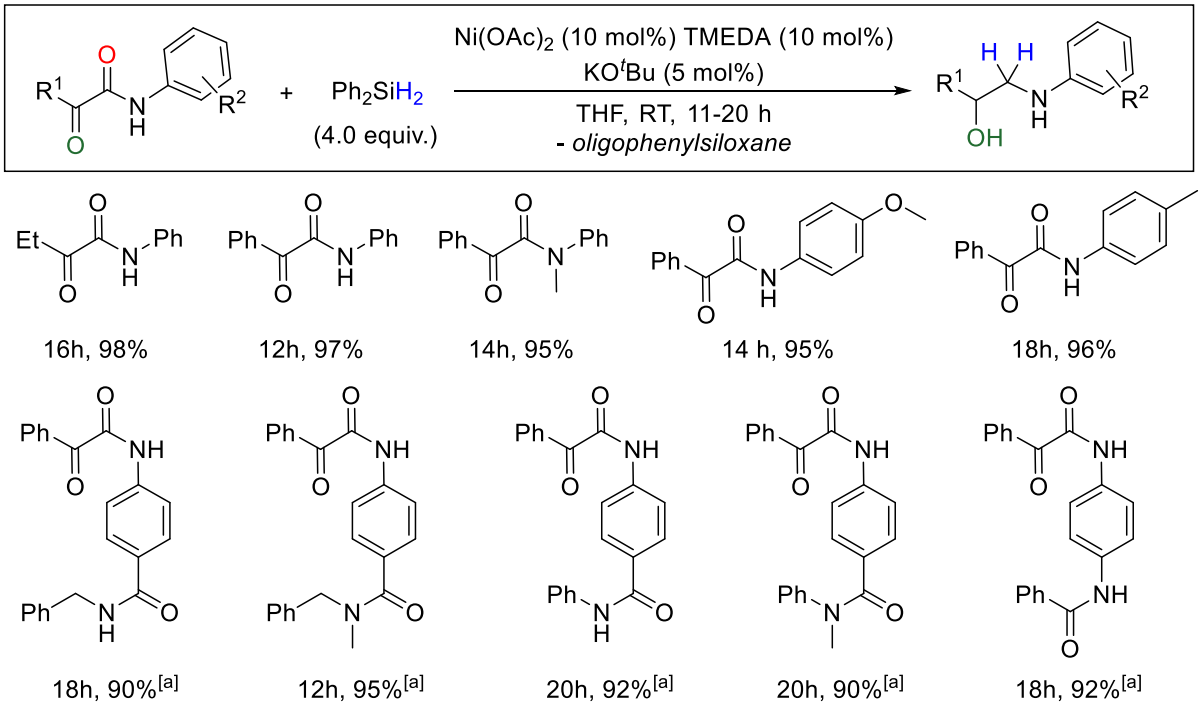

[a] Chemoselective reduction tolerating another amide functional group was detected

Interestingly, the developed catalytic system was found to chemoselectively reduce the α-keto amide substrates in the presence of other amide functional groups, as depicted in Scheme 11. Also, when PMHS was used as reducing agent instead of Ph_2SiH_2, hydrosilylation of α-keto amides resulted in highly chemoselective formation of α-hydroxy amines, tolerating ketone functionalities in the substrate [78].

In 2019 Garg and co-workers demonstrated $NiCl_2$(dme)-catalyzed (dme = 1,2-dimethoxyethane) reduction of secondary and tertiary amides with $PhSiH_3$ (Schemes 12 and 13) [79]. Even though, rather forcing conditions (10 mol% of pre-catalyst 115 °C, 24 h) were applied, the system did not require any external activator. The substrate scope included synthetically useful lactams, N-alkyl and N-aryl substituted aliphatic, aromatic, and heterocyclic substrates.

Scheme 12. Hydrosilylative reduction of tertiary amides catalyzed by $NiCl_2$(dme).

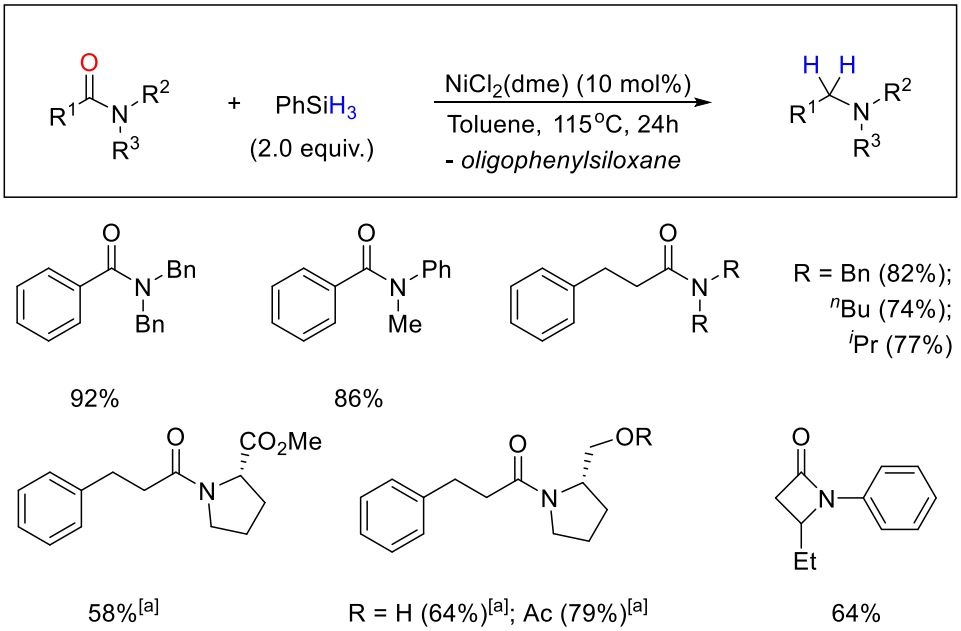

[a] 2.0-4.0 eq. of $PhSiD_3$ was used giving a-deuterated amines. Isolated yields are shown

Mild hydrosilylative reduction of tertiary and secondary amides with 2 equivalents of $PhSiH_3$ was performed in 2019 using N-phosphinoamidinate (κ^2-P,N)NiX pre-catalysts (X = $N(SiMe_3)_2$, NHdipp, O^{t}Bu, and Odmp; dipp = 2,6-^{i}Pr$_2$C$_6$H$_3$, dmp = 2,6-Me$_2$C$_6$H$_3$) [75]. The *tert*-butoxide derivative was found to be the most active resulting in >95% conversion of *N*,*N*-diisopropylbenzamide, and 84% isolated yield of the corresponding amine product at room temperature in 18 hours (Table 2).

Scheme 13. Hydrosilylative reduction of secondary amides catalyzed by $NiCl_2$(dme).

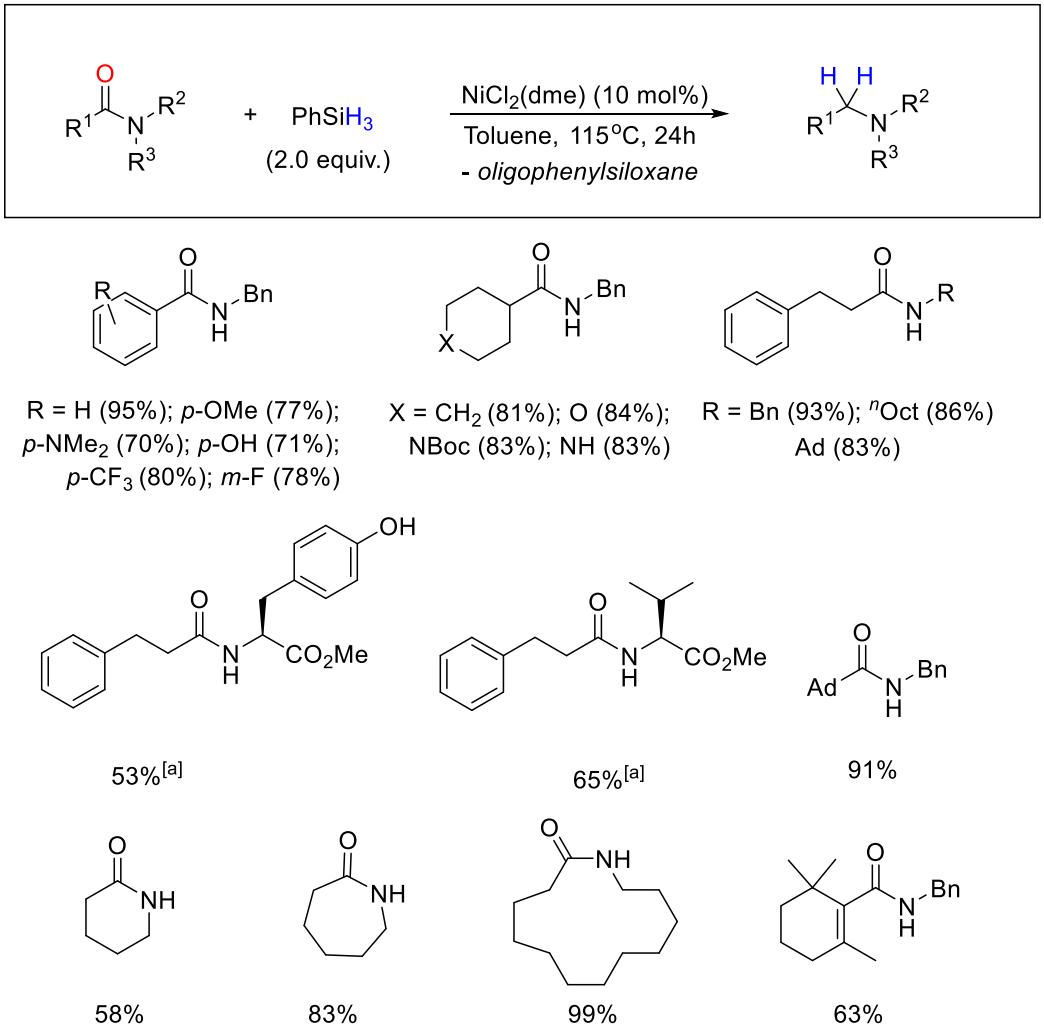

[a] 2.0-4.0 eq. of $PhSiD_3$ was used giving a-deuterated amines. Isolated yields are shown

Other N-phosphinoamidinate nickel derivatives also demonstrated high catalytic activity. For example, *N*,*N*-diisopropylbenzamide was transformed to the corresponding amine with 83% and 74% yields using (κ^2-P,N)Ni{$N(SiMe_3)_2$} in 18 h at 75 °C and (κ^2-P,N)Ni(NHdipp) in 18 h at room temperature, respectively. Assuming that hydrosilylative reduction is initiated by the formation of a catalytically active nickel hydride species, different activities of N-phosphinoamidinate nickel derivatives may correspond to different catalyst activation rates. Control experiments in the absence of the substrate were performed for (κ^2-P,N)Ni{$N(SiMe_3)_2$} and (κ^2-P,N)Ni(O^tBu) with large excess of $PhSiH_3$ (40 equivalents). Both compounds showed formation of a mixture of the hydride dimer [(κ^2-P,N)NiH]$_2$ with unidentified decomposition products; however, faster pre-catalyst consumption was observed for NiO^tBu derivative. Additionally, the *tert*-butoxy complex (κ^2-P,N)Ni(O^tBu) was also used for deoxygenative hydrosilylation of several secondary amides, such as *N*-benzylbenzamide and caprolactam, showing 79% and 84% isolated yields, respectively (Table 2). In contrast, no selective

deoxygenative reduction of primary amides was observed for any of the N-phosphinoamidinate nickel pre-catalysts. The reactions of primary amides with $PhSiH_3$ resulted in formation of complex mixtures of products.

Table 2. Hydrosilylative reduction of tertiary and secondary amides catalyzed by (κ^2-P,N)NiX pre-catalysts (X = $N(SiMe_3)_2$, NHdipp, O^{t}Bu, and Odmp).

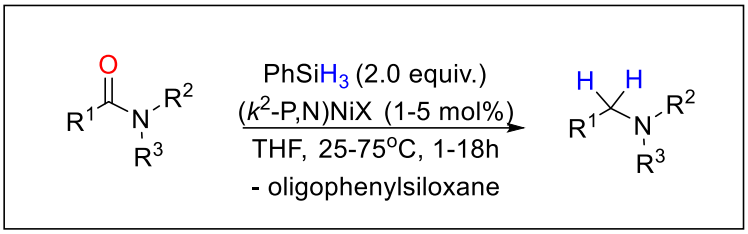

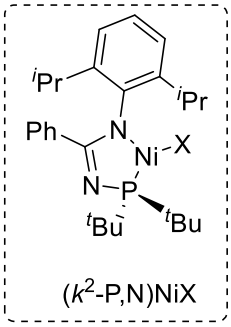

Substrate	[L]Ni-derivative	Cat. loading	Conditions	Conversion/(Yield), %
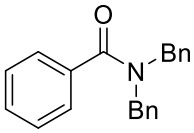	$N(SiMe_3)_2$	2 mol% of Ni	1h, 75°C	>95 (85)
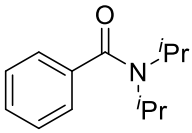	$N(SiMe_3)_2$	2 mol% of Ni	1h, 75°C	84 (67)
		5 mol% of Ni	18h, 75°C	>95 (83)
		5 mol% of Ni	18h, 25°C	74 (54)
	NHdipp	5 mol% of Ni	18h, 25°C	95 (74)
	Odmp	5 mol% of Ni	18h, 25°C	>95 (80)
	O^{t}Bu	5 mol% of Ni	18h, 25°C	>95 (84)
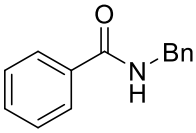	O^{t}Bu	5 mol% of Ni	18h, 75°C	(79)
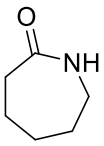	O^{t}Bu	1 mol% of Ni	18h, 25°C	(84)

2.2 Hydroboration of amides

Oppositely to hydrosilylation, deoxygenative hydroboration of amides is not so common. Hydroborative reduction of amides to amines was first performed in 2015 using magnesium-based complex To^{M}MgMe (To^{M} = tris(4,4-dimethyl-2-oxazolinyl)phenylborate) by Sadow and co-workers (Scheme 14) [61]. The developed catalytic system allowed for deoxygenative hydroboration of tertiary amides under mild conditions (room temperature, 2-5 mol% of catalyst); however, a huge excess of HBPin (20 equivalents) as reducing agent was required. In fact, such an excess of HBPin proved necessary for selective C-O bond cleavage reactions giving the desired tertiary amine products. On the other hand, low concentrations of HBPin resulted in the formation of RCH_2OBPin and R_2NBPin by-products, produced *via* the C–N bond cleavage of the amides. Thus, a series of aliphatic, aromatic tertiary amides, including the substrates with potentially reducible nitro- and azo substituents, were converted to the corresponding amines, which were isolated as ammonium salts in good yields. For secondary amides, the reduction proved more challenging, required significantly larger pre-catalyst loadings (10 mol%) and was limited to only 4 examples of formamide substrates (Scheme 14).

Scheme 14. To^{M}MgMe-catalyzed deoxygenative hydroboration of tertiary and secondary amides.

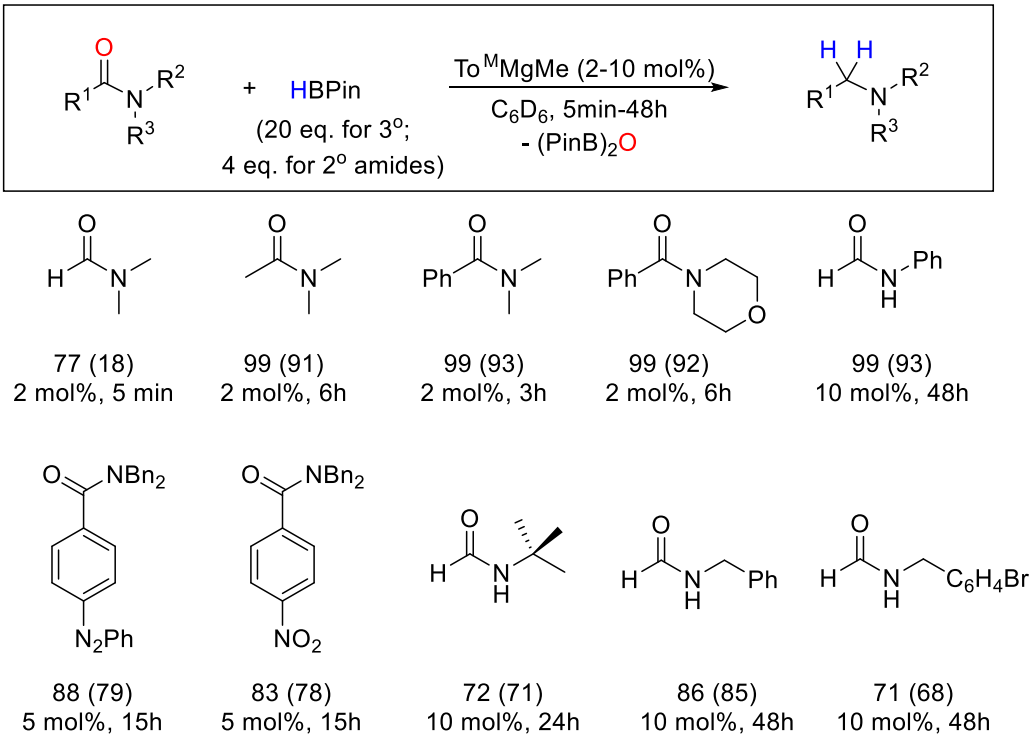

Isolated yields for the corresponding hydrochloride salts after tacidic work-up are given in parentheses

In 2016, Okuda *et al.* have reported the deoxygenative hydroboration of *N*,*N*-dimethylacetamide to *N*,*N*-dimethylethylamine using HBPin and magnesium borohydride $[Mg(THF)_6][HBPh_3]_2$ as a catalyst [62]. This system turned out to be less active and required more harsh conditions (8 h at 60 °C) compared to aforementioned $To^{M}MgMe$ complex (6 h at 25 °C for reduction of *N*,*N*-dimethylacetamide).

More recently, deoxygenative hydroboration of amides employing an aluminum-based complex [κ^2-$\{Ph_2P(Se)NC_9H_6N\}Al(Me)_2$] has been reported by Panda and co-workers [80]. The system was found to reduce a series of tertiary amides using 2 equivalents of HBPin and 5 mol% of the catalyst under mild conditions (room temperature, 12 h) (Scheme 15) [80]. Moreover, the reactions were shown to be chemoselective, tolerating ester, ether, nitro and cyano functionalities. Various aliphatic, aromatic and heterocyclic amides were reduced with HBPin to the corresponding amines, which can be isolated in the form of ammonium salts in good yields.

Scheme 15. [κ^2-$\{Ph_2P(Se)NC_9H_6N\}Al(Me)_2$]-catalyzed deoxygenative hydroboration of tertiary amides.

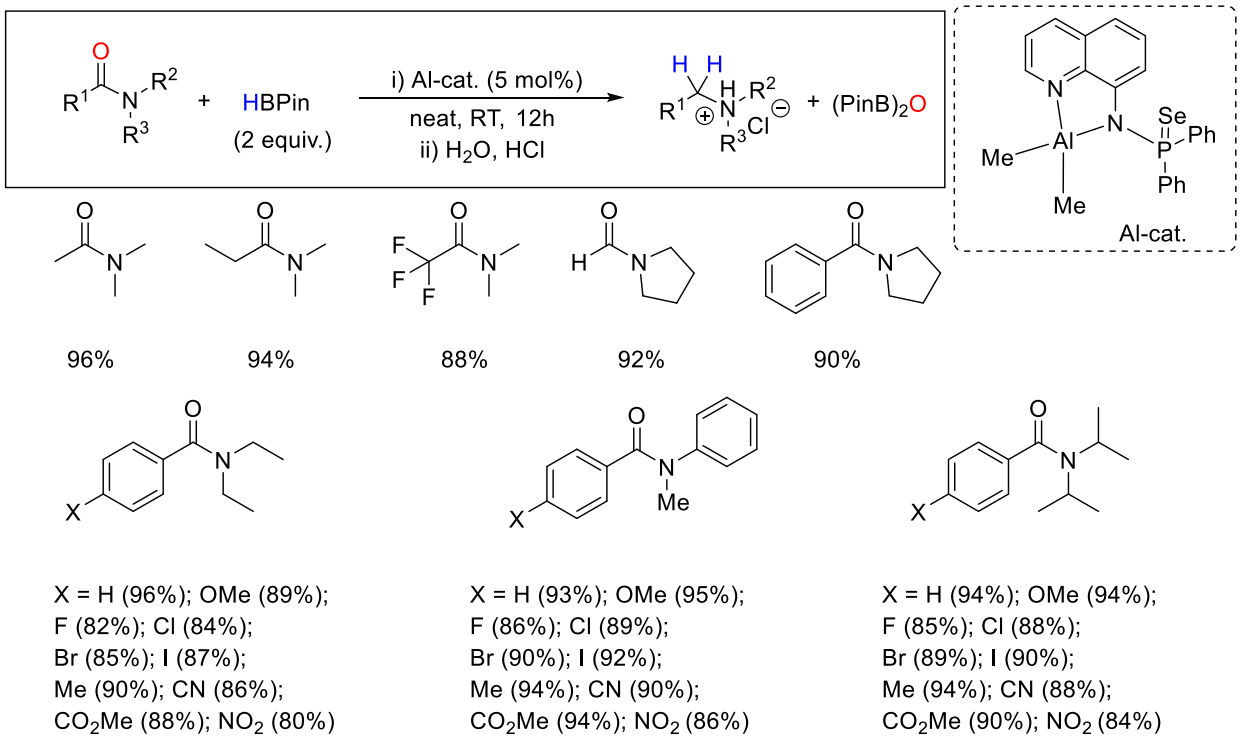

Yields of isolated products after acidic work-up are shown

In 2019, chemoselective reduction of C=X (X = O, N) functionalities, including amides, was demonstrated by Zhang, Mao, Dub *et al.* using the combination of vanadium-based complexes, obtained by the treatment of terpyridine ligand with VCl_3 in THF, followed by the addition of $LiCH_2TMS$ in ether (Scheme 16) [81]. Deoxygenative hydroboration of tertiary and secondary amides with 0.5 mol% of pre-catalysts (as a mixture of complexes, shown in Scheme

Scheme 16. Hydroborative reduction of secondary and tertiary amides catalyzed by the combination of V-based complexes.

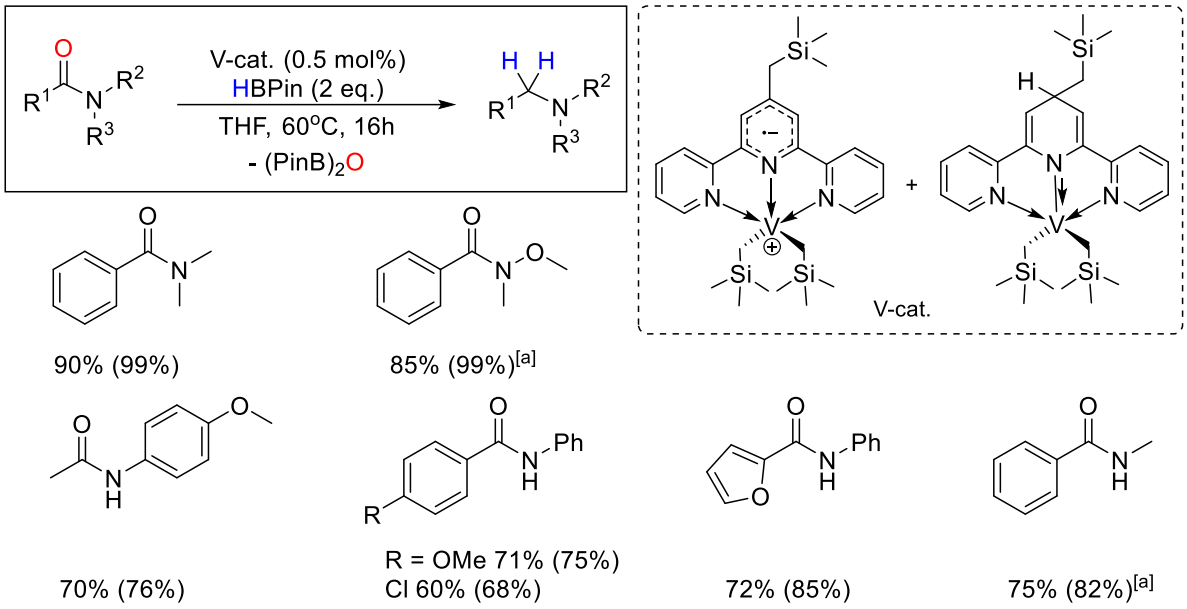

Yields of isolated products are given. GC yields are shown in parentheses. [a] Isolated as ammonium salt

16) at 60 °C for 16 h afforded the corresponding amines, some of which were isolated as ammonium salts after treatment with HCl. In contrast, the attempted V-catalyzed hydroborative reduction of primary amides, such as benzamide, resulted in the dehydration reaction and formation of benzonitrile [81].

The only one example of a base metal catalytic system capable of hydroborating all tertiary, secondary and even more challenging primary amides has been recently reported by our group (Scheme 17) [64]. The reactions were performed with HBPin as reducing agent and are mediated by an iminophosphinite nickel(II) complex ($^{i\text{Pr}}$POCN$^{\text{Ar}}$)NiMe. Thus, using 5 mol% of ($^{i\text{Pr}}$POCN$^{\text{Ar}}$)NiMe and 2 equivalents of HBPin, dimethylformamide was quantitatively reduced to triethylamine within 4 hours at room temperature. On the other hand, deoxygenative hydroboration of *N*-methylsuccinimide resulted in selective formation of *O*-borylated aminal after 5 hours at room temperature. Moreover, as the first examples of reductive hydroboration of primary and secondary amides beyond formamides, acetamide and *N*-phenylpropanamide were fully converted to the corresponding N-borylated amines, albeit the reactions required an excess of HBPin (5 equivalents) and slightly more forcing conditions (60 °C and 24 hours).

In 2020, Mandal and co-workers reported hydroboration of primary amides with HBPin (4 equivalents), catalyzed by an abnormal N-heterocyclic carbene (NHC) based potassium complex{(NHC)K[μ^2-N(SiMe$_3$)$_2$]}$_2$ (2 mol%) [82]. The reactions were performed under mild conditions (40 °C, 12 h), and various aliphatic, aromatic and heterocyclic primary amide substrates were reduced to the corresponding N-borylamines, which were hydrolyzed to the corresponding

Scheme 17. (^{iPr}POCN^{Ar})NiMe-catalyzed deoxygenative hydroboration of tertiary, secondary and primary amides.

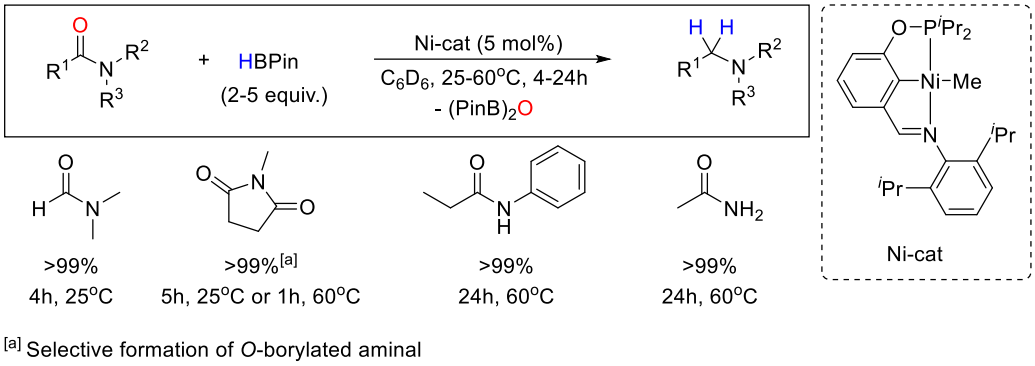

[a] Selective formation of *O*-borylated aminal

hydrochloride salts (Scheme 18). Notably, chemoselective hydroboration of the amide functionalities was observed in the presence of nitro and cyano substituents.

Scheme 18. Hydroboration of primary amides catalyzed by {(NHC)K[μ^2-N(SiMe$_3$)$_2$]}$_2$.

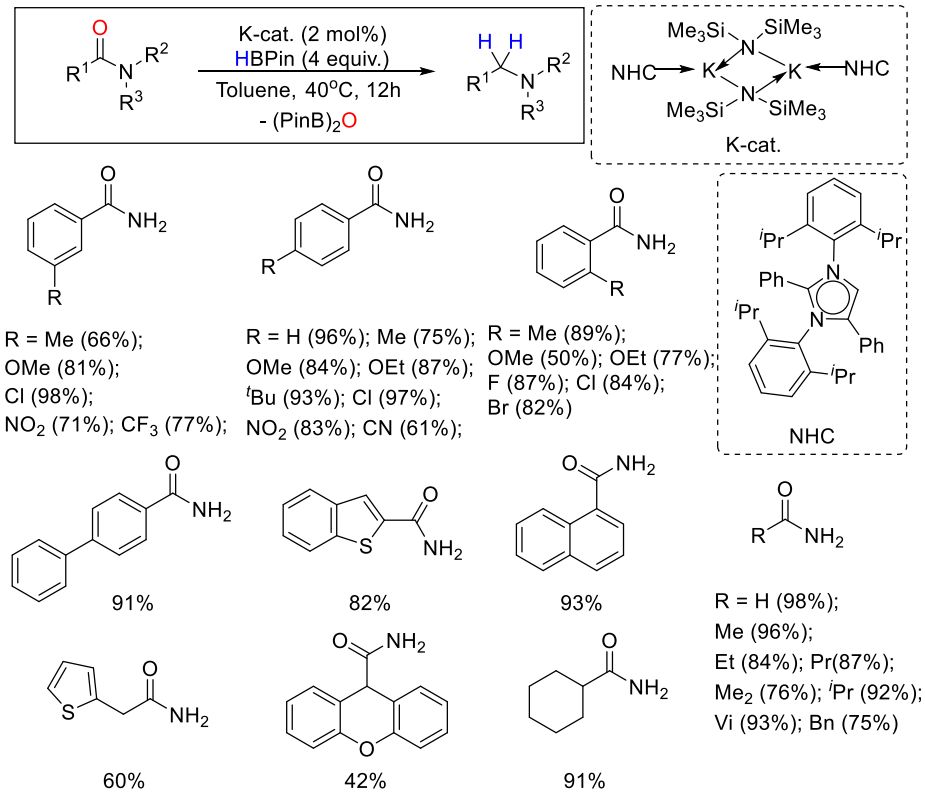

The first example of rare-earth metal-catalyzed deoxygenative hydroboration of tertiary and secondary amides has been demonstrated by Shao, Zhang, Chen *et al.* in 2020 [83]. Various aromatic and cyclic substrates, including those bearing nitro, cyano and vinyl groups, were chemoselectively reduced to the corresponding amines in good to excellent yields (60-98%) using the ytterbium amide Y[N(SiMe$_3$)$_2$]$_3$ (Scheme 19). However, in contrast to the previously described

systems, comparatively harsh reaction conditions (100-120 °C, 24-48 h) and high catalyst loading (10 mol%) were required for such transformations.

Scheme 19. $Y[N(SiMe_3)_2]_3$-catalyzed deoxygenative hydroboration of tertiary and secondary amides.

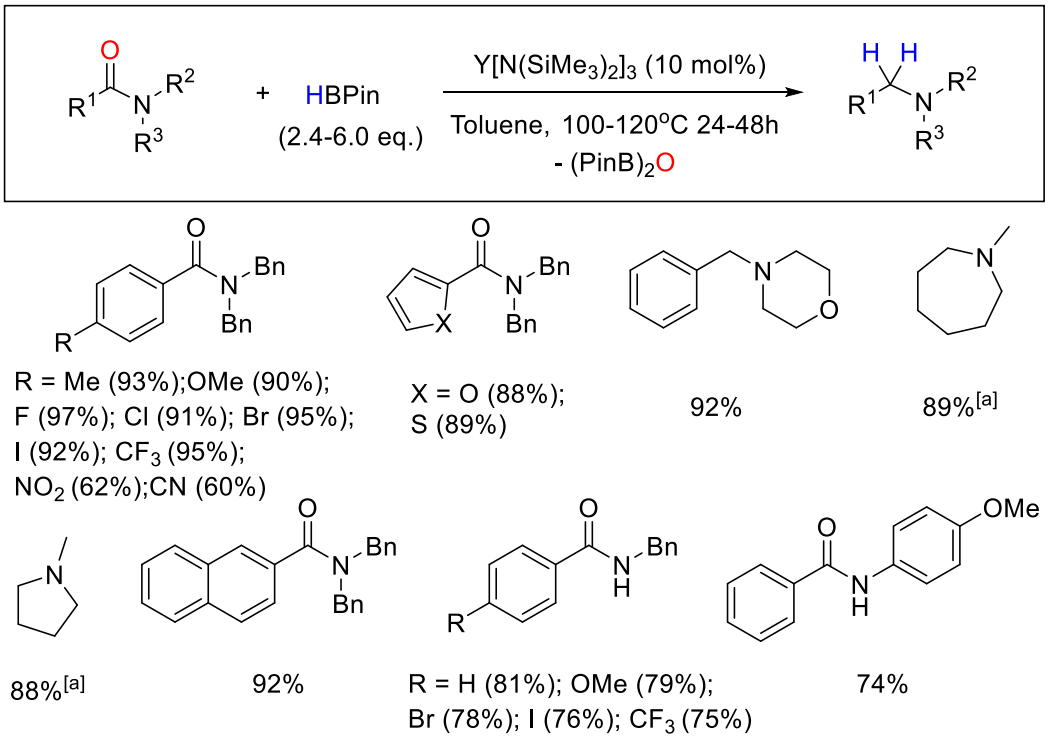

[a] NMR yield (mesitylene was used as internal standard).

Significantly milder hydroboration of tertiary and secondary amides with HBPin (5 equivalents) has been recently reported by Lohr, Marks and co-workers using the related tris[*N*,*N*-bis(trimethylsilyl)amido] lanthanum complex $La[N(SiMe_3)_2]_3$ in C_6D_6 [63]. Tertiary amides were converted to the corresponding amines at room temperature; however, sterically demanding substrates, such as *N*,*N*-diisopropylformamide, and lactams required heating to 60 °C (Scheme 20). Thus, full conversions of both *N*-methylsuccinamide and *N*,*N*-diisopropylformamide were observed in 24 hours, whereas 72 h and 96 h required to achieve complete conversions of these amines at room temperature, respectively. Similarly, no or little hydroboration of more challenging secondary amides was observed at room temperature, and the reactions required heating at 60 °C. Control experiments on hydroboration of *N*,*N*-dimethylbenzamide in the presence of 1-octene and 1-octyne showed high selectivity of the introduced catalytic system for reduction of tertiary amides over alkenes and alkynes.

Scheme 20. $La[N(SiMe_3)_2]_3$-catalyzed deoxygenative hydroboration of tertiary and secondary amides.

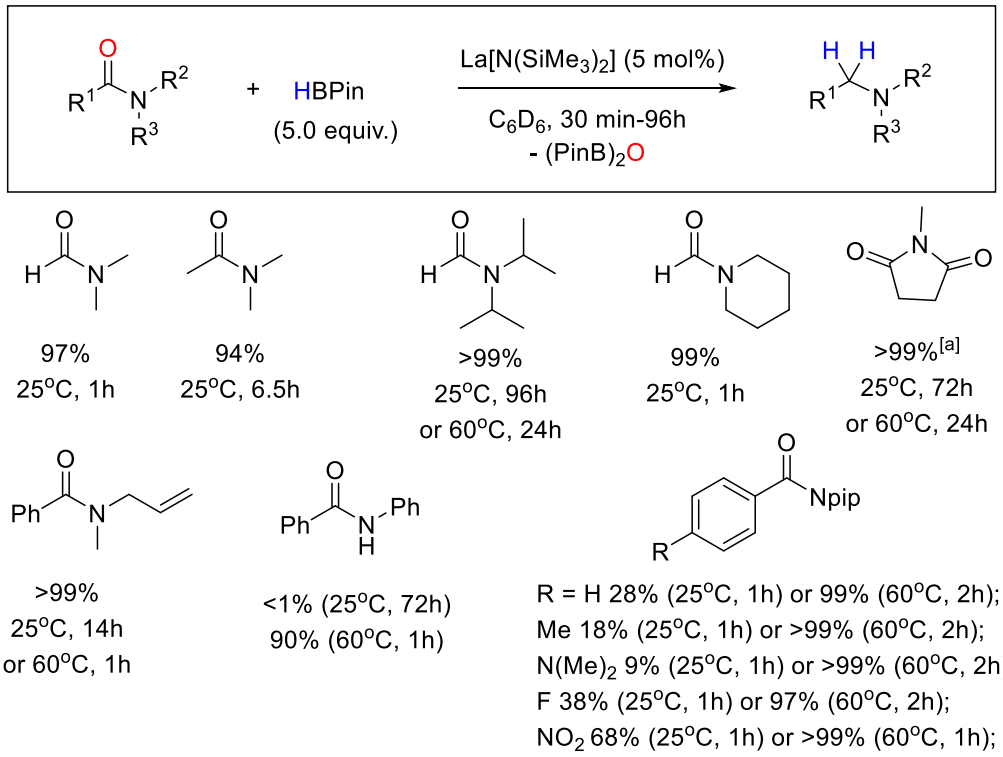

NMR yields are given (hexamethylbenzene was used as internal standard);
[a] 10 equivalents of HBPin were used

More recently, catalytic hydroboration of carboxamides, including tertiary, secondary and primary substrates, has been reported for polynuclear lanthanum-diketonato clusters $La_4(O)(acac)_{10}$ (Schemes 21-22) [84]. Using 3 equivalents HBPin and 1.5 mol% of the catalyst tertiary amides were efficiently reduced to the corresponding tertiary amines under comparatively mild conditions (50 °C, 7-10 h), apart from several examples when longer reaction times (20-24 h) were needed (see Scheme 21). In contrast, secondary and primary amides required significantly increased temperatures and longer reaction times (110 °C, 24 h) combined with higher catalyst loadings (3 mol%) and HBPin concentrations (4 equivalents) (Scheme 22).

Lastly, thorium metallocene-catalyzed ($Cp^*_2ThMe_2$) reductive hydroboration of primary, secondary, and tertiary amides to amines was disclosed by Eisen *et al.* (Scheme 23) [85]. The substrate scope mostly consisted of aliphatic and aromatic secondary amides with only a few examples of tertiary and even less examples primary amide substrates (benzamide and *n*-butyramide). The reactions were performed in C_6D_6 at 70 °C for 24 hours, and the amide conversions to amines were determined by ^1H NMR. Only a few amine products were isolated in

Scheme 21. $La_4(O)(acac)_{10}$-catalyzed deoxygenative hydroboration of tertiary amides.

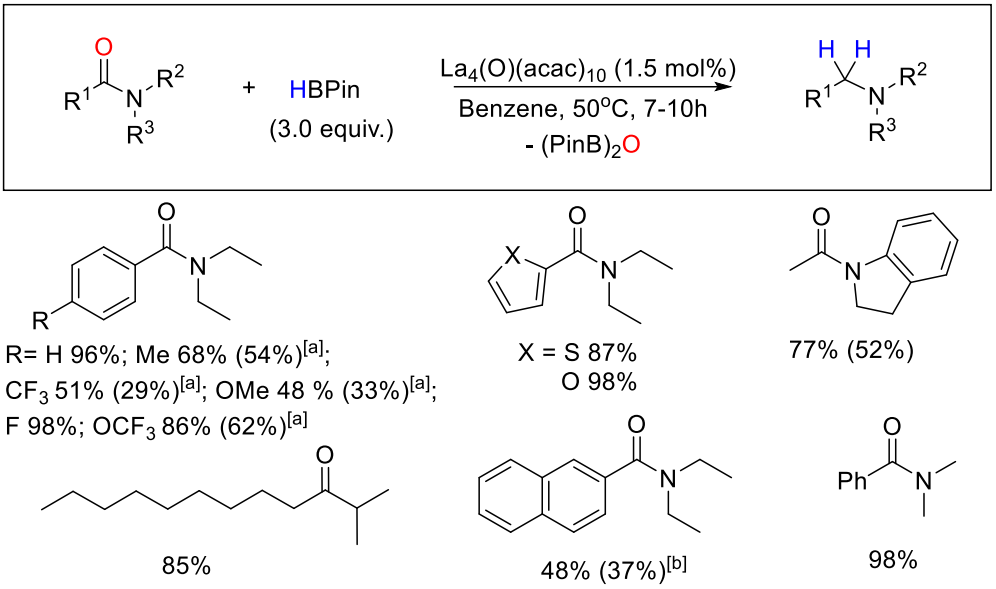

NMR yields are given (tetraethylsilane was used as internal standard). Yields in parentheses show isolated yields after column chromatography.
[a] Reaction proceeds under 24 h; [b] 20h

Scheme 22. $La_4(O)(acac)_{10}$-catalyzed deoxygenative hydroboration of secondary and primary amides.

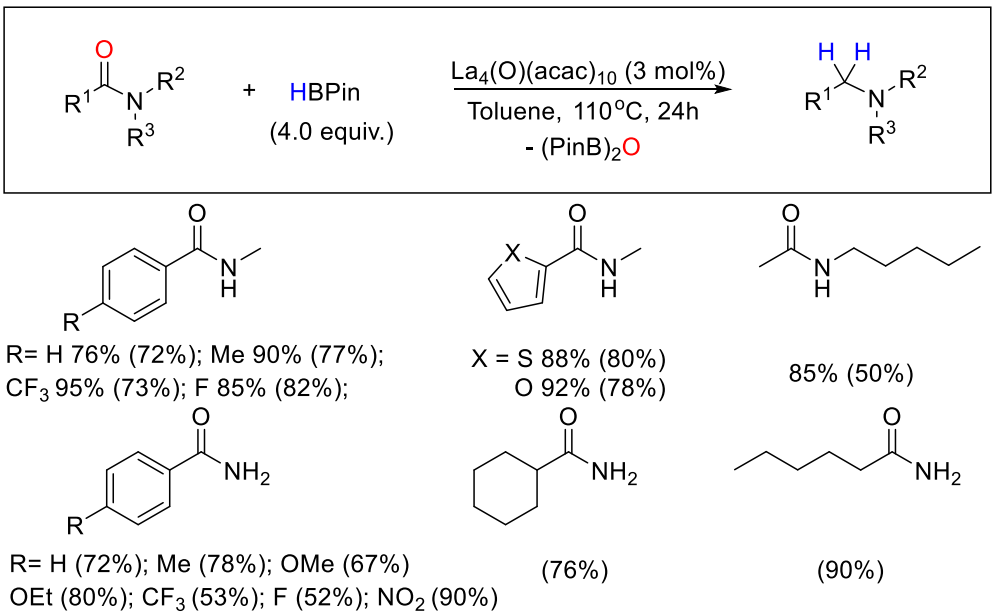

NMR yields are given for secondary amines ($SiEt_4$ was used as internal standard).
Yields in parentheses show isolated yields of hydrochloride salts after acidic work-up

analytically pure form. Also, for some substrates along with the desired deoxygenated products, formation of C-N cleavage by-products was observed by NMR (% of C-O/C-N bond cleavage products are given in Scheme 23).

Scheme 23. Deoxygenative hydroboration of tertiary, secondary and primary amides catalyzed by $Cp^*_2ThMe_2$.

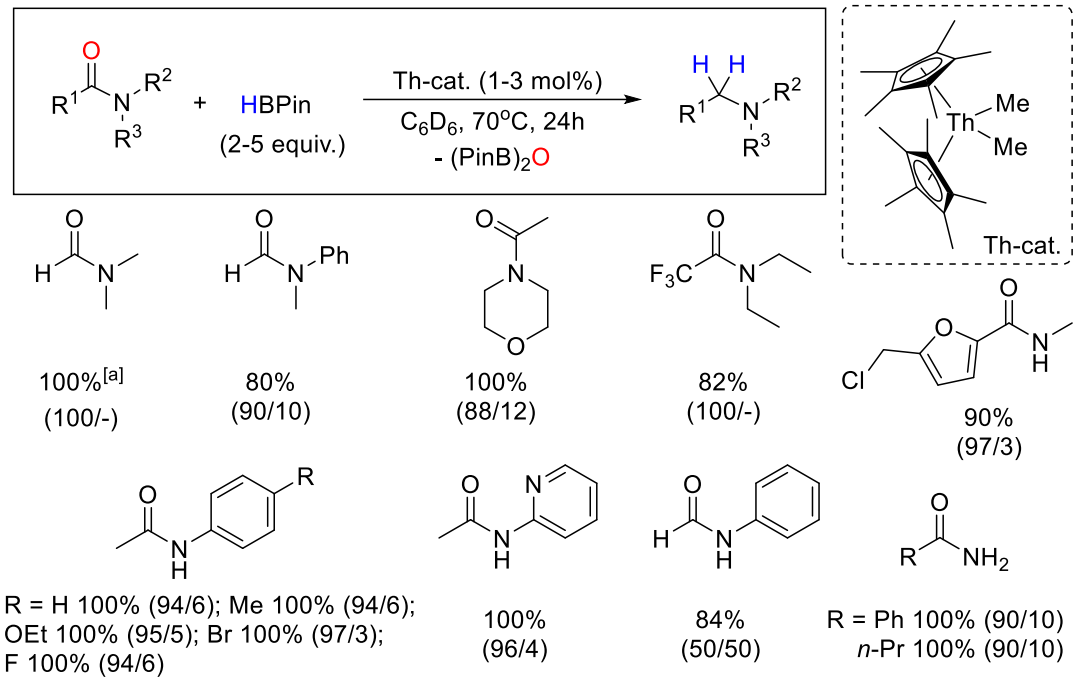

Conversions of the products are shown. Chemoselective percentage of C-O/C-N bond cleavage products are given in parentheses; [a] The reaction proceeds under 6h

In summary, despite numerous base metal catalytic systems developed for deoxygenative hydrosilylation of amides, most of the reported catalysts still require rather harsh experimental conditions. Moreover, hydrosilylation of secondary and especially primary amides is still a challenging task since these substrates are prone to formal dehydration (such as conversion of primary amides to nitriles) under catalytic conditions. On the other hand, compared to hydrosilylation approach, deoxygenative hydroboration of amides is developed to a significantly lesser extent with only a few catalytic systems based on d-block metals (namely one vanadium complex and one nickel complex) being reported to date. Despite these scarce examples, such hydroboration systems have already attracted significant attention since they seem to require milder reaction conditions compared to hydrosilylation reactions and can be applied in reduction of secondary and more importantly primary amide substrates, presenting an appealing approach for development of economical and efficient routes to amines from a wide range of amides. Deoxygenative hydroboration of secondary and primary amides have yet another advantage over analogous hydrosilylation reactions. In particular, hydroboration of $R^1C(O)N(H)R^2$ and $R^1C(O)NH_2$ with HBPin allow for direct preparation of N-borylated amines, $R^1CH_2N(BPin)R^2$ and $R^1CH_2N(BPin)_2$, which due to the presence of reactive B-N bonds can be *in situ* used for construction of more complex N-containing organic molecules, thus, opening new venues in synthetic organic chemistry [9].

3 Results and Discussion

3.1 Synthesis and characterization of iminophosphinite nickel complexes

Iminophosphinite nickel bromide complexes (^{iPr}POCN^{imine})NiBr were synthesized using slightly modified methodology reported previously by Zargarian and co-workers [86]. The synthetic approach to ^{iPr}POCN^{imine} pincer ligands starts with the commercially available 3-hydroxybenzaldehyde, which was treated with 2,6-dialkylanilines (where alkyl is either 2-propyl or methyl) resulting in the formation of imine derivatives. The latter products were reacted with $^{i}Pr_2PCl$ in the presence of NEt_3 excess giving the desired iminophosphinite ^{iPr}POCN^{imine} ligands **1-2** (Scheme 24) [64]. Formation of pincer complexes was achieved by metalation of the prepared ligands with $NiBr_2(CH_3CN)_2$ (Scheme 24), which was synthesized *via* bromination of Ni powder in acetonitrile [87]. Extraction with a mixture of hexanes and toluene (80:20 by volume, respectively) allowed the isolation of dark red products **1-Ar** and **1-Ar'** (Ar = 2,6-diisopropylphenyl, Ar' = 2,6-dimethylphemyl) in 60-69% yields. The obtained nickel bromide complexes **1-Ar** and **1-Ar'** were used as precursors for further derivatization *via* substitution of the bromide ligand for preparation of potential pre-catalysts for hydroboration reactions.

Since formation of the hydride complexes is essential in most of the catalytic reduction reactions (i.e. hydrogenation, hydrosilylation and hydroboration), including the intended deoxygenative hydroboration of carboxamides, conversion of the obtained bromides **1-Ar** and **1-Ar'** to the corresponding hydride derivatives (^{iPr}POCN^{imine})NiH seems the first logical reaction to

Scheme 24. Synthesis of (^{iPr}POCN^{imine})NiBr complexes.

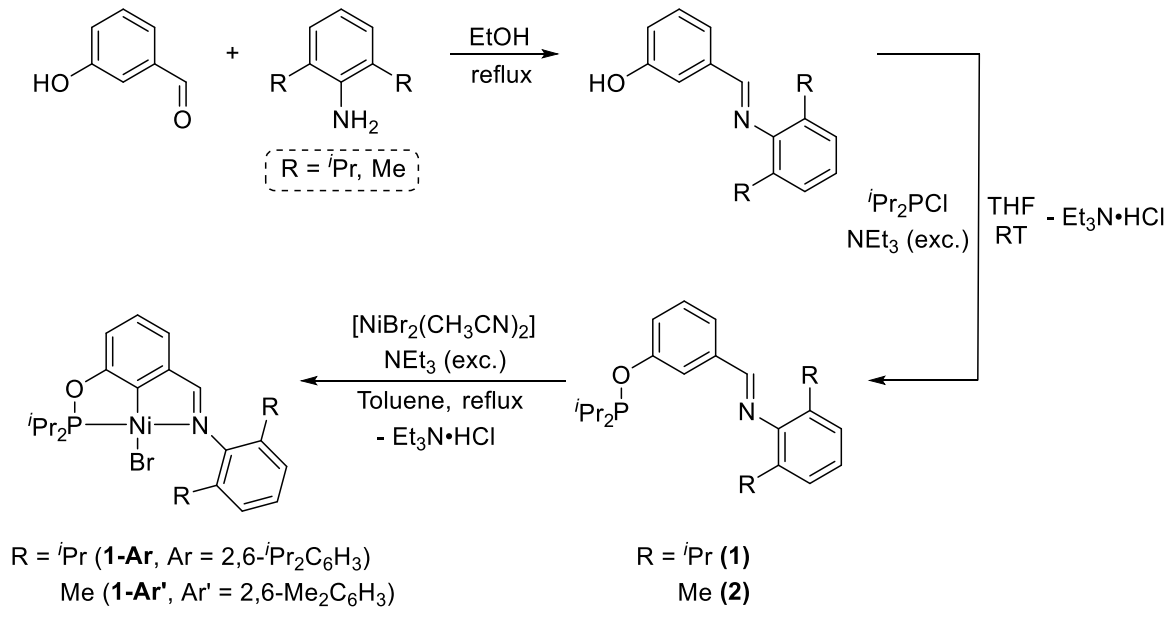

Scheme 25. NMR scale generation of (^{iPr}POCN^{Ar})NiH **(2-Ar**).

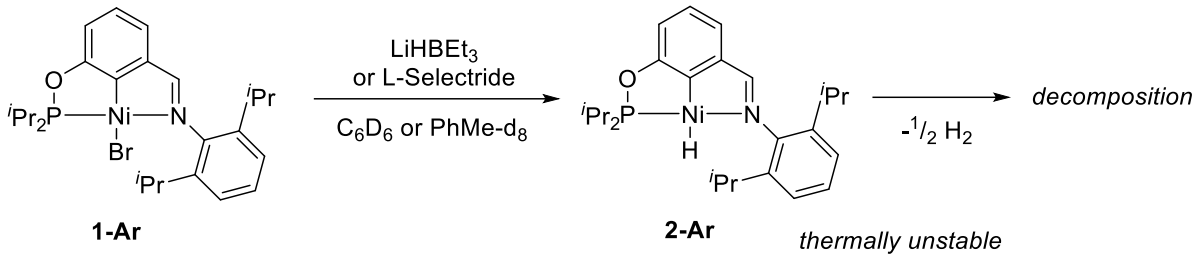

test. As was previously demonstrated in our laboratory [64], treatment of **1-Ar** with either $LiBHEt_3$ or L-Selectride (lithium tri-*sec*-butylborohydride) in C_6D_6 or toluene-d_8 allowed to generate the hydride complex (^{iPr}POCN^{Ar})NiH (**2-Ar**; Scheme 25); however, similarly to many other nickel hydrides [88], **2-Ar** turned out to be thermally unstable and decomposes at room temperature with liberation of hydrogen and deposition of metallic nickel. Therefore, we thought of preparing stable nickel pre-catalysts that would generate the hydride species akin to **2-Ar** *in situ* during the catalytic hydroboration reactions. Previously, it has been shown that effective generation of the hydride **2-Ar** could be achieved upon reaction of HBPin with the methyl derivative (^{iPr}POCN^{Ar})NiMe (**3-Ar**), which was prepared by the treatment of the bromide complex **1-Ar** with MeLi (Scheme 26) [64]. The preliminary studies have also indicated high catalytic activity of **3-Ar** in deoxygenative hydroboration of DMF, *N*-phenylpropanamide and acetamide at 60 °C, presenting the first example of d-block transition metal catalytic system for mild deoxygentaive hydroboration of carboxamides to amines [64]. However, **3-Ar** turned out to be unstable in solution and this precluded the detailed studies of the scope of amide hydroboration reactions. We hypothesized that decomposition of **3-Ar** may occur *via* migration of the methyl ligand from nickel to an electrophilic imine carbon of the iminophosphinite ligand (Scheme 27). To tackle this problem of stability, two major modifications of the pre-catalyst structure were proposed. In the first approach, we suggested that increasing the steric hindrance of the alkyl substituent at nickel may enhance the stability of the iminophosphinite compounds. The second approach is based on the substitution of the iminophosphinite ligands with saturated aminophsophinite surrogates and is described in

Scheme 26. Preparation of (^{iPr}POCN^{Ar})NiMe **(3-Ar**) and its reactivity with HBPin.

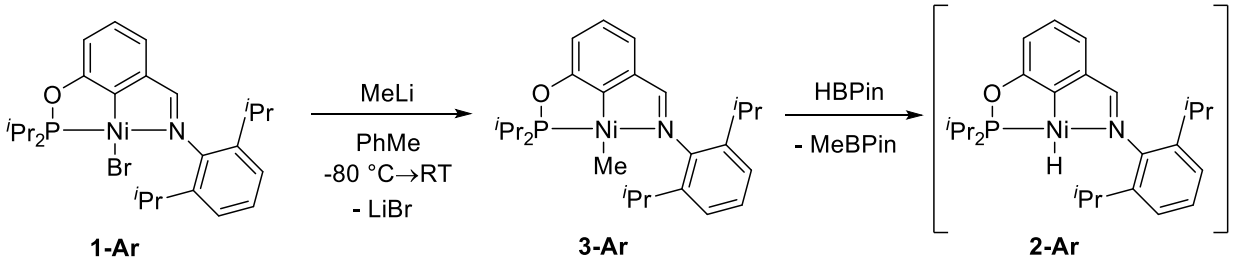

Scheme 27. Proposed pathway for decomposition of (^{iPr}POCN^{Ar})NiMe **(3-Ar)**.

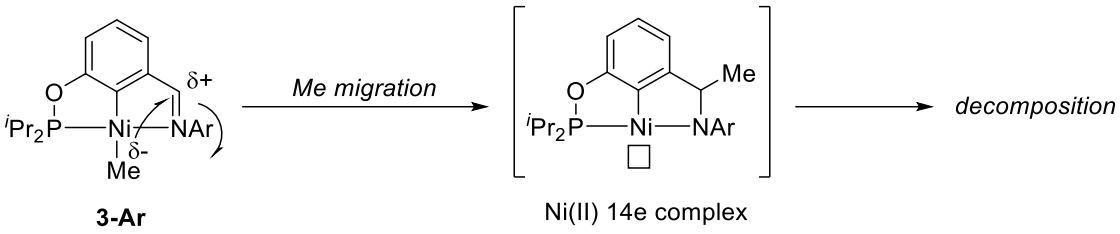

details in the second part of this section. With regards to preparation of sterically demanding nickel pre-catalysts, the bromide complex **1-Ar** was treated with $LiCH_2SiMe_3$ in toluene to give the (trimethylsilyl)methyl derivative (^{iPr}POCN^{Ar})Ni(CH_2TMS) (**4-Ar**; Scheme 28), which was isolated in 82% yield. As expected, due to the steric hindrance imposed by the trimethylsilyl group, **4-Ar** turned out to be significantly more stable compared to its methyl analogue **3-Ar**. The NMR features of **4-Ar** are similar to those previously reported for the methyl derivative **3-Ar**. Thus, compared to the starting bromide complex **1-Ar**, the $^{31}P\{^1H\}$-NMR spectrum of **4-Ar** reveals an up-field ^{31}P resonance at δ_P = 193.8 ppm (compare to δ_P = 199.2 ppm for the previously reported **3-Ar** [64]). The CH_2TMS ligand gives rise to the characteristic ^{1}H-NMR resonance at δ_H = -0.97 ppm (doublet) for the methylene protons of Ni-CH_2 moiety, coupled to the phosphorus nucleus of the POCN ligand with $^3J_{H\text{-}P}$ = 5.1 Hz. A similar up-field chemical shift (δ_H = -0.81 ppm) and the value of H-P coupling constant ($^3J_{H\text{-}P}$ = 3.6 Hz) was previously found for the nickel-bound CH_3 ligand of **3-Ar** [64]. The preparation of (^{iPr}POCN$^{Ar'}$)Ni(CH_2TMS) (**4-Ar'**) derivative, having 2,6-dimethylphenyl substituent at the iminophosphinite nitrogen atom, was also attempted by treatment of **1-Ar'** with $LiCH_2$TMS in toluene (Scheme 28). However, compared to **4-Ar**, using less sterically hindered ^{iPr}POCN$^{Ar'}$ ligand significantly lowered the stability of the resulting alkyl complexes, and **4-Ar'**

Scheme 28. Reactivity of (^{iPr}POCN^{imine})NiBr complexes **1-Ar** and **1-Ar'** with $LiCH_2$TMS and KO^{t}Bu.

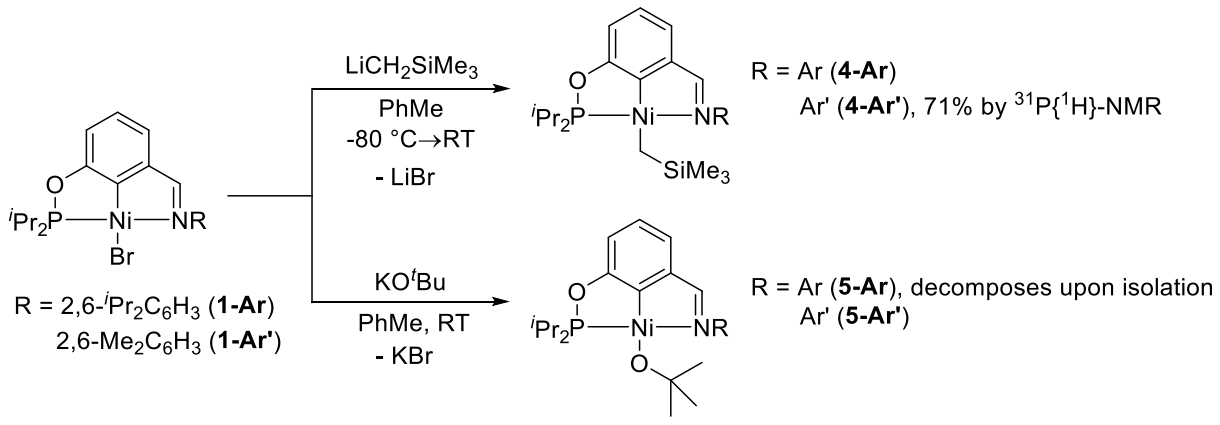

could be obtained only with 71% purity (by $^{31}P\{^{1}H\}$-NMR). All attempts to isolate **4-Ar'** in analytically pure forms were unsuccessful.

We then looked at the other pre-catalysts that can potentially give the catalytically active hydride species upon reaction with HBPin. Thus, treatment of **1-Ar** with KO^{t}Bu in either benzene, toluene or THF at room temperature leads to the formation of a *tert*-butoxide complex (^{iPr}POCN^{Ar})Ni(O^{t}Bu) (**5-Ar**; Scheme 28), which was characterized by ^{1}H and ^{31}P-NMR spectroscopy. The ^{1}H-NMR spectrum of **5-Ar** is very similar to the spectra of **1-Ar** and **4-Ar** except for the absence of alkyl ligands and the presence of the resonance for the *tert*-butoxide ligand found at δ 1.04 ppm (singlet). The $^{31}P\{^{1}H\}$-NMR spectrum of **5-Ar** showed an up-field (compared to **1-Ar**) ^{31}P resonance at δ 185.9 ppm for the iminophosphinite ligand. Although, **5-Ar** can be cleanly generated *in situ* on the NMR scale, leaving the complex in solution under argon atmosphere results in its partial decomposition to a mixture of unknown products. Such decomposition of **5-Ar** was also observed upon its attempted isolation. Analogously to **5-Ar**, the 2,6-dimethylphenyl derivative (^{iPr}POCN$^{Ar'}$)Ni(O^{t}Bu) (**5-Ar'**) can be quantitatively generated by treatment of **1-Ar'** with KO^{t}Bu in C_6D_6 or toluene on NMR scale, but turned out to be unstable upon isolation. Notably, similar instability of the nickel *tert*-butoxide complexes has been previously reported by Zargarian *et al.* for the related bis(phosphinite) POCOP pincer complexes (POC$_{sp2}$OP)Ni(O^{t}Bu) and (POC$_{sp3}$OP)Ni(O^{t}Bu) (Figure 3) and was explained by the presence of destabilizing dπ–pπ interactions in the Ni-O^{t}Bu moiety [89-90].

Figure 3. Bis(phosphinite) pincer complexes (POC$_{sp2}$OP)Ni(O^{t}Bu) and (POC$_{sp3}$OP)Ni(O^{t}Bu).

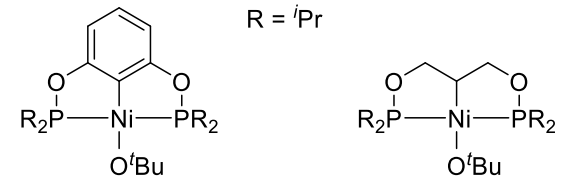

(POC$_{sp2}$OP)Ni(O^{t}Bu) (POC$_{sp3}$OP)Ni(O^{t}Bu)

Apart from alkyl and alkoxy ^{iPr}POCN^{imine} nickel complexes discussed above, we proposed that generation of the hydride species akin to **2-Ar**, active in hydroboration catalysis, could be achieved upon reactions of HBPin with (^{iPr}POCN^{imine})Ni(η^2-BH$_4$) and (^{iPr}POCN^{imine})Ni(η^1-BF$_4$), the synthetic routes to which were previously developed in our laboratory [64]. Thus, nickel bromide precursor **1-Ar** was reacted with either LiBH$_4$ or AgBF$_4$ in toluene at room temperature to produce barberry red nickel borohydride **6-Ar** and yellow nickel tetrafluoroborate complexes **7-Ar** in 93% and 59% yields, respectively (Scheme 29). Both compounds have similar ^{1}H and $^{31}P\{^{1}H\}$-NMR spectra with the bromide precursor **1-Ar**, considering that all complexes have similar structures. Notably, the borohydride ligand of **6-Ar** gives rise to two broad resonances at

δ_H = -0.95 ppm and δ_H = -0.72 ppm in the ^{1}H-NMR spectrum and a broad resonance at δ_B = -30.8 ppm in the ^{11}B{^{1}H}-NMR spectrum. For **7-Ar**, ^{19}F and ^{11}B resonances for the BF_4 ligand were observed at δ_F = -173.8 ppm (br s) and δ_B = -1.4 ppm (br s), respectively. These spectroscopic features of **6-Ar** and **7-Ar** are in agreement with those previously published in the literature [64].

Scheme 29. Synthesis of the borohydride and tetrafluoroborate nickel complexes **6-Ar** and **7-Ar**.

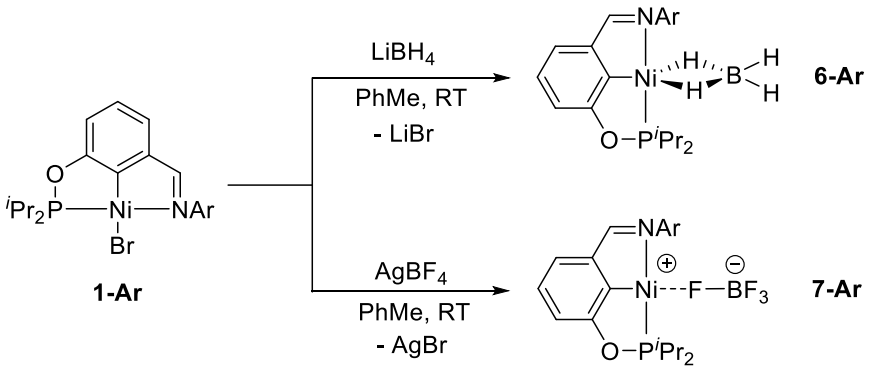

3.2 Synthesis, characterization and reactivity of aminophosphinite nickel complexes

3.2.1 Synthesis of aminophosphinite Ni(II) bromides

Taking into account the observed thermal instability of the iminophosphinite ^{iPr}POCN^{imine} complexes of nickel and their possible decomposition pathway depicted in Scheme 27, we proposed that substitution of the iminophosphinite pincer ligands with aminophosphinite ^{iPr}POCN^{amine} ligands should enhance the stability of nickel pre-catalysts while maintaining their reactivity. Thus, a series of aminophosphinite ^{iPr}POCN^{amine} nickel pre-catalysts, having saturated amine donors in the ligand side-arm positions, have been prepared. First, three aminophosphinite nickel bromide complexes (^{iPr}POCN^{R2})NiBr (R = Me (**8-Me$_2$**), Et (**8-Et$_2$**), ^{i}Pr (**8-^{i}Pr$_2$**)) have been synthesized using slightly modified literature procedure, reported previously by Zargarian *et al.* [91]. Thus, readily available 3-hydroxybenzaldehyde was converted to 3-(dialkylamino)methyl)phenol (Alk = Me, Et, ^{i}Pr) *via* reductive amination reactions using either $NaBH_4$ (for Alk = Me) or $NaBH(OAc)_3$ (for Alk = Et, ^{i}Pr) with 70%, 87% and 74% isolated yields, respectively (Scheme 30). Further room temperature reaction of 3-(dialkylamino)methyl)phenol derivatives with ^{i}Pr$_2$PCl in the presence of NEt_3 excess allowed for isolation of the target aminophosphinite ^{iPr}POCN^{amine} ligands (Scheme 30). Similar to iminophosphinite reactions, metallation of these ligands was performed with $NiBr_2(CH_3CN)_2$ (Scheme 30) [91]. Notably, compared to methyl and ethyl substituted derivatives, which showed complete conversion to the corresponding bromide complexes **8-Me$_2$** and **8-Et$_2$** within a few hours at 60 °C, the reaction of more sterically hindered isopropyl pincer ^{iPr}POCN^{iPr2} with $NiBr_2(CH_3CN)_2$ required higher

Scheme 30. Synthesis of (^{iPr}POCN^{amine})NiBr complexes.

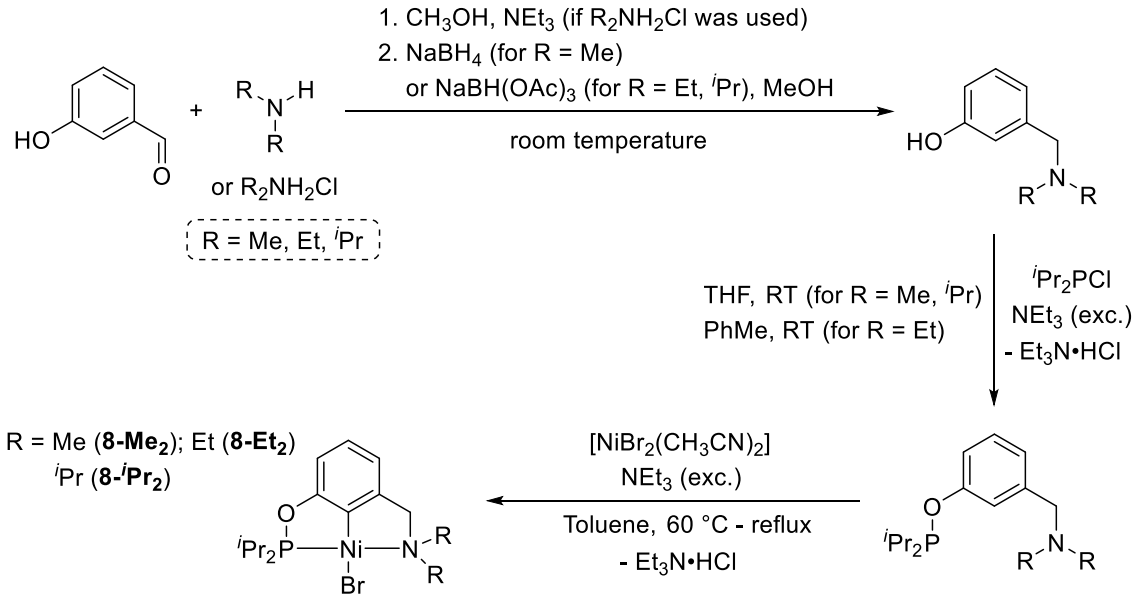

reaction temperatures (up to 110 °C) and longer reaction times (up to two days) to achieve complete conversion to **8-^{i}Pr$_2$**. Moreover, in contrast to the related iminophosphinite bromides (^{iPr}POCN^{imine})NiBr (**1-Ar** and **1-Ar'**) more rigorous procedures, such as additional filtration through a pad of silica gel, required for isolation of the aminophosphinite derivatives in a pure form. Despite this, complexes **8-Me$_2$**, **8-Et$_2$** and **8-^{i}Pr$_2$** were isolated in moderate to good yields (55%, 89% and 75%, respectively). Bromides **8-Me$_2$** and **8-Et$_2$** were characterized by NMR, showing good agreement with the previously published data. The isopropyl derivative **8-^{i}Pr$_2$** was not reported previously, but its ^{1}H, ^{13}C{^{1}H} and ^{31}P{^{1}H}-NMR features are very similar to those reported for **8-Me$_2$** and **8-Et$_2$** analogues.

3.2.2 Reactivity of aminophosphinite Ni(II) complexes

Having a series of the target aminophosphinite nickel bromides (**8-Me$_2$**, **8-Et$_2$** and **8-^{i}Pr$_2$**), we then examined their reactivity towards substitution of the bromide ligand in order to obtain suitable pre-catalysts for hydroboration studies. Similarly to the iminophosphinite complexes, we first targeted the preparation of alkyl compounds (^{iPr}POCN^{amine})NiR (where R = CH_3, CH_2SiMe_3). Thus, (^{iPr}POCN^{Me2})NiBr (**8-Me$_2$**) was treated with either MeLi or $LiCH_2TMS$ in toluene to produce (^{iPr}POCN^{Me2})NiMe (**9-Me$_2$**) and (^{iPr}POCN^{Me2})Ni(CH_2SiMe_3) (**10-Me$_2$**), respectively (Scheme 31). Oppositely to the iminophosphinite analogue (^{iPr}POCN^{Ar})NiMe (**3-Ar**), the methyl derivative **9-Me$_2$** turned out to be significantly more stable and was isolated by extraction with hexanes as yellow solid in 79% yield. The complex was fully characterized by

multinuclear NMR analysis. The ^{1}H-NMR spectrum of **9-Me$_2$** shows a characteristic up-field ^{1}H resonance for the

Scheme 31. Reactivity of (^{iPr}POCN^{Me2})NiBr (**8-Me$_2$**) with MeLi and LiCH$_2$TMS.

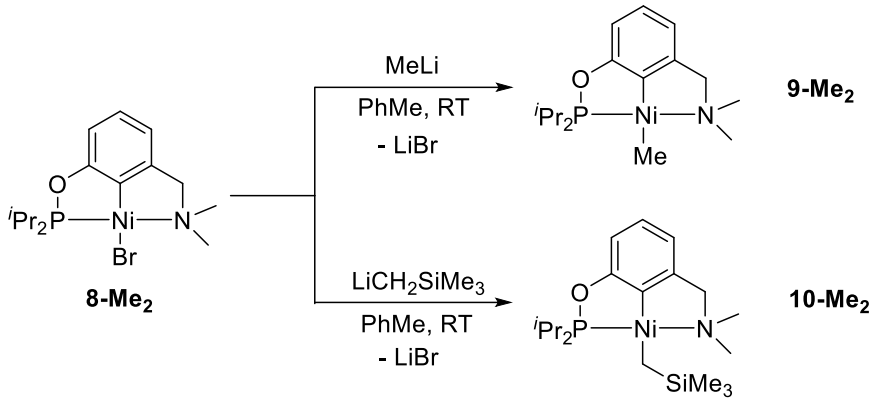

nickel-bound methyl group found at δ_H = -0.82 ppm (doublet, $^{3}J_{H\text{-}P}$ = 3.1 Hz) coupled in ^{1}H-^{31}P HSQC NMR to the ^{31}P resonance at δ_P = 197.1 ppm (singlet). The methyl ligand of **9-Me$_2$** also gives rise to an up-field ^{13}C resonance at δ_H = -10.2 ppm (doublet), which also shows coupling to the phosphorus of the aminophosphinite ligand ($^{2}J_{C\text{-}P}$ = 21.1 Hz). Analogous NMR features we detected for the (trimethylsilyl)methyl derivative **10-Me$_2$** ($\delta_{Ni\text{-}CH2}$ = -1.21 ppm (doublet, $^{3}J_{H\text{-}P}$ = 5.0 Hz); δ_P = 193.5 ppm). All these features are similar to those of the iminophosphinite methyl derivative **3-Ar** [64] and are consistent with a square-planar geometry of **9-Me$_2$** and **10-Me$_2$** with the methyl and (trimethylsilyl)methyl ligands, respectively, positioned *cis*- to the phosphinite side-arm of the ^{iPr}POCN^{Me2} ligand.

We have also attempted the preparation of the analogous ethyl complex (^{iPr}POCN^{Me2})NiEt (**11-Me$_2$**) by the reaction of the nickel bromide **8-Me$_2$** with EtMgBr in C_6D_6. Formation of $MgBr_2$ precipitate was observed indicating the successful substitution of the bromide ligand with the ethyl group. However, NMR analysis of the reaction mixture showed formation of a difficult-to-separate mixture of decomposition products, among which free ethylene and H_2 gas were detected in the ^{1}H NMR spectrum (δ_H = 5.26 ppm and 4.47 ppm in C_6D_6, respectively). Therefore, we believe that **11-Me$_2$** forms initially but decomposes subsequently *via* β-H elimination resulting in extrusion of C_2H_4 and formation of thermally unstable nickel hydride species (^{iPr}POCN^{Me2})NiH (**12-Me$_2$**) (Scheme 32).

Next, preparation of the *tert*-butoxy aminophosphinite complexes (^{iPr}POCN^{R2})Ni(O^{t}Bu) (R = Me (**13-Me$_2$**), Et (**13-Et$_2$**) and ^{i}Pr (**13-^{i}Pr$_2$**; Scheme 33) was attempted. The reactions of the bromides **8-Me$_2$**, **8-Et$_2$** and **8-^{i}Pr$_2$** with KO^{t}Bu in either benzene or toluene were found to be significantly slower compared to those for the iminophosphinite analogues **1-Ar** and **1-Ar'** (Scheme 28). Thus, for **8-Me$_2$** full conversion to the desired **13-Me$_2$** was observed in one hour at

room temperature, whereas for **8-Et2** the reaction with KO^{t}Bu in benzene requires stirring for several days. In contrast, using more polar THF instead of benzene or toluene allowed for almost instantaneous conversion (by $^{31}P\{^1H\}$-NMR) of **8-Me2**, **8-Et2** and **8-^{i}Pr2** to the corresponding *tert*-

Scheme 32. Reaction of the bromide complex **8-Me2** with EtMgBr.

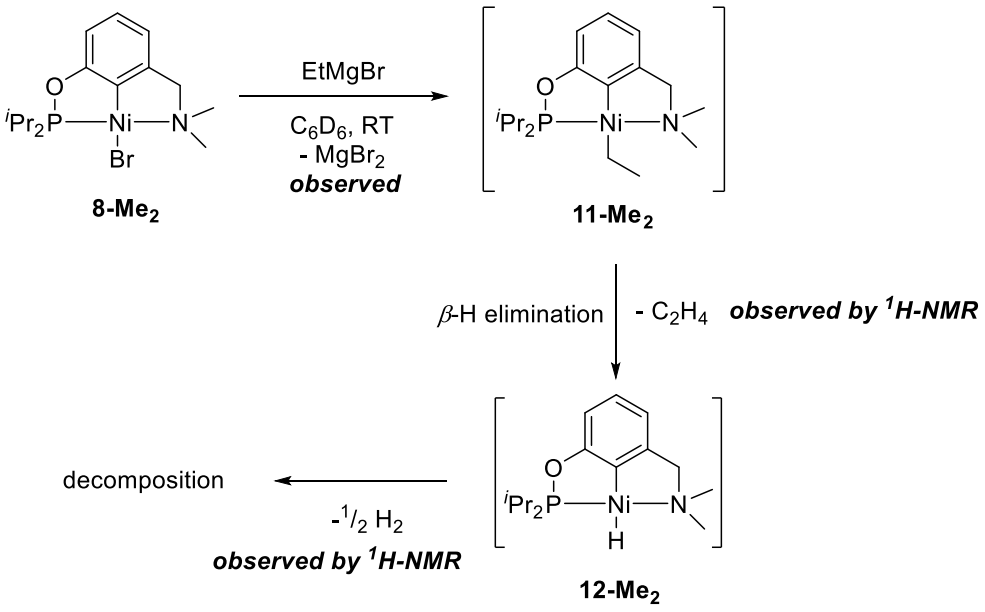

Scheme 33. Reactivity of the bromides **8-Me2**, **8-Et2** and **8-^{i}Pr2** with KO^{t}Bu.

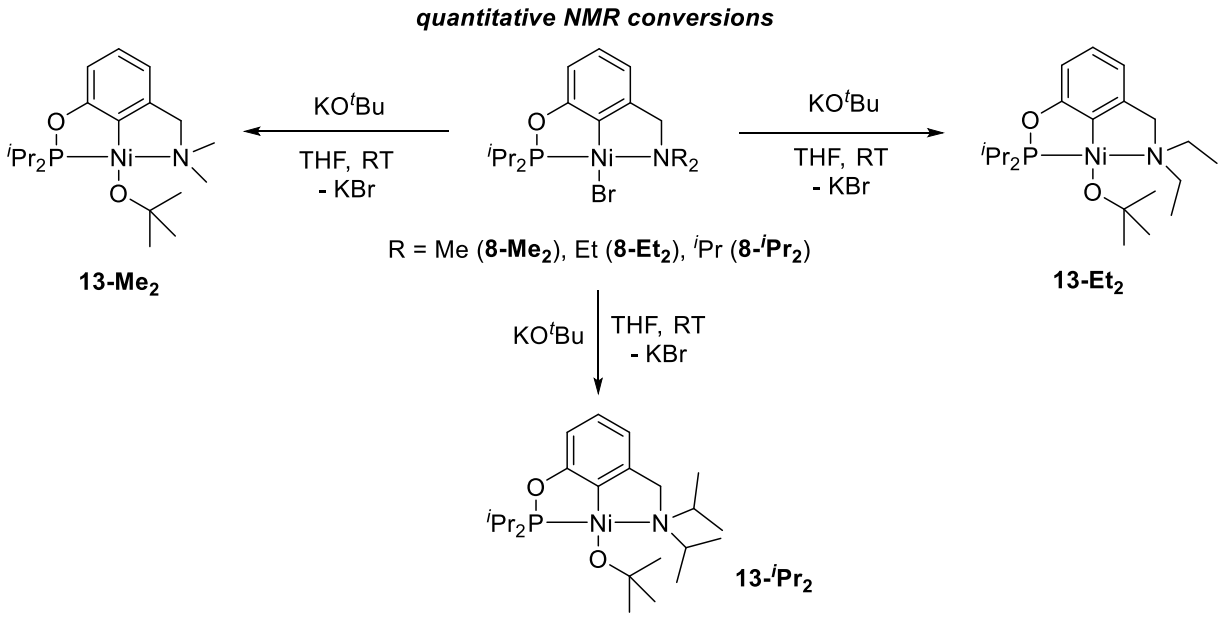

butoxide derivatives **13- Me2**, **13-Et2** and **13-^{i}Pr2**. Whereas quantitative formation of both **13-Me2** and **13-^{i}Pr2** was observed by NMR, the reaction of **8-Et2** with KO^{t}Bu turned out to be less clean, showing by $^{31}P\{^1H\}$-NMR formation of a mixture of **13-Et2** (approx. 68%) and unidentified decomposition products. The NMR features of complexes **13-Me2**, **13-Et2** and **13-^{i}Pr2** are very

similar to those observed for the related iminophosphinite compounds **5-Ar** and **5-Ar'**. Preparation and NMR characterization of the ethyl derivative **13-Et$_2$** have been previously reported by Miller *et al.* [92]. Following this literature procedure, extraction of the product with cold (-30 °C) hexanes afforded an orange oil, NMR analysis of which revealed the presence of two isomers of **13-Et$_2$** (two sets of very similar resonances were observed in ^{1}H and ^{31}P{^{1}H}-NMR spectra of **13-Et$_2$**; see the experimental section for details). Compared to less sterically crowded **13-Me$_2$**, formation of isomers of **13-Et$_2$** can be rationalized by restricted rotation of the bulky *tert*-butoxide ligand; however, this has not been previously reported by Miller *et al.* [92]. In contrast, despite even more sterically crowded isopropyl groups, formation of only one isomer was detected for **13-^{i}Pr$_2$** derivative. Even though **13-Me$_2$** can be cleanly, efficiently and quantitatively generated *in situ*, the complex turned out to be extremely hygroscopic and could not be isolated in analytically pure form. Similar, however less pronounced problems were encountered upon attempted isolation of **13-Et$_2$** and **13-^{i}Pr$_2$** derivatives. Hygroscopic nature of **13-Et$_2$** has been previously mentioned by Miller *et al.* [92] and the instability of the related bis(phosphinite) species, (POC$_{sp2}$OP)Ni(O^{t}Bu)and (POC$_{sp3}$OP)Ni(O^{t}Bu) (Figure 3), disclosed by Zargarian *et al.* [89] was discussed above.

To probe the proposed potential of *tert*-butoxy complexes to convert to the nickel hydride akin to (^{iPr}POCN^{Me2})NiH (**12-Me$_2$**) under hydroboration reaction conditions, complex **13-Me$_2$** was generated *in situ* on NMR scale by reaction of the bromide **8-Me$_2$** with KO^{t}Bu in C_6D_6 and treated with one equivalent of HBPin at room temperature (Scheme 34). Immediate change of the color of the reaction mixture from yellow to brown and shortly to dark brown was observed, and the reaction mixture was checked with ^{1}H and ^{31}P{^{1}H}-NMR analysis, showing formation of a new compound having two mutually coupled non-equivalent hydride resonances at δ_H = -10.01 ppm (doublet of triplets, J = 91.3 Hz and 21.8 Hz) and δ_H = -12.08 ppm (multiplet), also coupled to two phosphorus nuclei. On the other hand, the ^{31}P{^{1}H}-NMR spectrum of this new compound revealed only one ^{31}P resonance (singlet) at δ_P = 209.0 ppm. Similar observations were recorded when (^{iPr}POCN$^{Ar'}$)Ni(O^{t}Bu) (**5-Ar'**) was treated with excess HBPin (5 equivalents) to give a hydride species, characterized by the hydride resonances at δ_H = -8.96 ppm (doublet of triplets, 96.3 Hz and 22.6 Hz) and δ_H = -14.02 ppm (multiplet), coupled to the ^{31}P resonance at δ_P = 210.3 ppm. These NMR features suggest formation of a hydride bridged dimeric nickel species akin to [(^{iPr}POCN$^{Ar'}$)Ni(μ-H)]$_2$ (**14-Ar'**) and [(^{iPr}POCN^{Me2})Ni(μ-H)]$_2$ (**14-Me$_2$**), which can form from the corresponding monomeric hydride intermediates (^{iPr}POCN$^{Ar'}$)NiH (**2-Ar'**) and (^{iPr}POCN^{Me2})NiH (**12-Me$_2$**; Scheme 34). Such inequivalence of the bridging hydrides in **14-Ar'** and **14-Me$_2$** could be rationalized by slightly twisted [(^{iPr}POCN)Ni] fragments in these complexes (see Figure 2 below), reducing the symmetry of the system. Similar dimerization is often considered as a

pathway for liberation of H_2 upon decomposition of nickel(II) hydride complexes. And indeed, leaving the C_6D_6 solutions of either **14-Ar'** and **14-Me$_2$** at room temperature for 15 minutes results in its complete decomposition to a mixture of unidentified products accompanied by the release of H_2 gas (determined by ^{1}H-NMR, δ_H = 4.47 ppm in C_6D_6 [93]).

Scheme 34. Reaction of the *tert*-butoxy complexes **5-Ar'** and **13-Me$_2$** with HBPin.

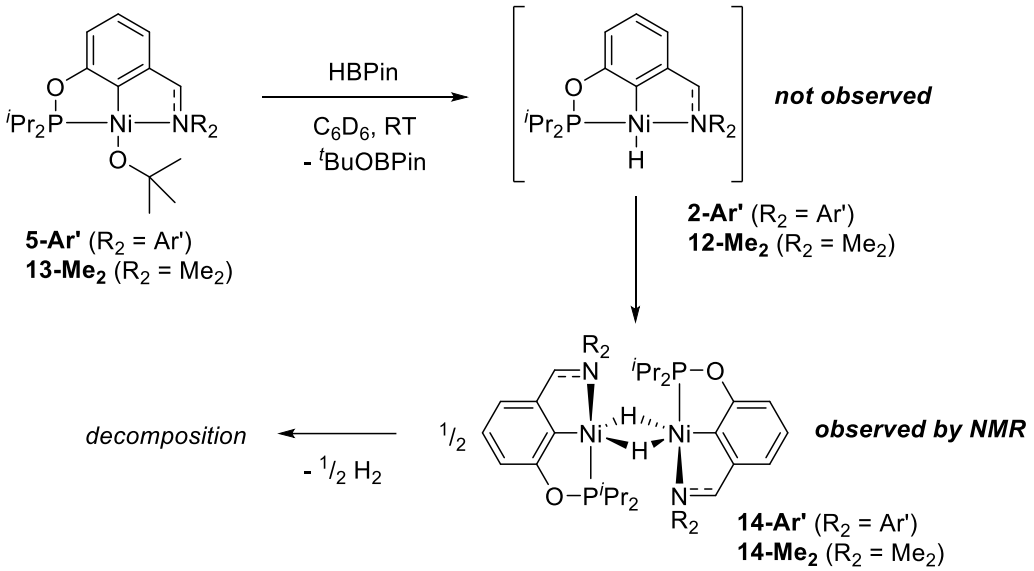

In contrast to dimethyl derivative, higher stability of the monomeric hydride species was observed with ^{iPr}POCN^{iPr2} ligand, presumably due to the enhanced steric hindrance of the diisopripylamino side-arm. Thus, room temperature treatment of (^{iPr}POCN^{iPr2})NiBr (**8-*i*Pr$_2$**) with one equivalent of $LiBHEt_3$ in toluene results in slow (64% in 19 hours by ^{31}P{^{1}H}-NMR) but exclusive formation of the monomeric hydride complex (^{iPr}POCN^{iPr2})NiH (**15-*i*Pr$_2$**) (Scheme 35). Compared to the starting bromide **8-*i*Pr$_2$**, the aminophosphinite ligand of **15-*i*Pr$_2$** gives rise to a down-field ^{31}P resonance (δ_P = 202.2 ppm *vs.* δ_P = 191.0 ppm for **8-*i*Pr$_2$** in PhMe) in the ^{31}P{^{1}H}-NMR spectrum. The presence of the hydride in **15-*i*Pr$_2$** is evident from the ^{1}H-NMR spectrum showing a characteristic up-field hydride resonance at δ_P = -11.67 ppm (doublet), coupled to the phosphorus with ^2J = 81.0 Hz. The complex proved stable at room temperature in solution and no decomposition to the dimeric species akin to **14-Me$_2$** in Scheme 11 and further H_2 evolution were observed by NMR within a few days. However, all attempts to fully convert (^{iPr}POCN^{iPr2})NiBr (**8-*i*Pr$_2$**) to the hydride product **15-*i*Pr$_2$** were unsuccessful resulting in difficult-to-separate mixtures of **15-*i*Pr$_2$** and the starting bromide **8-*i*Pr$_2$**. This precluded the isolation of **15-*i*Pr$_2$** in analytically pure form.

By analogy with the iminophosphinite complexes, the bromide **8-Me$_2$** was also treated with $LiBH_4$ in toluene to afford the borohydride derivative (^{iPr}POCN^{Me2})Ni(η^2-BH_4) (**16-Me$_2$**; Scheme 36) in 77% yield. The product was fully characterized, including X-Ray diffraction analysis. The

molecular structure of **16-Me2** is depicted in Figure 4. The selected bond distances and angles are shown in Table 3 and crystallographic parameters for **16-Me2** are summarized Materials and Methods section of this thesis. Similarly to **6-Ar** [64], the presence of the η^2-coordinated borohydride ligand in **16-Me2** is evident from the observation of two broad hydride resonances at δ_H = -0.49 ppm (broad doublet with J = 76.1 Hz) and δ_H = -0.82 ppm (broad doublet with J = 78.3

Scheme 35. Reaction of (^{iPr}POCN^{iPr2})NiBr (**8-*i*Pr2**) with excess LiBHEt$_3$.

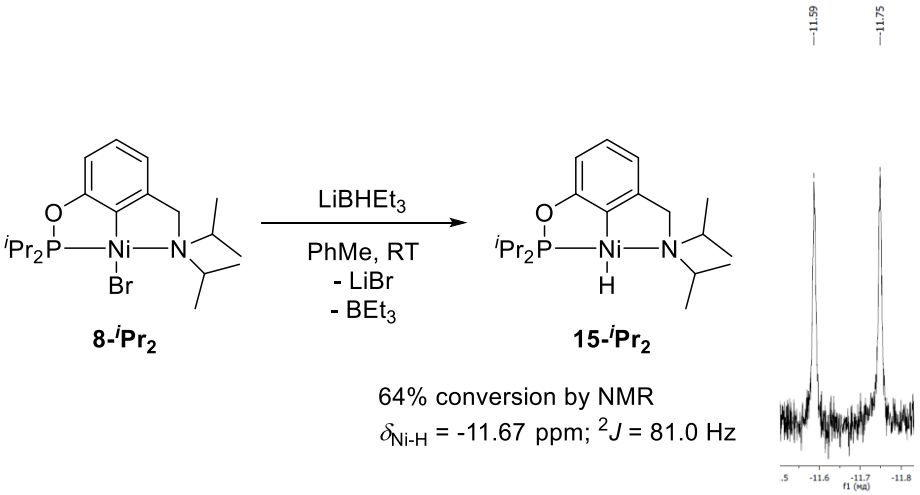

Hz) in its ^{1}H-NMR spectrum and a broad resonance at δ_B = -36.5 ppm in its ^{11}B{^{1}H}-NMR spectrum. The molecular structure of **16-Me2** also shows the η^2-coordination of the borohydride ligand (Figure 4). Single crystals of **16-Me2** suitable for X-ray diffraction analysis were obtained by crystallization from Et_2O solution at -28 °C. These crystals turned out to be co-crystals of **16-Me2** and the bromide complex **8-Me2**. The refinement of Br and BH_4 occupancies led to the non-integer number for B, Br and H of the BH_4 ligand (Figure 4A). Therefore, The Ni-C9 and Ni-B1 bond distances should be discussed with caution. Nonetheless, it is evident that the structure of **16-Me2** adopts a square-planar geometry, similar to the previously reported iminophosphinite derivative (^{iPr}POCN^{Ar})Ni(η^2-BH$_4$) (**6-Ar**) [64]. It is noteworthy, that compared to previously reported structurally characterized iminophosphinite pincer complexes [64], the planarity of the [(^{iPr}POCN^{Me2})Ni] fragment is distorted (Figure 4B) due to the absence of conjugation in the aminophosphinite ligand.

Using similar strategy for substitution of the bromide ligand in (^{iPr}POCN^{Me2})NiBr (**8-Me2**) we have prepared a series of other aminophosphinite pincer nickel(II) complexes containing Ni-O bonds prone to reactions with HBPin to generate the nickel-hydride species under the catalytic hydroboration conditions. Thus, salt metathesis reactions between **8-Me2** and AgOAc in THF, AgOTf in toluene and $AgNO_3$ in THF afforded the respective (^{iPr}POCN^{Me2})Ni(OAc) (**17-Me2**), (^{iPr}POCN^{Me2})Ni(OTf) (**18-Me2**) and (^{iPr}POCN^{Me2})Ni(ONO$_2$) (**19-Me2**) complexes (Scheme 37). The rates of the reactions varied significantly depending on the solubility of the silver salts. In

particular, due to low solubility of $AgNO_3$ in THF compared to AgOAc and AgOTf, the reaction of **8-Me$_2$** with former salt required 4 days of intensive stirring at room temperature. In contrast,

Scheme 36. Preparation of (^{iPr}POCN^{Me2})Ni(η^2-BH_4) (**16-Me$_2$**).

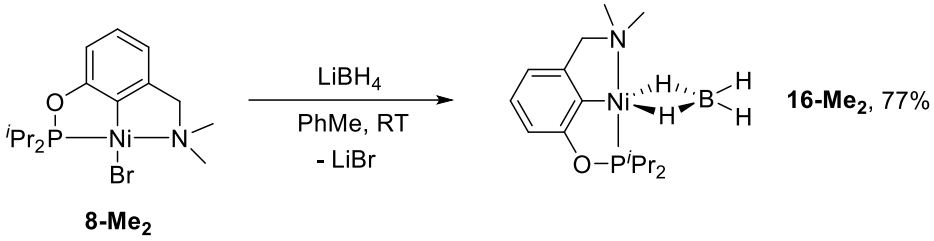

Figure 4. Molecular structure of (^{iPr}POCN^{Me2})Ni(η^2-BH_4) (**16-Me$_2$**) co-crystallized with (^{iPr}POCN^{Me2})NiBr (**8-Me$_2$**); thermal ellipsoids are drawn at the 50% probability level): (A) general view illustrating the superposition of B1 and Br1. (hydrogen atoms except for the BH_4^- are omitted for clarity); (B) front view showing non-planarity of [(^{iPr}POCN^{Me2})Ni] fragment (all hydrogen atoms are omitted for clarity).

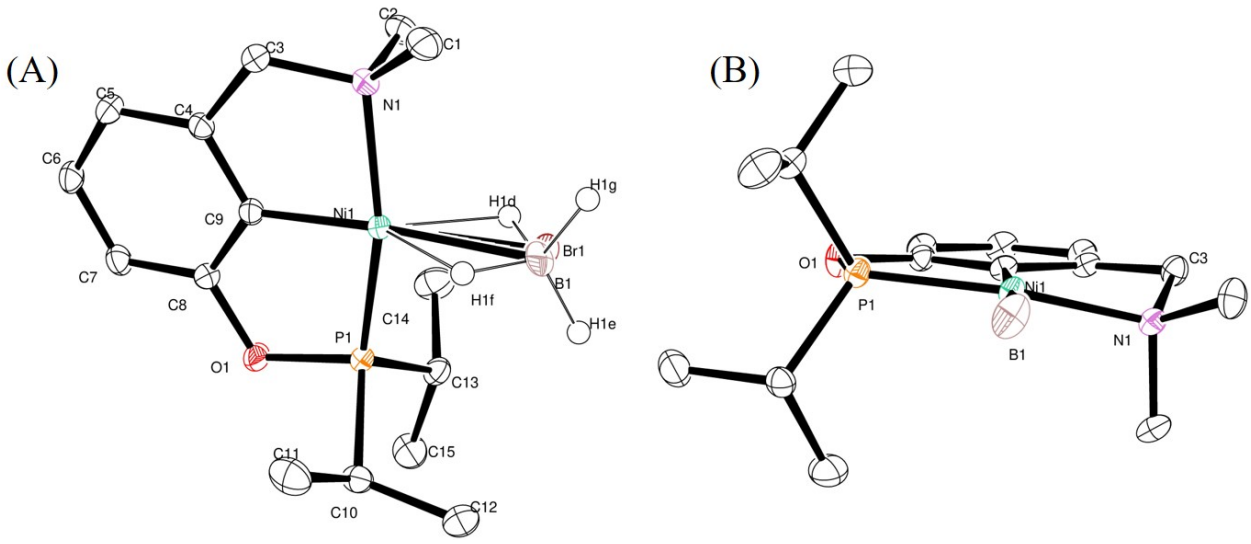

Table 3. Selected bond distances (Å) and bond angles (°) for (^{iPr}POCN^{Me2})Ni(η^2-BH_4) (**16-Me$_2$**).

Bond distances (Å)		**Bond angles (°)**	
Ni1-C9	1.8669(14)	C9-Ni1-B1	175.8(4)
Ni1-P1	2.1250(5)	C9-Ni1-N1	83.49(6)
Ni1-N1	2.0220(13)	C9-Ni1-P1	81.34(5)
Ni1-B1	2.270(10)	N1-Ni1-P1	162.74(4)
N1-C3	1.5018(18)	N1-Ni1-B1	100.5(3)
P1-O1	1.6642(11)	P1-Ni1-B1	94.8(3)

full conversions to **17-Me2** and **18-Me2** upon treatment of **8-Me2** with AgOAc and AgOTf in THF were observed within 24 hours. Compounds **17-19** were found to be thermally stable, were isolated in good yields (71-84%) and were fully characterized by multinuclear NMR and elemental analysis. The ^{1}H, $^{13}C\{^{1}H\}$ and $^{31}P\{^{1}H\}$-NMR features of all these complexes are very similar to each other and to other previously discussed aminophosphinite Ni(II) complexes, implying the similarity of the structures of these compounds. In addition, the acetate ligand in **17-Me2** gives rise to characteristic ^{1}H resonance for the acetate methyl group and ^{13}C resonance for the carbonyl carbon at δ_H = 2.10 ppm and δ_C = 175.4 ppm in its ^{1}H and $^{13}C\{^{1}H\}$-NMR spectra, respectively. For the triflate derivative **18-Me2**, the presence of the nickel-bound OTf ligand is supported by the observation of a ^{19}F resonance at δ_H = -77.58 ppm in its ^{19}F-NMR spectrum. Compared to the parent nickel bromide **8-Me2** (δ_P = 201.2 ppm) and consistent with the other substituted aminophosphinite pincer complexes of Ni(II), compounds **17-19** show an up-field ^{31}P resonance at δ_H = 192.7 ppm, δ_H = 199.6 ppm and δ_C = 195.5 ppm, respectively.

Scheme 37. Reactions of ($^{iPr}POCN^{Me2}$)NiBr (**8-Me2**) with AgX (X = OAc, OTf, NO_3) and NaSPh.

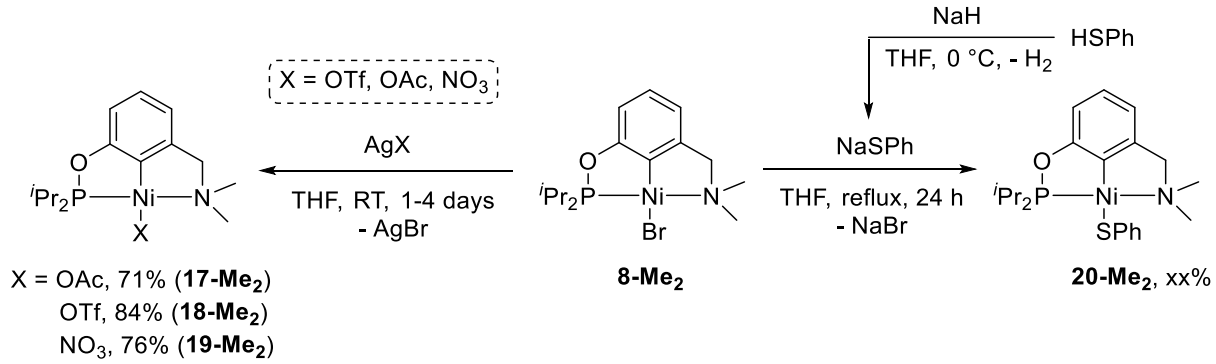

To compare the catalytic hydroboration activity of aminophosphinite complexes with oxo-substituents at the nickel center with those having thiolate ligands, the bromide complex **8-Me2** was treated with NaSPh, which was *in situ* prepared from HSPh by reaction with NaH (Scheme 37). An analogous procedure was previously reported by Zhang and Chen an co-workers for the synthesis of the related bis(phosphinite) nickel complexes ($POC_{sp2}OP$)Ni(SR) (where R = CH_2Ph, Ph, C_6H_4-*p*-OCH_3, C_6H_4-*p*-CH_3, C_6H_4-*p*-CF_3) [94]. The reaction was performed in refluxing THF for 24 hours using 5 equivalents of NaSPh and resulted in ($^{iPr}POCN^{Me2}$)Ni(SPh) (**20-Me2**) in 83% isolated yield. Compound **20-Me2** was found to be thermally stable and was fully characterized by multinuclear NMR spectroscopy, showing structural similarities with the oxo-derivatives **17-19**.

3.3 Comparative study of catalytic activities of imino- and aminophosphinite Ni(II) complexes in deoxygenative hydroboration of carboxamides

Having a series of the iminophosphinite and aminophosphinite Ni(II) complexes in hands, we then performed comparative studies of their catalytic activity in deoxygenative hydroboration of carboxamides to the corresponding amines. Considering the previously reported examples of **3-Ar**-catalyzed hydroboration of DMF, N-phenylpropanamide and acetamide [64], 5 mol% of a nickel complexes was chosen as an optimal pre-catalyst loading for test reactions. Since primary carboxamides are considered as the most challenging substrates for deoxygenative reduction reactions, and the catalytic systems for mild hydroborative conversion of primary amides to the corresponding primary amines are underdeveloped, we mostly focused our studies on deoxygenative hydroboration of benzamide as a model substrate (Scheme 38). The reactions were performed with excess HBPin (5 equivalents to benzamide) under argon atmosphere on NMR scale in C_6D_6 using NMR tubes equipped with Teflon valves and were monitored by ^{1}H-NMR spectroscopy. Under these conditions, $PhC(O)NH_2$ was converted to *N,N*-bis(pinacolboryl)benzylamine, $PhCH_2N(BPin)_2$, with release of an equivalent of $(PinB)_2O$ as a by-product. Vigorous hydrogen gas evolution was observed immediately after initiation of the reactions and the H_2 pressure built up in the system had to be released at the beginning of the reaction. No vigorous hydrogen gas release was detected again later during the course of the reaction. The conversions of benzamide were determined by integration of ^{1}H-NMR spectra using 1,3,5-trimethoxybenzene as internal standard. The results of these catalytic trials are summarized in Table 4.

Scheme 38. Deoxygenative hydroboration of benzamide with HBPin catalyzed by POCN complexes of Ni(II).

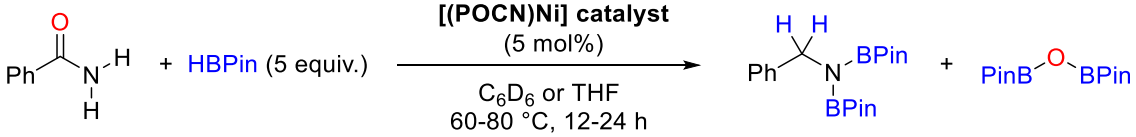

First, we tested the catalytic activity of the (trimethylsilyl)methyl derivative **4-Ar** in deoxygenative hydroboration of $PhC(O)NH_2$ (Table 4, entry 1). At 5 mol% loading, the complex turned out to be less active compared to the previously reported methyl derivative **3-Ar** and showed 52% conversion of benzamide to $PhCH_2N(BPin)_2$ within 24 hours at 60 °C (although, **3-Ar**-catalyzed hydroboration of benzamide was not previously attempted, **3-Ar** showed full conversion of both acetamide and *N*-phenylpropanamide after 24 hours at 60 °C [64]). Increasing

the temperature of the reaction to 80 °C did not result in the improved yield of the amine product. An analogous reaction of the borohydride derivative (^{iPr}POCN^{Ar})Ni(η^2-BH_4) (**6-Ar**) resulted in almost the same conversion of $PhC(O)NH_2$ to $PhCH_2N(BPin)_2$ (55% in 24 h at 80 °C; Table 4, entry 2). Slightly increased yield of *N*,*N*-bis(pinacolboryl)benzylamine (66%) was observed when the reaction with **6-Ar** was performed at 110 °C for 24 hours. In contrast, better conversion of

Table 4. Catalytic deoxygenative hydroboration of benzamide with HBPin using 5 mol% of imino- and aminophosphinite ^{iPr}POCN pincer complexes of Ni(II) as pre-catalysts.[a]

Entry	Pre-catalyst system	Solvent	T, °C	Time, h	Yield, %[b]
1	(^{iPr}POCN^{Ar})Ni(CH_2TMS) (**4-Ar**)	C_6D_6	60	24	52
			80	24	52
2	(^{iPr}POCN^{Ar})Ni(η^2-BH_4) (**6-Ar**)[c]	C_6D_6	80	24	55
			110	24	66
3	(^{iPr}POCN^{Ar})Ni(η^1-BF_4) (**7-Ar**)	C_6D_6	110	24	84
4	(^{iPr}POCN$^{Ar'}$)Ni(CH_2TMS) (**4-Ar'**)	C_6D_6	80	24	>99
				12	>99
5	(^{iPr}POCN^{Me2})NiMe (**9-Me$_2$**)	C_6D_6	80	24	63
6	(^{iPr}POCN^{Me2})Ni(O^{t}Bu) (**13-Me$_2$**)	C_6D_6	80	24	85
	via (^{iPr}POCN^{Me2})NiBr (**8-Me$_2$**) + KO^{t}Bu	THF	80	24	63
7	(^{iPr}POCN^{Et2})Ni(O^{t}Bu) (**13-Et$_2$**) *via* (^{iPr}POCN^{Et2})NiBr (**8-Et$_2$**) + KO^{t}Bu	THF	80	24	66
8	(^{iPr}POCN^{Me2})Ni(η^2-BH_4) (**16-Me$_2$**)[d]	C_6D_6	80	24	62
9	(^{iPr}POCN^{Me2})Ni(OAc) (**17-Me$_2$**)	C_6D_6	80	24	41
10	(^{iPr}POCN^{Me2})Ni(OTf) (**18-Me$_2$**)	C_6D_6	80	24	13
11	(^{iPr}POCN^{Me2})Ni(ONO_2) (**19-Me$_2$**)	C_6D_6	80	24	44
12	(^{iPr}POCN^{Me2})Ni(SPh) (**20-Me$_2$**)	C_6D_6	80	24	13

[a]C(benzamide) = 0.21 mol/L. [b]Calculated by integration of ^{1}H-NMR spectra using 1,3,5-trimethoxybenzene (0.2 equivalents to benzamide) as internal standard. [c]47% conversion to $EtN(BPin)_2$ was observed for **6-Ar**-catalyzed hydroboration of acetamide in C_6D_6 for 24 hours at 80 °C. [d]76% conversion to $EtN(BPin)_2$ was observed for 1**6-Me$_2$**-catalyzed hydroboration of acetamide in C_6D_6 for 24 hours at 80 °C.

benzamide (84% in 24 hours) was detected for (^{iPr}POCN^{Ar})Ni(η^1-BF_4) (**7-Ar**) but the reaction required rather high temperature of 110 °C (Table 4, entry 3). The borohydride complex **6-Ar** was also tested in hydroboration of acetamide but, surprisingly, compared to benzamide, showed lower conversion to N,N-diborylethylamine (47% in 24 hours at 80 °C).

The observed lower catalytic activity of (^{iPr}POCN^{Ar})Ni(CH_2TMS) (**4-Ar**) *vs.* (^{iPr}POCN^{Ar})NiMe (**3-Ar**) is likely explained by the presence of more sterically demanding (trimethylsilyl)methyl ligand in **4-Ar**. Considering that decreasing the steric hindrance of the Ni-bound alkyl ligand leads to the decreased thermal stability of the alkyl complexes (**3-Ar** was found to be less stable compared to **4-Ar**), we thought that decreasing the steric hindrance in the imine side-arm of the ligand (i.e. switching from ^{iPr}POCN^{Ar} to ^{iPr}POCN$^{Ar'}$) but keeping the CH_2TMS group at nickel will lead to an increased catalytic activity of the system while maintaining the necessary thermal stability of the complex. Indeed, hydroboration of benzamide with HBPin using 5 mol% of the 2,6-dimethyl-substituted iminophosphinite derivative (^{iPr}POCN$^{Ar'}$)Ni(CH_2TMS) (**4-Ar'**) proved more efficient and showed complete conversion of $PhC(O)NH_2$ to $PhCH_2N(BPin)_2$ at 80 °C within 24 and even 12 hours (Table 4, entry 4). However, as discussed above, the pre-catalyst **4-Ar'** can not be obtained in the analytically pure form (in the best case, the complex was formed in 71% purity by $^{31}P\{^1H\}$-NMR), what somewhat questions its use for further catalytic studies.

To address the issues of the pre-catalyst stability and reproducibility we then turned to investigation of catalytic activities of the related aminophosphinite derivatives, which in many cases showed greater thermal stability compared to analogous iminophosphinite complexes. Disappointingly, deoxygenative hydroboration of benzamide catalyzed by (^{iPr}POCN^{Me})NiMe (**9-Me$_2$**) turned out to be more sluggish than for the iminophosphinite methyl complex **3-Ar** [64] and somewhat similar to the iminophosphinite (trimethylsilyl)methyl complex **4-Ar** (Table 4, entry 1) and showed 63% NMR conversion of $PhC(O)NH_2$ in 24 hours 80 °C (Table 4, entry 5). In contrast, fast pre-catalyst activation and significantly more efficient hydroboration of $PhC(O)NH_2$ was observed for the *tert*-butoxy derivative (^{iPr}POCN^{Me2})Ni(O^{t}Bu) (**13-Me$_2$**), which was generated *in situ* from (^{iPr}POCN^{Me2})NiBr (**8-Me$_2$**) and KO^{t}Bu prior to catalysis. Using 5 mol% of pre-formed **13-Me$_2$** in C_6D_6 showed 85% conversion of benzamide at 80 °C within 24 hours, whereas an analogous reaction at 60 °C resulted in 77% yield of $PhCH_2N(BPin)_2$ (Table 4, entry 6). Interestingly, switching from C_6D_6 to THF revealed lower activity of **13-Me$_2$** resulting in only 63% of *N,N*-bis(pinacolboryl)benzylamine after 24 hours at 80 °C. Somewhat similar results were obtained for hydroboration of $PhC(O)NH_2$ using pre-formed (^{iPr}POCN^{Et2})Ni(O^{t}Bu) (**13-Et$_2$**; Table 4, entry 7).

Further screening of the aminophosphinite nickel pre-catalysts in hydroboration of benzamide with HBPin using (^{iPr}POCN^{Me2})Ni(η^2-BH$_4$) (**16-Me$_2$**), (^{iPr}POCN^{Me2})Ni(OAc) (**17-Me$_2$**), (^{iPr}POCN^{Me2})Ni(OTf) (**18-Me$_2$**), (^{iPr}POCN^{Me2})Ni(ONO$_2$) (**19-Me$_2$**) and (^{iPr}POCN^{Me2})Ni(SPh) (**20-Me$_2$**) did not reveal any starling improvements in conversions of PhC(O)NH$_2$, and for these systems the yields of the hydroboration products after 24 hours at 80 °C were found in the range of 13-62% (Table 4, entries 8-12).

In contrast to primary amides, catalytic deoxygenative hydroboration of secondary amides was found to proceed more efficiently resulting in formation of secondary N-borylamines. So far, we have tested only (^{iPr}POCN^{Ar})Ni(CH$_2$TMS) (**4-Ar**) as a pre-catalysts for deoxygenative addition of HBPin to *N*-methylbenzamide and *N*-phenylpropanamide, but both secondary amides showed good conversions (71-98%) to the corresponding N-borylated secondary amines (Scheme 39). In contrast, no or very low catalytic activity of **4-Ar** were detected in deoxygenative hydroboration of tertiary amides, such as *N*,*N*-dimethylbenzamide and *N*,*N*-dibenzylacetamide (Scheme 40).

Scheme 39. Deoxygenative hydroboration of *N*-methylbenzamide and *N*-phenylpropanamide with HBPin catalyzed by (^{iPr}POCN^{Ar})Ni(CH$_2$TMS) (**4-Ar**). Conditions: C(amide) = 0.21 mol/L; yields are determined by integration of ^{1}H-NMR spectra using 1,3,5-trimethoxybenzene (0.2 equivalents to amide substrate) as internal standard.

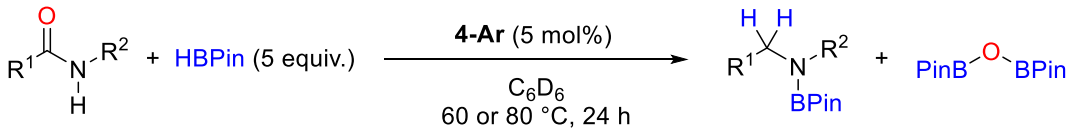

R^1 = Ph, R^2 = Me: 60 °C, 71% yield
R^1 = Et, R^2 = Ph: 80 °C, 98% yield

Scheme 40. Deoxygenative hydroboration of *N*,*N*-dimethylbenzamide and *N*,*N*-dibenzylacetamide with HBPin catalyzed by (^{iPr}POCN^{Ar})Ni(CH$_2$TMS) (**4-Ar**). Conditions: C(amide) = 0.21 mol/L; yields are determined by integration of ^{1}H-NMR spectra using 1,3,5-trimethoxybenzene (0.2 equivalents to amide substrate) as internal standard.

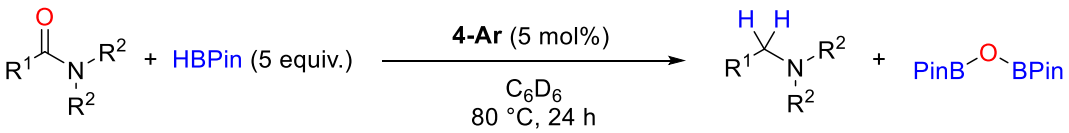

R^1 = Ph, R^2 = Me: 13% yield
R^1 = Me, R^2 = CH$_2$Ph: no reaction

Notably, such lack of reactivity of tertiary amide substrates contradicts the generally accepted trend for deoxygenative reduction of carboxamides (tertiary > secondary > primary) [9]. As has been already discussed in the literature review of this thesis, typically tertiary amides are

easier to reduce compared with the secondary and tertiary ones, whereas the reduction of the primary amides is the most challenging among all others [9]. One can suggest, that compared to the secondary and primary substrates, tertiary amides possess more steric crowding around the carbonyl function, leading to unfavorable steric repulsions between the amides and rather bulky iminophosphinite ^{iPr}POCN^{Ar} and ^{iPr}POCN$^{Ar'}$ ligands. On the other hand, the difference in reactivity of tertiary *vs.* secondary and primary amides could be rationalized based on the different reaction pathways for these substrates. The mechanistic aspects of deoxygenative hydroboration of carboxamides catalyzed by the imino- and amino-phosphinite pincer complexes complexes of Ni(II) are discussed in the next chapter of this thesis.

3.4 Mechanistic aspects of Ni-catalyzed deoxygenative hydroboration reactions

To shed some light on the mechanism of deoxygenative hydroboration of carboxamides by imino- and aminophosphinite complexes of Ni(II) we performed a number of control experiments. First, benzamide was treated with 5 equivalents of HBPin in C_6D_6 in the absence of nickel pre-catalysts. The reaction was monitored by ^{1}H-NMR showing release of H_2 gas (δ_H = 4.47 ppm in C_6D_6) and full conversion of $PhC(O)NH_2$ after 20 hours at room temperature. Formation of three major products was observed, which based on their NMR features were tentatively assigned to PhC(O)N(H)BPin (64%), an *O*-addict $PhC(O)NH_2$•HBPin (26%) [85] and PhC(H)=NBPin (9%) (Scheme 41). Trace amounts of the final deoxygentive hydroboration product $PhCH_2N(BPin)_2$ (<1%) were also observed in the ^{1}H-NMR spectrum. Repeating the reaction at 80 °C for 24 hours also resulted in complete conversion of benzamide and formation of a mixture of PhC(O)N(H)BPin (88%), PhC(H)=NBPin (11%) and $PhCH_2N(BPin)_2$ (<1%). Interestingly, the same mixture with approximately the same product distribution was observed when the reaction was performed for 1 hour at 80 °C. This suggests a fast pre-activation of benzamide to form N-borylbenzamide, which compared to benzamide itself possess higher electrophilic character of the carbonyl group allowing for easier addition of HBPin across C=O bond.

Formation of a similar N-borylamide species $CH_3C(O)N(CH_3)BPin$ has been previously

Scheme 41. Reactivity of $PhC(O)NH_2$ with excess HBPin in the absence of Ni(II) pre-catalysts.

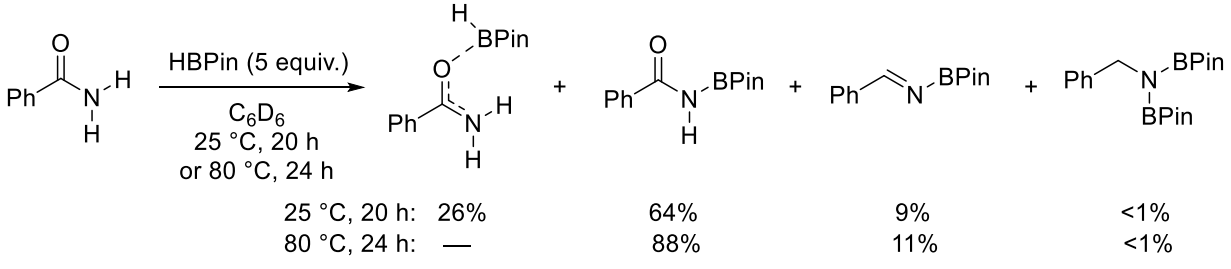

reported by Eisen *et al.* upon reaction of *N*-methylacetamide with HBPin [85]. In contrast, our studies have indicated no reaction between *N*-phenylbenzamide and excess HBPin (5 equivalents) within 24 hours at both room temperature and 80 °C.

Scheme 42. Nickel catalyst activation during hydroboration reactions.

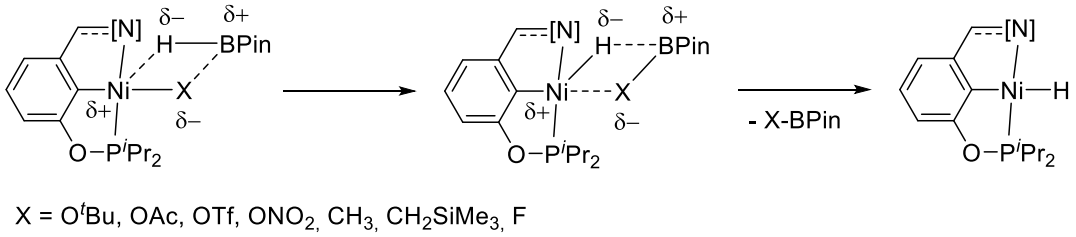

X = O^{t}Bu, OAc, OTf, ONO_2, CH_3, CH_2SiMe_3, F

On the other hand, we have previously discussed that the reaction of Ni-O^{t}Bu complexes with HBPin efficiently generates the Ni(II) hydride species akin to (POCN)NiH, which are known to undergo migratory insertions of C=O bonds of carbonyl compounds into the Ni-H bond to form the alkoxy intermediates [64]. Similar formation of a nickel hydride can be suggested to occur *via* metathesis of HBPin with other *O*-substituted nickel pre-catalysts as well as with nickel alkyl complexes (Scheme 42). Based on these experimental findings and previous literature precedents on reduction of carboxamides to amines we propose the mechanism for deoxygenative hydroboration of benzamide depicted in Scheme 43. The reaction is initiated by HBPin, which activates both the nickel catalyst forming the nickel hydride species **A** and the amide to give N-borylbenzamide **B**. Due to the presence of a Lewis acidic boryl substituent at nitrogen and hence the increased electrophilic character of the carbonyl moiety, **B** can undergo a migratory insertion into the Ni-H bond of the hydride complex **A** to give and intermediate **C**, which in turn reacts with another molecule with HBPin to recover the nickel hydride species **A** and produce O-borylated hemiaminal **D**. Decomposition of the latter species *via* release of either PinBOH or $(PinB)_2O$ yields the imine intermediates **E** and **F** (**E** can be converted to **F** in the presence of HBPin). Similarly to N-borylbenzamide **B**, N-borylated phenylmethanimine **F** undergoes insertion into the Ni-H bond of **A** to give an amide complex **G**. Following σ-bond metathesis with HBPin regenerates the hydride catalyst and affords the final product, *N*,*N*-bis(pinacolboryl)benzylamine.

An analogous mechanism that proceeds through formation of an imine $R^1C(H)=NR^2$ can be proposed for Ni-catalyzed deoxygenative hydroboration of secondary amides (Scheme 44). However, in this case, as suggested based on the control experiments between *N*-phenylbenzamide and HBPin indicated above, no pre-activation of the amide substrates by HBPin forming secondary N-borylamides takes place. Nonetheless, the reaction should follow the pathways similar to those for primary amides, involving migratory insertion of the carbonyl moiety into the Ni-H bond,

Scheme 43. Proposed mechanism for deoxygenative hydroboration of benzamide with HBpin catalyzed by imino- and aminophosphinite complexes of Ni(II).

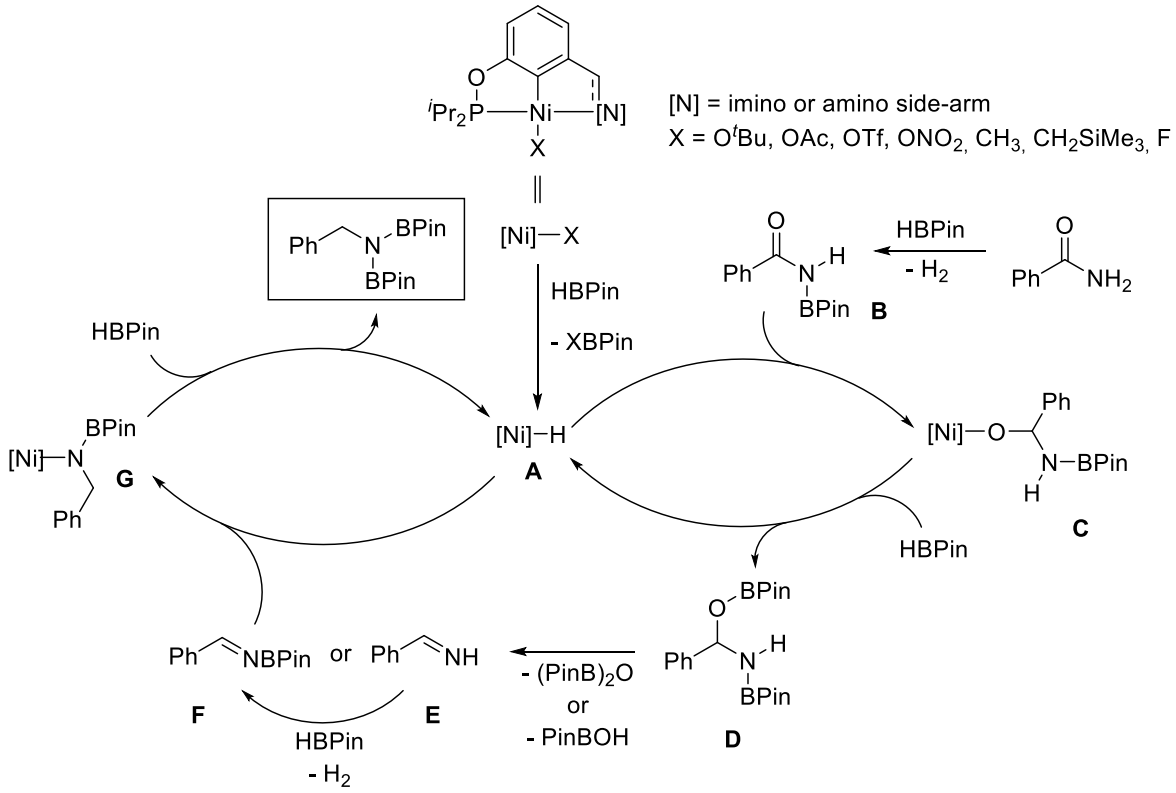

Scheme 44. Proposed mechanism for deoxygenative hydroboration of secondary amides with HBpin catalyzed by imino- and aminophosphinite complexes of Ni(II).

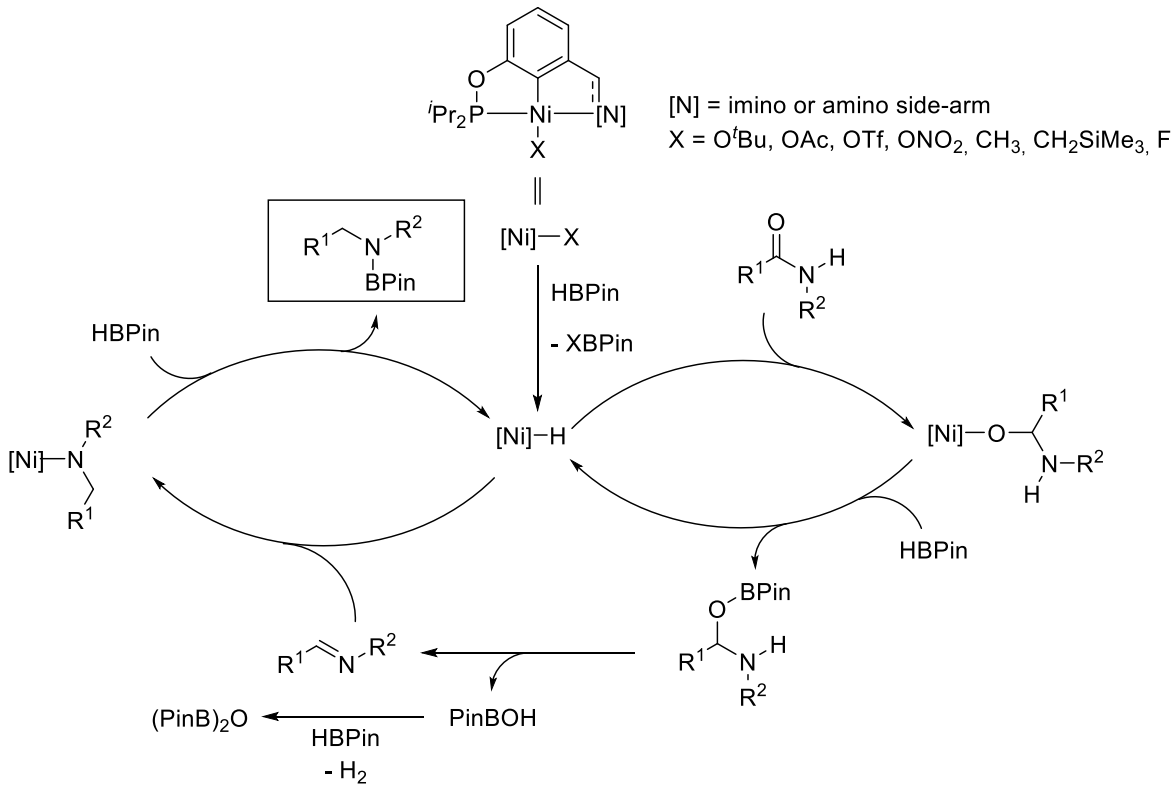

followed by reaction with HBPin and generation of the imine species. The latter intermediate undergoes another cycle of insertion and σ-bond metathesis reactions to recover the hydride catalyst and generate the secondary *N*-borylamine product (Scheme 44).

For tertiary carboxamides, the insertion of an amide substrate into the Ni-H bond of catalytic hydride species, followed by metathesis with HBPin would generate a tertiary O-borylated hemiaminal $R^1C(H)(OBPin)NR^2R^3$ **H** (Scheme 45), which could potentially give the iminium intermediate $[R^1C(H)=NR^2R^3][OBPin]$ (**I**) [83]. However, formation of this latter species in such non-polar solvents as benzene or toluene would be unfavorable compared to the neutral imine intermediates generated during deoxygenative hydroboration of primary and secondary carboxamides. This correlates well with the observed low activity of the prepared iminophosphinite and aminophosphinite nickel complexes in the reactions with tertiary amides (see Scheme 40).

Scheme 45. Proposed mechanism for deoxygenative hydroboration of tertiary amides with HBpin catalyzed by imino- and aminophosphinite complexes of Ni(II).

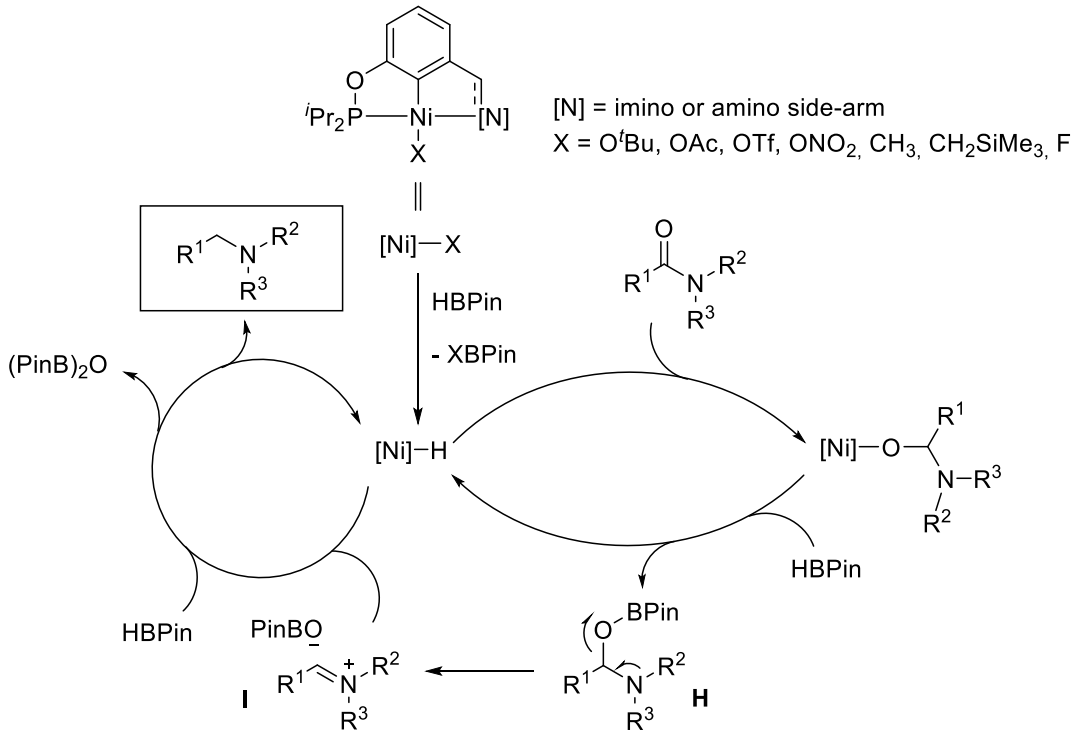

4 Materials and Methods

4.1 Materials

3-hydroxybenzaldehyde, 2,6-diisopropylaniline, 2,6-dimethylaniline, dimethylammonium chloride, $HNEt_2$, NEt_3, HN^iPr_2, $NaBH_4$, $NaHB(OAc)_3$, $NaHCO_3$, Ni powder, Br_2, $LiBHEt_3$ (1.0 M in THF), L-Selectride (lithium tri-*sec*-butylborohydride; 1.0 M in THF), MeLi (1.6 M in Et_2O), $LiCH_2SiMe_3$ (1.0 M in pentane), KO^tBu, $LiBH_4$ (2.0 M in THF), $AgBF_4$, EtMgBr (3.0 M in Et_2O), AgOAc, AgOTf, $AgNO_3$, NaH, HSPh, benzamide, *N*,*N*-dimethylbenzamide, *N*,*N*-dibenzylacetamide, *N*-methylbenzamide, *N*-phenylbenzamide *N*-phenylpropanamide, HBPin, 1,3,5-trimethoxybenzene, anhydrous $MgSO_4$, anhydrous Na_2SO_4, concentrated HCl, aqueous ammonia were purchased from Sigma Aldrich and used without further purification. All protonated and deuterated solvents (toluene, THF, hexane, Et_2O, CH_3CN, C_6D_6 and toluene-d_8) were dried either by distillation from appropriate drying agents or using LC Technology Solutions Inc. SPBT103 benchtop solvent purification system. MeOH and EtOH were dried with 4 Å molecular sieves.

4.2 Equipment

All manipulations were done using standard inert atmosphere LC Technologies single station glovebox and Schlenk techniques. Schlenk glassware was used for reactions that includes substances sensitive to oxygen and/or moisture. NMR analysis was performed using JNM-ECA 500 MHz (Nazarbayev University) and Bruker Avance 300 MHz (Brock University) spectrometers (^{1}H: 500 MHz and 300 MHz; ^{13}C: 125.8 MHz; ^{31}P: 202.5 MHz and 121 MHz; ^{19}F: 470.6 MHz). The ^{1}H and ^{13}C NMR chemical shifts were referenced to the residual proton and naturally abundant ^{13}C resonances of the deuterated solvents, respectively. ^{31}P and ^{19}F-NMR spectra were referenced to 85% H_3PO_4 and C_6F_6 (δ = -163.0 ppm), respectively. NMR analysis was done at room temperature under argon atmosphere using NMR tube equipped with Teflon valves (J Young NMR tubes). Elemental analysis was performed at Nazarbayev University Core Facilities using either 2400 Series II CHNS/O Elemental Analyzer or CHNS-O Unicube Organic Elemental Analyzer. X-ray analysis was performed at Brock University by Anton Dmitrienko and Prof. Melanie Pilkington with a Bruker APEX-II CCD diffractometer equipped with an Oxford Cryosystems lowt emperature device operating at 150.0(1) K.

4.3 Experimental procedures

4.3.1 Preparation and characterization of alcohol precursors to iminophosphinite POCN pincer ligands

1-(HO)-3-(CH=NAr)-C_6H_4 (Ar = 2,6-^{i}Pr$_2$$C_6H_3$)

To a solution of 3-hydroxybenzaldehyde (5.25 g, 0.043 mol) in EtOH 2,6-diisopropylaniline (2.3 mL, 0.056 mol) was added dropwise. The reaction mixture was refluxed overnight. After the evaporation of the volatiles, the residue was extracted with hexane. The solvent was pumped off and the residue was dried in vacuum to give a product (10.23 g, 85%). ^{1}H-NMR (500 MHz; C_6D_6; δ, ppm): 1.18 (d, $^3J_{H-H}$ = 6.8 Hz, 12H, 4 CH_3, N*Ar*); 3.13 (sept, $^3J_{H-H}$ = 6.8 Hz, 2H, 2 CH, N*Ar*); 4.21 (br s, O*H*); 6.61 (br d, $^3J_{H-H}$ = 8.2 Hz, 1H); 6.98 (t, $^3J_{H-H}$ = 7.8 Hz, 1H); 7.13-7.19 (m, 3H); 7.24 (d, $^3J_{H-H}$ = 7.5 Hz, 1H); 7.26 (s, 1H); 7.95 (s, C*H*=NAr). The spectral data are consistent with those previously published in the literature [64]

1-(HO)-3-(CH=NAr')-C_6H_4 (Ar' = 2,6-$Me_2C_6H_3$)

To a solution of 3-hydroxybenzaldehyde (5.30 g, 0.043 mol) in EtOH 2,6-diisopropylaniline (8.1 mL, 0.065 mol) was added dropwise. The reaction mixture was then refluxed overnight, after which the volatiles were evaporated in vacuum, and the residue was extracted with hexane. The solvent was pumped off, and the product was dried to give a product (7.67 g, 79%).^{1}H-NMR (500 MHz; C_6D_6; δ, ppm): 2.12 (s, 6H, 2 CH_3, N*Ar'*); 4.22 (br s, O*H*); 6.61 (br d, $^3J_{H-H}$ = 8.4 Hz, 1H); 6.98 (m, 2H); 7.04 (m, 2H); 7.19 (d, $^3J_{H-H}$ = 7.6 Hz, 1H); 7.27 (s, 1H); 7.74 (s, C*H*=NAr'). The spectral data are consistent with those previously published in the literature [64]

4.3.2 Preparation and characterization of iminophosphinite POCN pincer ligands

1-(^{i}Pr$_2$PO)-3-(CH=NAr)-C_6H_4 (Ar = 2,6-^{i}Pr$_2$$C_6H_3$)

To a solution of ClP^iPr$_2$ (0.628 mL, 0.004 mmol) in THF was added a solution of 1-(HO)-3-(CH=NAr)-C_6H_4 (1.01 g, 0.0035 mmol) and NEt_3 (1.25 mL, 0.009 mmol) at RT. The resulting mixture was stirring for 10 h, after which the volatiles were evaporated in vacuum and the residue was extracted with toluene. After the evaporation of the volatiles the substance was dried to give an oily product (1.18 g, 83%). ^{1}H-NMR (500 MHz; C_6D_6; δ, ppm): 0.95 (dd, *J* = 7.3 and 15.8 Hz, 6H, 2 CH_3 of ^{i}*Pr*$_2$P); 1.10 (dd, *J* = 6.9 and 10.6 Hz, 6H, 2 CH_3 of ^{i}*Pr*$_2$P); 1.15 (d, $^3J_{H-H}$ = 6.9 Hz, 12H, 4 CH_3 of N*Ar*); 1.74 (m, 2H, 2CH of ^{i}*Pr*$_2$P); 3.12 (sept, $^3J_{H-H}$ = 6.9 Hz, 2H, 2CH of N*Ar*); 7.09 (t, $^3J_{H-H}$ = 7.8 Hz, 1H, C*H*); 7.11-7.18 (m, 3H, C*H*); 7.33 (m, 1H, C*H*); 7.41 (m, 1H, C*H*);

7.99 (s, 1H, C*H*); 8.07 (br s, 1H, C*H*=NAr). $^{31}P\{^{1}H\}$-NMR (202.5 MHz; C_6D_6; δ, ppm): 149.1 (s, O*P*$^{i}Pr_2$). The spectral data are consistent with those previously published in the literature [64]

1-($^{i}Pr_2PO$)-3-(CH=NAr')-C_6H_4 (Ar' = 2,6-$Me_2C_6H_3$)

To a solution of Cl$P^{i}Pr_2$ (2.47 mL, 0.0155 mmol) in THF was added a solution of 1-(HO)-3-(CH=NAr')-C_6H_4 (3.18 g, 0.014 mmol), followed by the addition of NEt_3 (4.92 mL, 0.035 mmol) at room temperature. The resulting mixture was stirring for 10 h. The volatiles were pumped off in vacuum, and the residue was extracted with toluene. The solvent was evaporated, and the compound was dried to yield a product (2.86 g, 60%). ^{1}H-NMR (500 MHz; C_6D_6; δ, ppm): 0.97 (dd, J = 7.2 and 16 Hz, 6H, 2 CH_3 of $^{i}Pr_2$P); 1.12 (dd, J = 6.9 and 10.5 Hz, 6H, 2 CH_3 of $^{i}Pr_2$P); 1.76 (m, 2H, 2CH of $^{i}Pr_2$P); 2.08 (s, 6H, 2 CH_3 of N*Ar'*); 6.95 (m, 1H, C*H*); 7.01 (m, 2H, 2 C*H*); 7.09 (t, $^{3}J_{H\text{-}H}$ = 7.8 Hz, 1H, C*H*); 7.32 (br d, $^{3}J_{H\text{-}H}$ = 8.1 Hz, 1H, C*H*); 7.4 (br d, $^{3}J_{H\text{-}H}$ = 7.5 Hz, 1H, C*H*); 7.76 (s, 1H, C*H*); 8.01 (s, C*H*=NPh). $^{31}P\{^{1}H\}$-NMR (202.5 MHz; C_6D_6; δ, ppm): 149.0 (s, O*P*$^{i}Pr_2$). The spectral data are consistent with those previously published in the literature [64]

4.3.3 Preparation and characterization of iminophosphinite POCN nickel bromide complexes

($^{i\text{-}Pr}POCN^{Ar}$)NiBr (1-Ar)

A solution of the ligand 1-($^{i}Pr_2PO$)-3-(CH=NAr)-C_6H_4 (313.5 mg, 0.793 mmol) in toluene was added to a suspension of [$NiBr_2(CH_3CN)_2$] (310.15 mg, 1.031 mmol) in toluene, followed by the addition of an excess of NEt_3 (0.17 mL, 1.19 mmol) at RT. The resulting reaction mixture was heated for 3h at 110°C, after which the solvent was evaporated in vacuum. The residue was extracted with 80:20 mixture of hexane:toluene, followed by the evaporation of the volatiles. The solid was dissolved in a small amount of Et_2O and put at -25°C for recrystallization and the precipitate that had appeared after several days was collected to give a dark red product (549.2 mg, 69%). ^{1}H-NMR (500 MHz; C_6D_6; δ, ppm): 1.15 (m, 12H, 2 CH_3 of $^{i}Pr_2$P and 2 CH_3 of NAr); 1.40 (dd, J = 7.2 and 17.9 Hz, 6H, 2 CH_3 of $^{i}Pr_2$P); 1.57 (d, J = 6.8 Hz, 6H, 2 CH_3 of NAr); 2.19 (m, 2H, 2CH of $^{i}Pr_2$P); 3.60 (sept, J = 6.8 Hz, 2H, 2 CH of NAr); 6.65 (m, 2H, aromatic CH); 6.76 (t, $^{3}J_{H\text{-}H}$ = 7.7 Hz, 1H, aromatic CH); 7.14 7 (m, 3H, aromatic CH); 7.48 (d, J = 4.0 Hz, 1H, CH=NAr). $^{31}P\{^{1}H\}$-NMR (202.5 MHz; C_6D_6; δ, ppm): 203.1 (s, O$P^{i}Pr_2$). The obtained NMR data are consistent with those previously published in the literature [64].

($^{i\text{-}Pr}POCN^{Ar'}$)NiBr (1-Ar')

To a suspension of [$NiBr_2(CH_3CN)_2$] (407.93 mg, 1.370 mmol) in toluene a solution of the ligand 1-($^{i}Pr_2PO$)-3-(CH=NAr')-C_6H_4 (Ar' = 2,6-$Me_2C_6H_3$) (356.4 mg, 1.044 mmol) in toluene was

added dropwise at room tempearture. The color of the reaction mixture changed immediately from greenish-yellow to dark cherry red. An excess of NEt_3 (0.22 mL, 1.566 mmol) was added dropwise to the reaction mixture followed by the heating the reaction mixture for 3 hours at 110°C. After that toluene was evaporated, and the residue was extracted with a 80:20 mixture of hexane:toluene. The evaporation of the solvent mixture resulted in the appearance of dark red solid. The solid was dissolved in a small amount of Et_2O and put at -25°C for recrystallization and the precipitate that had appeared after several days was collected to give dark red solid (401.7 mg, 80.3%). ^{1}H-NMR (500 MHz; C_6D_6; δ, ppm): 1.14 (dd, *J* = 6.9 and 15.0 Hz, 6H, 2 CH_3 of ^{i}Pr$_2$P); 1.40 (dd, *J* = 7.2 and 17.8 Hz, 6H, 2 CH_3 of ^{i}Pr$_2$P); 2.18 (m, 2H, 2 CH of ^{i}Pr$_2$P); 2.33 (s, 6H, 2 CH_3 of NAr'); 6.62 (d, $^3J_{H-H}$ = 7.4 Hz, 1H, aromatic CH); 6.68 (d, $^3J_{H-H}$ = 8.0 Hz, 1H, aromatic CH); 6.78 (t, $^3J_{H-H}$ = 7.6 Hz, 1H, aromatic CH); 6.98 (m, 4H, 3 aromatic CH and CH=NAr). ^{31}P{^{1}H}-NMR (202.5 MHz; C_6D_6; δ, ppm): 203.0 (s, OP^{i}Pr$_2$). The obtained NMR data are consistent with those previously published in the literature [64].

4.3.4 Preparation and characterization of iminophosphinite POCN nickel derivatives

(i-PrPOCNAr)NiMe (3-Ar)

A solution of MeLi in Et_2O (1.6 M, 0.2025 mmol) was added to a solution of **1-Ar** (103.2 mg, 0.1929 mmol) in toluene at -80 °C. The mixture allowed to warm up to room temperature slowly and then stirred for additional 1.5 h (in total took app. 12 h). During this time the colour of the reaction mixture turned to crimson red. All volatiles were evaporated in vacuum, the residue was dried and the product was extracted with hexanes (3 x 20 mL) to give dark-red solid (69 mg, 76%). ^{1}H-NMR (500 MHz; C_6D_6; δ, ppm): -0.81 (d, *J* = 3.6 Hz, 3H, $NiCH_3$); 1.10 (d, *J* = 6.8 Hz, 6H, 2 CH_3 of NAr); 1.15 (m, 6H, 2 CH_3 of ^{i}Pr$_2$P); 1.19 (dd, *J* =3.2 and 7.1 Hz, 6H, 2 CH_3 of ^{i}Pr$_2$P); 1.38 (d, J = 6.8 Hz, 6H, 2 CH_3 of NAr); 2.05 (m, 2H, 2 CH of ^{i}Pr$_2$P); 3.49 (sept, *J* = 6.8 Hz, 2H, 2 CH of NAr); 6.84-6.90 (m, 3H, C_6H_3/NAr); 7.13-7.16 (m, 3H, C_6H_3/NAr overlapping with the residual resonance of C_6D_6); 7.73 (d, J = 4.2 Hz, 1H, CH=NAr). ^{31}P{^{1}H}-NMR (202.5 MHz; C_6D_6; δ, ppm): 199.2 (s, OP^{i}Pr$_2$). The obtained NMR data are consistent with those previously published in the literature [64].

(i-PrPOCNAr)Ni(CH2SiMe3) (4-Ar)

A solution of $LiCH_2SiMe_3$ (0.531 ml, 0.531 mmol; 1.0 M in pentane) was added dropwise by syringe to a solution of ($^{i\text{-}Pr}$POCN^{Ar})NiBr (**1-Ar**) (284 mg, 0.531 mmol) in toluene -78 °C. The reaction mixture was stirred for 30 mins at -80 °C and then allowed to warm up to room temperature and stirred overnight. The color of the reaction mixture turned to dark red. Volatiles were removed under reduced pressure and the residue was extracted with hexanes to afford dark-

red solid (236 mg, 82%). ^{1}H-NMR (500 MHz; C_6D_6; δ, ppm): -0.97 (d, *J* = 5.1 Hz, 2H, $NiCH_2TMS$); 0.07 (s, 9H, $SiMe_3$); 1.00 (d, *J* = 6.8 Hz, 6H, 2 CH_3 of NAr); 1.17 (d, 3H, *J* = 6.9 Hz, 3H, CH_3 of $^{i}Pr_2P$); 1.19 (d, *J* = 7.0 Hz, 3H, CH_3 of $^{i}Pr_2P$); 1.26 (d, *J* = 7.2 Hz, 3H, CH_3 of $^{i}Pr_2P$); 1.30 (d, *J* = 7.2 Hz, 3H, CH_3 of $^{i}Pr_2P$); 1.38 (d, *J* = 6.8 Hz, 6H, 2 CH_3 of NAr); 2.21 (m, 2H, 2 CH of $^{i}Pr_2P$); 3.48 (sept, *J* = 6.8 Hz, 2H, 2 CH of NAr); 6.81-6.84 (m, 3H, C_6H_3/NAr); 7.13-7.16 (m, 3H, C_6H_3/NAr overlapping with the residual resonance of C_6D_6); 7.96 (d, *J* = 3.8 Hz, 1H, CH=NAr). $^{31}P\{^{1}H\}$-NMR (202.5 MHz; C_6D_6; δ, ppm): 193.8 (s, $OP^{i}Pr_2$).

($^{i\text{-Pr}}$POCN$^{Ar'}$)Ni(CH_2SiMe_3) (4-Ar')

A solution of $LiCH_2TMS$ (1.0 M in pentane, 142.5 μL, 0.14 mmol) was added dropwise by syringe to a solution of ($^{i\text{-Pr}}$POCN$^{Ar'}$)NiBr (**1-Ar'**) (52.5 mg, 0.11 mmol) in toluene -80 °C (liq. N_2/acetone bath). The reaction mixture stirred and allowed to warm up to room temperature overnight. The color of the reaction mixture turned to dark red. All volatiles were removed under reduced pressure and the residue was extracted with hexanes to afford dark-red solid (39 mg, 73%). The NMR analysis of this substance revealed its 71% purity (by $^{31}P\{^{1}H\}$-NMR) in a mixture with unknown decomposition products. All attempts to isolate **4-Ar'** in analytically pure forms were unsuccessful. ^{1}H-NMR (500 MHz; C_6D_6; δ, ppm): -0.92 (d, *J* = 3.9 Hz, 2H, $NiCH_2TMS$); 0.10 (s, 9H, $SiMe_3$); 1.18 (d, *J* = 6.6 Hz, 3H, CH_3 of $^{i}Pr_2P$); 1.20 (d, *J* = 6.6 Hz, 3H, CH_3 of $^{i}Pr_2P$); 1.26 (d, *J* = 6.9 Hz, 3H, CH_3 of $^{i}Pr_2P$); 1.29 (d, *J* = 6.9 Hz, 3H, CH_3 of $^{i}Pr_2P$); 2.21 (m, 2H, 2 CH of $^{i}Pr_2P$); 2.28 (s, 6H, 2 CH_3 of NAr'); 6.79 (m, 1H, C_6H_3/NAr); 6.86 (m, 2H, C_6H_3/NAr); 6.99 (m, 3H, C_6H_3/NAr'); 7.19 (d, *J* = 2.6 Hz, 1H, CH=NAr'). $^{31}P\{^{1}H\}$-NMR (202.5 MHz; C_6D_6; δ, ppm): 195.3 (s, $OP^{i}Pr_2$).

NMR scale generation of ($^{i\text{-Pr}}$POCN^{Ar})Ni($O^{t}Bu$) (5-Ar)

A solution of ($^{i\text{-Pr}}$POCN^{Ar})NiBr (**1-Ar**) (15.6 mg, 0.029 mmol) in 0.6 ml of THF was added at room temperature to solid $NaO^{t}Bu$ (change in R&D, it is KOtBu there) (2.8 mg, 0.029 mmol). The color of the solution changed to red-brown immediately after addition and formation of white precipitate of NaBr was observed. The mixture was transferred to an NMR tube, left for 10 minutes at room temperature, and was checked by NMR spectroscopy showing quantitative conversion of **1-Ar** to **5-Ar**. In attempt to isolate complex **5-Ar**, all volatiles were pumped off, the residue was dried and extracted with hexanes. Hexanes were removed under reduced pressure to give an oily red material, which upon NMR analysis turn out to be a mixture of the target complex **5-Ar** and unknown decomposition products. All attempts to separate this mixture and obtain **5-Ar** in analytically pure form were unsuccessful.

5-Ar: ^{1}H-NMR (300 MHz; C_6D_6; δ, ppm): 1.04 (s, 9H, 3 CH_3 of NiO^{t}Bu); 1.13 (d, *J* = 6.8 Hz, 6H, 2 CH_3 of NAr); 1.23 (dd, *J* = 13.6 Hz and 7.0 Hz, 6H, 2 CH_3 of P^{i}Pr$_2$); 1.46 (dd, *J* = 17.9 Hz and 7.2 Hz, 6H, 2 CH_3 of P^{i}Pr$_2$); 1.55 (d, *J* = 6.8 Hz, 6H, 2 CH_3 of NAr); 2.21 (m, 2H, 2 CH of P^{i}Pr$_2$); 3.91 (sept, *J* = 6.8 Hz, 2H, 2 CH of NAr); 6.58 (d, *J* = 7.6 Hz, 1H, C_6H_3 or NAr); 6.65 (d, *J* = 7.3 Hz, 1H, C_6H_3 or NAr); 6.75 (t, *J* = 7.4 Hz, 1H, C_6H_3 or NAr); 7.09-7.26 (m, 3H, C_6H_3 or NAr); 7.66 (d, *J* = 4.6 Hz, 1H, CH=NAr). ^{31}P{^{1}H}-NMR (121 MHz; C_6D_6; δ, ppm): 185.9 (s, OP^{i}Pr$_2$).

($^{i\text{-Pr}}$POCN$^{Ar'}$)Ni(O^{t}Bu) (5-Ar')

A solution of ($^{i\text{-Pr}}$POCN$^{Ar'}$)NiBr (**1-Ar'**) (147.4 mg, 0.308 mmol) in toluene (100 ml) was added at room temperature to solid KO^{t}Bu (41.4 mg, 0.369 mmol). The color of the reaction mixture changed to dark red almost immediately. The reaction mixture was stirred for 2 hours at room temperature. Quantitative formation of **5-Ar'** was confirmed by NMR analysis of the crude sample taken directly from the reaction mixture. All volatiles were removed under reduced pressure and the residue was extracted with cold (-30 °C; liq. N_2/CH_3CN bath) hexanes to afford dark-red oily material (126.5 mg, 87%). NMR analysis of this substance revealed a mixture of **5-Ar'** (61% by ^{31}P{^{1}H}-NMR) with unidentified decomposition products. All attempts to separate this mixture and obtain **5-Ar'** in analytically pure form were unsuccessful.

5-Ar': ^{1}H-NMR (500 MHz; C_6D_6; δ, ppm): 1.08 (s, 9H, 3 CH_3 of NiO^{t}Bu); 1.24 (d, *J* = 6.9 Hz, 3H, CH_3 of ^{i}Pr$_2$P); 1.27 (d, *J* = 6.8 Hz, 3H, CH_3 of ^{i}Pr$_2$P); 1.44 (d, *J* = 7.2 Hz, 3H, CH_3 of ^{i}Pr$_2$P); 1.47 (d, *J* = 7.2 Hz, 3H, CH_3 of ^{i}Pr$_2$P); 2.20 (m, 2H, 2 CH of ^{i}Pr$_2$P); 2.51 (s, 6H, 2 CH_3 of NAr'); 6.59 (d, *J* = 6.8 Hz, 1H, C_6H_3/NAr); 6.64 (d, *J* = 7.3 Hz, 1H, C_6H_3/NAr); 6.78 (t, J = 7.8 Hz, 2H, C_6H_3/NAr'); 6.96-7.04 (m, 3H, 2H of C_6H_3/NAr and 1H, CH=NAr'). ^{31}P{^{1}H}-NMR (202.5 MHz; C_6D_6; δ, ppm): 185.4 (s, OP^{i}Pr$_2$).

NMR scale reaction of ($^{i\text{-Pr}}$POCN$^{Ar'}$)Ni(O^{t}Bu) (5-Ar') with HBPin

HBPin (5.7 µl, 0.039 mmol, 5 equivalents) was added at room temperature *via* syringe to **5-Ar'** (3.7 mg, 0.00783 mmol, generated in situ by treatment of **1-Ar'** with KO^{t}Bu in C_6D_6) in 0.6 ml of C_6D_6 in and NMR tube. Immediately after addition the color of the reaction mixture changed to dark brown and the reaction was checked with NMR after 5 minutes at room temperature. NMR analysis showed formation of a hydride species, which were tentatively assigned to [(^{iPr}POCN$^{Ar'}$)Ni(µ-H)]$_2$ (**14-Ar'**). The product turned out to be very unstable and full decomposition to a mixture of unknown products was observed after 15 minutes at room temperature.

[(^{iPr}POCN$^{Ar'}$)Ni(μ-H)]$_2$ (**14-Ar'**): selected characteristic NMR data: ^{1}H-NMR (500 MHz; C_6D_6; δ, ppm): -8.96 (dt, *J* = 96.3 Hz and 22.6 Hz, 1H, NiH); -14.02 (m, 1H, NiH). ^{31}P{^{1}H}-NMR (202.5 MHz; C_6D_6; δ, ppm): 210.3 (s, OP^{i}Pr$_2$).

($^{i\text{-}Pr}$POCN^{Ar})Ni(η^2-BH$_4$) (6-Ar)

A solution of $LiBH_4$ in THF (2.0 M, 96.3 μL, 0.1925 mmol) was added at room temperature to a solution of **1-Ar** (98.1 mg, 0.1833 mmol) in 20 mL of toluene. A color change from orange-red to barberry red with the formation of white precipitate were observed. The reaction mixture was left with stirring for 24 hours. All volatiles were evaporated followed by the extraction with hexanes (3 x 20 mL). Residue was dried in vacuum to give the barberry red powder of **6-Ar** (75 mg, 93%). ^{1}H-NMR (500 MHz; C_6D_6; δ, ppm): -0.95 (br s, 2H, BH_4); -0.72 (br s, 2H, BH_4); 1.07 (dd, *J* = 6.9 and 14.8 Hz, 6H, 2 CH_3 of ^{i}Pr$_2$P); 1.08 (d, *J* = 6.9 Hz, 6H, 2 CH_3 of NAr); 1.24 (dd, *J* = 7.2 and 18 Hz, 6H, 2 CH_3 of ^{i}Pr$_2$P); 1.50 (d, *J* = 6.9 Hz, 6H, 2 CH_3 of NAr); 2.06 (m, 2H, 2 CH of ^{i}Pr$_2$P); 3.56 (sept, *J* = 6.9 Hz, 2H, 2 CH of NAr); 6.74 (m, 3H, aromatic protons of C_6H_3/NAr); 7.12 (m, 2H, aromatic protons of C_6H_3/NAr); 7.18 (m, 1H, aromatic proton of C_6H_3/NAr); 7.57 (d, *J* = 3.5 Hz, 1H, CH=NAr). ^{31}P{^{1}H}-NMR (202.5 MHz; C_6D_6; δ, ppm): 208.2 (s, OP^{i}Pr$_2$). ^{11}B{^{1}H}-NMR (160.5 MHz; C_6D_6; δ, ppm): -30.8 (br s, BH_4). The obtained NMR data are consistent with those previously reported in the literature [64].

($^{i\text{-}Pr}$POCN^{Ar})Ni(η^1-BF$_4$) (7-Ar)

A solution of $AgBF_4$ (76.6 mg, 0.3934 mmol) in toluene was added at room temperature to a solution of **1-Ar** (200.5 mg, 0.3747 mmol) in toluene. A colour change (from orange-red to yellow) with the formation of white precipitate were observed. The reaction mixture was stirred at room temperature for 1 h, filtered and the residue was washed with a mixture of hexanes/toluene (5/1) until the filtrate became colourless. The solvent was removed in vacuum to give yellow powder of **7-Ar** which was additionally dried in vacuum for 5 h (120 mg, 59%). ^{1}H-NMR (500 MHz; C_6D_6; δ, ppm): 1.05 (dd, *J* = 7.1 and 14.7 Hz, 6H, 2 CH_3 of ^{i}Pr$_2$P); 1.09 (d, J = 6.9 Hz, 6H, 2 CH_3 of NAr); 1.41 (dd, *J* = 7.2 and 19.4 Hz, 6H, 2 CH_3 of ^{i}Pr$_2$P); 1.59 (d, *J* = 6.9 Hz, 6H, 2 CH_3 of NAr); 2.26 (m, 2H, 2 CH of ^{i}Pr$_2$P); 3.59 (sept, *J* = 6.9 Hz, 2H, 2 CH of NAr); 6.37 (d, *J* = 8.1 Hz, 1H, C_6H_3/NAr); 6.43 (d, *J* = 7.4 Hz, 1H, C_6H_3/NAr); 6.61 (t, *J* = 7.8 Hz, 1H, C_6H_3/NAr); 7.10 (m, 2H, C_6H_3/NAr); 7.19 (m, 1H, C_6H_3/NAr); the resonance of CH=NAr is obscured by the residual resonance of C_6D_6 (found by ^{1}H-^{13}C HSQC NMR). ^{31}P{^{1}H}-NMR (202.5 MHz; C_6D_6; δ, ppm): 199.5 (s, OP^{i}Pr$_2$). ^{11}B{^{1}H}- NMR (160.5 MHz; C_6D_6; δ, ppm): -1.4 (br s, BF_4). ^{19}F{^{1}H}-NMR (470.6 MHz; C_6D_6; δ, ppm): -173.8 (br s, BF_4). The obtained NMR data are consistent with those previously reported in the literature [64].

4.3.5 Preparation and characterization of alcohol precursors to aminophosphinite POCN pincer ligands

1-(HO)-3-(CH_2-NMe_2)-C_6H_4

To a solution of 3-hydroxybenzaldehyde (0.500g, 4.1 mmol) in MeOH a solution of dimethylammonium chloride (1.174g, 12.3 mmol) in MeOH was added at room temperature. NEt_3 (1.71 mL, 12.3 mmol) was added by syringe and the resulting mixture was stirred for 1 hour to obtain a yellow solution. Full conversion of 3-hydroxybenzaldehyde was confirmed by ^{1}H-NMR analysis of the sample taken directly from the reaction mixture. The mixture was cooled to -5 ^{o}C and $NaBH_4$ (0.2g, 5.3 mmol) has been in small portions added for 1 hour. The reaction mixture was concentrated and treated with 10% HCl to reach pH = 1 and washed with diethyl ether (3 x 10mL). The aqueous layer was treated with ammonia solution to get pH = 10 and extracted with Et_2O. Organic extracts were combined, dried with anhydrous $MgSO_4$, filtered, and evaporated to give a yellow powder (434.9 mg, 70%). ^{1}H-NMR (500 MHz; $CDCl_3$; δ, ppm): 2.26 (s, 6H, 2 CH_3), 3.39 (s, 2H, NCH_2), 6.74-6.67 (m, 2H, {Ar}$H^{2,6}$), 6.76 (d, ^3J = 8 Hz, 1H, {Ar}H^4), 7.13 (t, ^3J = 8 Hz, 1H, {Ar}H^5), 8.42 (br s, 1H, OH). The obtained NMR data are consistent with those previously reported in the literature [91].

1-(HO)-3-(CH_2-NEt_2)-C_6H_4

To a solution of 3-hydroxybenzaldehyde (0.5 g, 0.004 mol) and diethylamine (0.85 mL, 0.008 mol) in THF $NaHB(OAc)_3$ (1.74 g, 0.008 mol) was added portionwise at room temperature. The reaction mixture was left stirring overnight. After removing 2/3 of THF under reduced pressure, the mixture was quenched with saturated $NaHCO_3$ until it turns a clear solution. Then 10% HCl solution was added to the mixture until pH = 1. The resulting mixture was extracted with Et_2O (1 x 100mL, 2 x 50mL). The aqueous layer was collected, and saturated ammonia solution was added until pH = 10. After that the solution was extracted again with Et_2O (1 x 100mL, 2 x 50mL). The collected organic phase was dried with anhydrous Na_2SO_4. The solvent was evaporated first using rotary evaporator and the residue was dried in vacuum at 50 °C to give a product (0.65 g, 87%). ^{1}H-NMR (500 MHz; C_6D_6; δ, ppm): 1.01 (t, ^3J = 7 Hz, 6H, 2 CH_3), 2.50 (q, ^3J = 7 Hz, 4H, 2 NCH_2), 3.49 (s, 2H, NCH_2), 6.83 (dd, ^3J = 8 Hz, 2 Hz, 1H, {Ar}H^6), 6.96 (d, ^3J = 8 Hz, 1H, {Ar}H^4), 7.03 (br s, 1H, OH), 7.06 (s, 1H, {Ar}H^2), 7.17 (t, ^3J = 8 Hz, 1H, {Ar}H^5). The obtained NMR data are consistent with those previously published in the literature [91].

1-(HO)-3-(CH_2-N^iPr_2)-C_6H_4

To a solution of 3-hydroxybenzaldehyde (5.0g, 0.045 mol) and diisopropylamine (16.6 g, 0.164 mol) in THF $NaHB(OAc)_3$ (17.5 g, 0.082 mol) was added portionwise at room temperature. The reaction mixture was left stirring overnight. After removing 2/3 of THF under reduced pressure, the mixture was quenched with saturated $NaHCO_3$ until it turns a clear solution. Then 10% HCl solution was added to the mixture until pH = 1. The solution was extracted with Et_2O (1 x 100mL, 2 x 50mL). The aqueous layer was collected, and saturated ammonia solution was added until pH = 10. After that the solution was extracted again with Et_2O (1 x 100mL, 2 x 50mL). The collected organic phase was dried with anhydrous Na_2SO_4. The solvent was evaporated under reduced pressureand the residue was dried in vacuum at 80°C to give a product (6.257 g, 74%). ^{1}H-NMR (500 MHz; C_6D_6; δ, ppm): 0.93 (d, ^3J = 6.6 Hz, 12H, 4 CH_3); 2.93 (sept, ^3J = 6.6 Hz, 2H, 2 CH); 3.48 (s, 2H, NCH_2); 4.68 (br s, 1H, OH); 6.56 (m, 1H, {Ar}H^5); 6.95 (br s, 1H, {Ar}H^1); 6.97 (d, ^3J = 7.7 Hz, 1H, {Ar}H^3); 7.08 (t, ^3J = 7.8 Hz, 1H, {Ar}H^4). NMR data are consistent with those previously reported in the literature [95].

4.3.6 Preparation and characterization of aminophosphinite POCN pincer ligands

1-(^{i}Pr$_2$PO)-3-(CH_2-NMe_2)-C_6H_4

A solution of ^{i}Pr$_2$PCl (0.55 mL, 3.4 mmol) in THF was added to [3-((*N*,*N*-dimethylamino)methyl)phenol] (434.9 mg, 2.9 mmol) solution in THF. Then, NEt_3 (1 mL, 14.38 mmol) was added to the mixture and the reaction was stirred at room temperature for 1.5 hours. The solvent was evaporated, and the residue was extracted with toluene. All volatiles were pumped off and the residue was dried in vacuum to give a yellow oil (760.0 mg, 98%). ^{1}H-NMR (500 MHz; C_6D_6; δ, ppm): 0.68 (dd, $J_{H\text{-}P}$ = 15 Hz, $J_{H\text{-}H}$ = 7 Hz, 6H, 2 $CHCH_3$), 0.84 (dd, $J_{H\text{-}P}$=10 Hz, $J_{H\text{-}H}$= 7 Hz, 6H, 2 $CHCH_3$), 1.46 (m, 2H, 2 CH), 1.76 (s, 6H, 2 NCH_3), 2.94 (s, 2H, NCH_2), 6.68 (d, $J_{H\text{-}H}$ = 7 Hz, 1H, {Ar}H^6), 6.81 (t, $J_{H\text{-}H}$= 8, 1H, {Ar}H^5), 6.85 (s, 1H, {Ar}H^2), 6.89 (d, $J_{H\text{-}H}$= 8 Hz, 1H, {Ar}H^4). ^{31}P{^{1}H}-NMR (202.5 MHz; C_6D_6; δ, ppm): 147.4 (s, OP^iPr$_2$). The obtained NMR data are consistent with those previously published in the literature [91].

1-(^{i}Pr$_2$PO)-3-(CH_2-NEt_2)-C_6H_4

To a solution of 1-(HO)-3-(CH_2-NEt_2)-C_6H_4 (0.508 g, 0.0028 mol) in toluene a solution of ^{i}Pr$_2$PCl (0.473 mL, 0.003 mol) in toluene was added, after which NEt_3 (0.780 mL, 0.0056mol) was added dropwise and the resulting mixture was stirred at room temperature overnight. After that the mixture was filtered, the residue was washed with toluene, the filtrate was collected and all volatiles were evaporated to give a product (739 mg, 82%). ^{1}H-NMR (500 MHz; C_6D_6; δ, ppm): 0.56 (t, $^3J_{H\text{-}H}$= 7 Hz, 6H, 2 CH_2CH_3); 0.63 (dd, $^3J_{H\text{-}P}$ = 16 Hz, $J_{H\text{-}H}$ = 7 Hz, 6H, 2 $CHCH_3$); 0.79 (dd, $^3J_{H\text{-}P}$ = 11 Hz, $J_{H\text{-}H}$ = 7 Hz, 6H, 2 $CHCH_3$); 1.51-1.26 (m, 2H, 2 CH); 2.03 (q, $^3J_{H\text{-}H}$= 7 Hz,

4H, 2 CH_2); 3.06 (s, 2H, NCH_2); 6.67 (d, $^3J_{H-H}$ = 8 Hz, 1H, {Ar}H^6); 7.03-6.92 (m, 3H, {Ar}$H^{4,2,5}$). $^{31}P\{^1H\}$-NMR (202.5 MHz; C_6D_6; *δ*, ppm): 147.1 (s, O*P*^{i}Pr$_2$). The obtained NMR data are consistent with those previously published in the literature [91].

1-(^{i}Pr$_2$PO)-3-(CH$_2$-N^{i}Pr$_2$)-C$_6$H$_4$

To a solution of 1-(HO)-3-(CH_2-N^{i}Pr$_2$)-C_6H_4 (1.056 g, 0.0051 mol) in THF a solution of ^{i}Pr$_2$PCl (0.7 mL, 0.0054 mol) in THF was added, after which NEt_3 (1 mL, 0.0076mol) was added dropwise and the resulting mixture was stirred at room temperature overnight. After the removal of THF in vacuum, the residue was extracted with toluene. All volatiles were evaporated to give a product (1.442 g, 90%). ^{1}H-NMR (500 MHz; C_6D_6; δ, ppm): 0.93 (d, $^3J_{H-H}$= 6.6 Hz, 12H, 4 CH_3); 1.01 (dd, $^3J_{H-P}$ = 15.7 Hz, $^3J_{H-H}$ = 7.2 Hz, 6H, 2 $CHCH_3$); 1.18 (dd, $^3J_{H-P}$ = 10.4 Hz, $^3J_{H-H}$ = 7.0 Hz, 6H, 2 $CHCH_3$); 1.70-1.86 (m, 2H, 2 CH); 2.92 (sept, $^3J_{H-H}$= 6.8 Hz, 2H, 2 CH); 3.52 (s, 2H, NCH_2); 7.02 (m, 1H, {Ar}); 7.12-7.19 (m, 3H, {Ar}); 7.55 (s, 1H, {Ar}H^1). $^{31}P\{^1H\}$-NMR (202.5 MHz; C_6D_6; *δ*, ppm): 147.0 (s, O*P*^{i}Pr$_2$). NMR data are consistent with those previously reported in the literature [95].

4.3.7 Preparation and characterization of aminophosphinite POCN nickel bromide complexes

($^{i\text{-}Pr}$POCN^{Me2})NiBr (8-Me$_2$)

To a suspension of [$NiBr_2(CH_3CN)_2$] (0.684 g, 2.3 mmol) in toluene the solution of the ligand 1-(^{i}Pr$_2$PO)-3-(CH_2-NMe_2)-C_6H_4 (0.76 g, 2.3 mmol) in toluene was added at room temperature. This was followed by the addition of NEt_3 (1.58 mL, 11.37 mmol). The resulting mixture was stirring for 3 hours at 70 °C. The mixture was filtered through a pad of silica gel, after which the volatiles were evaporated in vacuum to give a yellow powder (509.4 mg, 55%). ^{1}H-NMR (500 MHz; C_6D_6; δ, ppm): 1.16 (d, 3H, CH_3); 1.19 (d, 3H, CH_3); 1.47 (d, 3H, CH_3); 1.50 (d, 3H, CH_3); 2.19 (m, 1H, CH); 2.22 (m, 1H, CH); 2.44 (d, 6H, 2 CH_3); 3.24 (s, 2H, NCH_2); 6.41 (d, 1H, CH aromatic); 6.64 (d, 1H, CH aromatic); 6.92 (t, 1H, CH aromatic). $^{31}P\{^1H\}$-NMR (202.5 MHz; C_6D_6; *δ*, ppm): 201.2 (s, O*P*^{i}Pr$_2$). The obtained NMR data are consistent with those previously reported in the literature [91].

($^{i\text{-}Pr}$POCN^{Et2})NiBr (8-Et$_2$)

A solution of the ligand 1-(^{i}Pr$_2$PO)-3-(CH_2-N^{i}Pr$_2$)-C_6H_4 (764.0 mg, 2.586 mmol) in toluene was added at room temperature to a suspension of [$NiBr_2(CH_3CN)_2$] (777.45 mg, 2.586 mmol) in toluene, followed by the addition of excess of NEt_3 (1.8 mL, 12.93 mmol). The resulting mixture was heated at 70 °C for 3 hours. The mixture was filtered through a pad of silica gel, the solvent

was pumped off and the residue was dried in vacuum to give a dark-yellow oily material, which after tituration with Et_2O turned to a yellow powder (0.995 mg, 89%). ^{1}H-NMR (500 MHz; C_6D_6; δ, ppm): 1.17 (dd, *J* = 14.4 Hz, 7.0 Hz, 6H, 2 CH_3 of P^{i}Pr); 1.41-1.57 (m, 12H, 2 CH_3 of P^{i}Pr and 2 CH_3 of NEt_2); 2.01-2.12 (m, 2H, 2 CH of P^{i}Pr); 2.16-2.29 (m, 2H, CH_2 of NEt_2); 3.35-3.42 (m, 2H, CH_2 of NEt_2); 3.43 (s, 2H, NCH_2); 6.41 (d, *J* = 7.5 Hz, 1H, C_6H_3); 6.62 (d, *J* = 7.9 Hz, 1H, C_6H_3); 6.91 (t, *J* = 7.7 Hz, 1H, C_6H_3). ^{31}P{^{1}H}-NMR (202.5 MHz; C_6D_6; *δ*, ppm): 198.1 (s, O*P*^{i}Pr$_2$). The obtained NMR data are consistent with those previously reported in the literature [91].

(i-PrPOCNi-Pr2)NiBr (8-iPr2)

A solution of the ligand 1-(^{i}Pr$_2$PO)-3-(CH_2-N^{i}Pr$_2$)-C_6H_4 (177 mg, 0.599 mmol) in toluene was added at room temperature to a suspension of [$NiBr_2(CH_3CN)_2$] (180 mg, 0.593 mmol) in toluene, followed by the addition of excess of NEt_3 (0.4 mL, 0.725 mmol). The resulting mixture was heated at 100 °C for 4 days. The mixture was filtered through a pad of silica gel, the solvent was pumped off and the residue was dried in vacuum to give a yellow powder (205 mg, 75%). ^{1}H-NMR (500 MHz; C_6D_6; δ, ppm): 1.02 (d, *J* = 6.4 Hz, 6H, 2 CH_3 of N^{i}Pr$_2$); 1.20 (dd, *J* = 14.4 Hz, 7.0 Hz, 6H, 2 CH_3 of N^{i}Pr$_2$); 1.53 (dd, *J* = 17.1 Hz, 7.2 Hz, 6H, 2 CH_3 of N^{i}Pr$_2$); 1.80 (d, *J* = 6.5 Hz, 6H, 2 CH_3 of N^{i}Pr$_2$); 2.26-2.38 (m, 2H, 2 CH of N^{i}Pr$_2$); 3.20-3.34 (m, 2H, 2 CH of P^{i}Pr$_2$); 3.49 (s, 2H, NCH_2); 6.43 (d, *J* = 7.5 Hz, 1H, C_6H_3); 6.61 (d, *J* = 7.8 Hz, 1H, C_6H_3); 6.92 (t, *J* = 7.7 Hz, 1H, C_6H_3). ^{13}C{^{1}H}-NMR (125.8 MHz; C_6D_6; δ, ppm): 16.9 (d, *J* = 2.0 Hz); 18.5 (d, *J* = 3.5 Hz); 19.3; 22.7; 28.9 (d, *J* = 24.6 Hz); 57.7; 60.8; 107.7 (d, *J* = 13.0 Hz); 114.0; 126.8; 155.4; 157.0; 159.8. ^{31}P{^{1}H}-NMR (202.5 MHz; C_6D_6; *δ*, ppm): 192.9 (s, O*P*^{i}Pr$_2$).

4.3.8 Preparation and characterization of aminophosphinite POCN nickel derivatives

(i-PrPOCNMe2)NiMe (9-Me2)

A solution of MeLi in Et_2O (1.6 M, 141μL, 0.225 mmol) was added to a yellow-orange solution of ($^{i\text{-Pr}}$POCN^{Me2})NiBr **(8-Me2)** (87.0 mg, 0.215 mmol) in toluene at -30 °C. Formation of white precipitate was observed almost immediately. The resulting mixture was allowed to warm up to room temperature and was stirred for additional 40 minutes. After that the mixture was filtered, all volatiles were pumped off and the residue was extracted with hexanes (3 x 5 mL). The hexanes solution was evaporated to give yellow-orange solid which was dried in vacuum (57.7 mg, 79%). The crystals suitable for X-ray analysis were obtained by crystallization from Et_2O solution at -30 °C. ^{1}H-NMR (500 MHz; C_6D_6; δ, ppm): -0.81 (d, $^3J_{H\text{-}P}$ = 3.1 Hz, 3H, $NiCH_3$); 1.22 (dd, *J* = 13.8 Hz, 6.9 Hz, 6H, 2 CH_3 of P^{i}Pr); 1.27 (dd, *J* = 16.9 Hz, 7.2 Hz, 6H, 2 CH_3 of P^{i}Pr); 2.04-2.13 (m, 2H, 2 CH of P^{i}Pr); 2.267 (s, 3H, CH_3 of NMe_2); 2.269 (s, 3H, CH_3 of NMe_2); 3.53 (s, 2H, NCH_2);

6.66 (d, J = 7.3 Hz, 1H, C_6H_3); 6.85 (d, J = 7.8 Hz, 1H, C_6H_3); 7.00-7.06 (m, 1H, C_6H_3). $^{13}C\{^1H\}$-NMR (125.8 MHz; C_6D_6; δ, ppm): -10.2 (d, J = 21.1 Hz); 17.1; 17.9 (d, J = 5.6 Hz); 27.7 (d, J = 24.1 Hz); 47.83; 47.84; 75.2; 107.3 (d, J = 13.0 Hz); 114.7; 125.8; 149.3; 156.1 (d, J = 28.4); 164.2 (d, J = 10.9). $^{31}P\{^1H\}$-NMR (202.5 MHz; C_6D_6; δ, ppm): 197.1 (s, O*P*^{i}Pr$_2$).

($^{i\text{-Pr}}$POCN^{Me2})Ni(CH$_2$SiMe$_3$) (10-Me$_2$)

A solution of LiCH$_2$TMS in pentane (1.0 M, 194.4 µL, 0.1944 mmol) was added at –80 °C (liq. N_2/acetone bath) to a solution of ($^{i\text{-Pr}}$POCN^{Me2})NiBr (**8-Me$_2$**) (49.2 mg, 0.1215 mmol) in 15 ml of toluene. The reaction mixture was stirred at –80 °C for 30 minutes and then was allowed to warm up to room temperature overnight. All volatiles were pumped off, and the residue was extracted with hexanes to give yellow-orange solid (32 mg, 64%). ^{1}H-NMR (500 MHz; C_6D_6; δ, ppm): -1.21 (d, $^3J_{H\text{-}P}$ = 5.0 Hz, 2H, NiCH$_2$); 0.44 (s, 9H, SiMe$_3$); 1.20 (dd, J = 13.8 Hz, 6.8 Hz, 6H, 2 CH$_3$ of P^{i}Pr); 1.27 (dd, J = 16.6 Hz, 7.2 Hz, 6H, 2 CH$_3$ of P^{i}Pr); 2.05-2.14 (m, 2H, 2 CH of P^{i}Pr); 2.28 (s, 6H, 2 CH$_3$ of NMe$_2$); 3.46 (s, 2H, NCH$_2$); 6.62 (d, J = 7.8 Hz, 1H, C_6H_3); 6.79 (d, J = 7.8 Hz, 1H, C_6H_3); 6.98-7.02 (m, 1H, C_6H_3). $^{31}P\{^1H\}$-NMR (202.5 MHz; C_6D_6; δ, ppm): 193.5 (s, O*P*^{i}Pr$_2$).

NMR reaction of ($^{i\text{-Pr}}$POCN^{Me2})NiBr (8-Me$_2$) with EtMgBr

Generation (*in situ*) of 13-Me$_2$ on NMR scale. A solution EtMgBr in Et$_2$O (3.0 M, 18.1 µl, 0.054 mmol) was added at room temperature to a solution of **8-Me$_2$** (20 mg, 0.049 mmol) 0.6 ml of C_6D_6 in an NMR tube. Formation of white precipitate was observed and the color of the reaction mixture became dark brown. The reaction mixture was left at room temperature for 15 minutes and then checked with NMR spectroscopy, showing formation of a difficult to separate mixture of decomposition products as well as ethylene (δ_H = 5.26 ppm) and H_2 (δ_H = 4.47 ppm).

($^{i\text{-Pr}}$POCN^{Me2})Ni(O^{t}Bu) (13-Me$_2$)

Generation (*in situ*) of 13-Me$_2$ on NMR scale. A solution of ($^{i\text{-Pr}}$POCN^{Me2})NiBr (**8-Me$_2$**) (4.0 mg, 0.034 mmol) in 0.6 ml of C_6D_6 was added at room temperature to solid KO^{t}Bu (10.4 mg, 0.041 mmol). The color changed immediately from yellow to orange and formation of white precipitate was observed. The mixture was transferred to an NMR tube and left at room temperature for 1 hour. NMR analysis showed quantitative conversion of **8-Me$_2$** to **13-Me$_2$**. All attempts to isolate the product *via* extraction with hexanes resulted in its partial decomposition and formation of difficult to separate mixtures of **13-Me$_2$** and unidentified decomposition products.

13-Me$_2$: ^{1}H-NMR (500 MHz; C_6D_6; δ, ppm): 1.22 (dd, J = 12.8 Hz, 6.9 Hz, 6H, 2 CH$_3$ of P^{i}Pr); 1.45-1.55 (m, 15H, 2 CH$_3$ of P^{i}Pr and 3 CH$_3$ of NiO^{t}Bu); 2.15-2.25 (m, 2H, 2 CH of P^{i}Pr); 2.42 (s, 6H, 2 CH$_3$ of NMe$_2$); 3.34 (s, 2H, NCH$_2$); 6.42 (d, J = 7.1 Hz, 1H, C_6H_3); 6.60 (d, J = 7.8 Hz, 1H,

C_6H_3); 6.91 (t, *J* = 7.6 Hz, 1H, C_6H_3). $^{31}P\{^1H\}$-NMR (202.5 MHz; C_6D_6; *δ*, ppm): 190.0 (s, O*P*^{i}Pr$_2$).

NMR scale reaction of ($^{i\text{-}Pr}$POCN^{Me2})Ni(O^{t}Bu) (13-Me$_2$) with HBPin

HBPin (4.0 µl, 0.028 mmol, 1.12 equivalents to Ni) was added at room temperature by syringe to a solution of ($^{i\text{-}Pr}$POCN^{Me2})Ni(O^{t}Bu) (**13-Me$_2$**) (generated *in situ* from 10 mg (0.025 mmol) of ($^{i\text{-}Pr}$POCN^{Me2})NiBr (**8-Me$_2$**) and 6.93 mg (0.062 mmol) of KO^{t}Bu in C_6D_6). The color of the reaction changed to dark brown immediately after HBPin addition. The reaction was left at room temperature for 5 minutes and then checked by NMR showing formation of a difficult-to-separate mixture of the hydride species (tentatively assigned to [(^{iPr}POCN^{Me2})Ni(µ-H)]$_2$ (**14-Me$_2$**)) and unidentified decomposition products. All attempts to generate **14-Me$_2$** cleanly and/or isolate it in analytically pure form were unsuccessful. [(^{iPr}POCN^{Me2})Ni(µ-H)]$_2$ (**14-Me$_2$**) showed full decomposition after 15 minutes at room temperature.

[(^{iPr}POCN^{Me2})Ni(µ-H)]$_2$ (**14-Me$_2$**): selected characteristic NMR data: ^{1}H-NMR (500 MHz; C_6D_6; δ, ppm): -10.01 (dt, *J* = 91.3 Hz and 21.8 Hz, 1H, NiH); -12.08 (m, 1H, NiH). $^{31}P\{^1H\}$-NMR (202.5 MHz; C_6D_6; δ, ppm): 209.0 (s, OP^{i}Pr$_2$).

($^{i\text{-}Pr}$POCN^{Et2})Ni(O^{t}Bu) (13-Et$_2$).

A solution of ($^{i\text{-}Pr}$POCN^{Et2})NiBr (**8-Et$_2$**) (244.1 mg, 0.564 mmol) in THF (30 ml) was added at room temperature to a suspension of KO^{t}Bu (69.6 mg, 0.62 mmol) in THF (10 ml). The color of the reaction mixture turned from yellow to orange almost immediately and formation of the white precipitate was observed. The reaction mixture was stirred at room temperature for 1 hour, after which all volatiles were pumped off and the oily residue was extracted with cold hexanes (-30 °C). Hexanes were removed in vacuum to give orange oil (227.3 mg, 86%), which was dried in vacuum and checked with NMR in C_6D_6. NMR analysis of this oil revealed the presence of two compounds (1:0.85 ratio by $^{31}P\{^1H\}$-NMR) which were assigned to two isomers of **13-Et$_2$** based on similarities of their ^{1}H and ^{31}P-NMR spectra. ^{1}H-NMR (500 MHz; C_6D_6; mixture of two isomers; *δ*, ppm): 1.16 (dd, *J* = 12.3 Hz, 6.9 Hz, 6 H, 2 CH_3 of P^{i}Pr$_2$, isomer 1); 1.21-1.26 (m, 6 H, 2 CH_3 of P^{i}Pr$_2$, isomer 2); 1.37 (s, 9H, NiO^{t}Bu, isomer 1); 1.38 (s, 9H, NiO^{t}Bu, isomer 2); 1.49-1.65 (m, 24 H, 4 CH_3 of NEt_2 for two isomers and 4 CH_3 of P^{i}Pr$_2$ for two isomers); 1.92 (m, 2H, CH_2 of NEt_2, isomer 1); 2.08 (m, 2H, CH_2 of NEt_2, isomer 2); 2.14-2.30 (m, 4H, 4 CH of P^{i}Pr$_2$ of two isomers); 3.20 (m, 2H, CH_2 of NEt_2, isomer 1); 3.33-3.41 (m, 2H, CH_2 of NEt_2, isomer 2); 3.48 (s, 2H, NCH_2, isomer 1); 3.53 (s, 2H, NCH_2, isomer 1); 6.39-6.45 (m, 2H, C_6H_3 for two isomers); 6.55-6.58 (m, 2H, C_6H_3 for two isomers); 6.86-6.94 (m, 2H, C_6H_3 for two isomers). $^{31}P\{^1H\}$-NMR

(202.5 MHz; C_6D_6; mixture of two isomers; δ, ppm): 189.3 (s, O*P*^{i}Pr$_2$, isomer 1); 189.8 (s, O*P*^{i}Pr$_2$, isomer 2).

($^{i\text{-Pr}}$POCN$^{i\text{-Pr2}}$)Ni(O^{t}Bu) (13-^{i}Pr$_2$)

Generation (*in situ*) of 13-^{i}Pr$_2$ on NMR scale. A solution of ($^{i\text{-Pr}}$POCN$^{i\text{Pr2}}$)NiBr (**8-^{i}Pr$_2$**) (15 mg, 0.033 mmol) in 0.6 ml of THF was added at room temperature to solid KO^{t}Bu (3.83 mg, 0.034 mmol). The color changed immediately from yellow to orange and formation of white precipitate was observed. The mixture was transferred to an NMR tube and left at room temperature overnight. NMR analysis showed quantitative conversion of **8-^{i}Pr$_2$** to **13-^{i}Pr$_2$**. All attempts to isolate the product *via* extraction with hexanes resulted in its partial decomposition and formation of difficult to separate mixtures of **13-^{i}Pr$_2$** and unidentified decomposition products.

13-^{i}Pr$_2$: ^{1}H-NMR (500 MHz; THF-H_8; δ, ppm): 0.99 (s, 9H, 3 CH_3 of NiO^{t}Bu); 1.26 (d, *J* = 6.8 Hz, 6H, 2 CH_3 of N^{i}Pr$_2$); 1.29 (dd, *J* = 8.6 Hz, 4.7 Hz, 6 H, 2 CH_3 of P^{i}Pr$_2$); 2.38-2.47 (m, 2H, 2 CH of N^{i}Pr$_2$); 6.12 (d, *J* = 7.8 Hz, 1H, C_6H_3); 6.28 (d, *J* = 7.1 Hz, 1H, C_6H_3); 6.64 (t, *J* = 7.6 Hz, 1H, C_6H_3); other resonances are obscured by the resonances of THF. ^{31}P{^{1}H}-NMR (202.5 MHz; THF-H_8; *δ*, ppm): 185.5 (s, O*P*^{i}Pr$_2$).

NMR reaction of ($^{i\text{-Pr}}$POCN$^{i\text{Pr2}}$)NiBr (8-^{i}Pr$_2$) with LiBHEt$_3$

Generation (*in situ*) of 13-Me$_2$ on NMR scale. A solution of $LiBHEt_3$ in THF (1.0 M, 65 μl, 0.065 mmol) was added by syringe at room temperature to a solution of ($^{i\text{-Pr}}$POCN$^{i\text{Pr2}}$)NiBr (**8-^{i}Pr$_2$**) (20 mg, 0.0434 mmol) in 0.6 ml of C_6D_6 in an NMR tube. The reaction mixture was left at room temperature for 30 mins and then was monitored by NMR. NMR analysis showed slow (64% in 19 hours by ^{31}P{^{1}H}-NMR) formation of ($^{i\text{Pr}}$POCN$^{i\text{Pr2}}$)NiH (**15-^{i}Pr$_2$**). All attempts to fully convert ($^{i\text{Pr}}$POCN$^{i\text{Pr2}}$)NiBr (**8-^{i}Pr$_2$**) to the hydride product **15-^{i}Pr$_2$** were unsuccessful resulting in difficult-to-separate mixtures of **15-^{i}Pr$_2$** and the starting bromide **8-^{i}Pr$_2$**.

($^{i\text{Pr}}$POCN$^{i\text{Pr2}}$)NiH (**15-^{i}Pr$_2$**): selected characteristic resonances: ^{1}H-NMR (500 MHz; THF-H_8; δ, ppm): -11.67 (d, *J* = 81.0 Hz, 1H, NiH). ^{31}P{^{1}H}-NMR (202.5 MHz; THF-H_8; *δ*, ppm): 202.2 (s, O*P*^{i}Pr$_2$).

($^{i\text{Pr}}$POCN$^{\text{Me2}}$)Ni(η^2-BH$_4$) (16-Me$_2$)

A solution of $LiBH_4$ in THF (2.0 M, 250.0 μL, 0.494 mmol) was added at room temperature to a solution of **8-Me$_2$** (200 mg, 0.494 mmol) in toluene. The color of the reaction mixture changed immediately from yellow to orange. The mixture was left with stirring for 2 hours, after which it was filtered and the volatiles were evaporated to give an orange powder (128.7 mg, 77%). The single crystals suitable for X-ray diffraction analysis were obtained by crystallization of **16-Me$_2$**

from Et_2O solution at -30 °C. ^{1}H-NMR (500 MHz; C_6D_6; δ, ppm): 6.90 (t, *J* = 7.7 Hz, 1H aromatic), 6.64 (d, *J* = 7.9 Hz, 1H aromatic), 6.43 (d, *J* = 7.4 Hz, 1H aromatic), 3.18 (s, 2H NCH_2), 2.31 (d, *J* = 1.3 Hz, 6H, 2 CH_3 of NMe_2), 2.12 – 2.03 (m, 2H, 2 CH of ^{i}Pr$_2$P), 1.36 (d, *J* = 7.1 Hz, 3H, CH_3 of ^{i}Pr$_2$P), 1.32 (d, *J* = 7.2 Hz, 3H, CH_3 of ^{i}Pr$_2$P), 1.13 (d, *J* = 6.9 Hz, 3H, CH_3 of ^{i}Pr$_2$P), 1.10 (d, *J* = 7.0 Hz, 3H, CH_3 of ^{i}Pr$_2$P), -0.49 (br d, *J* = 76.1 Hz, 2H of BH_4), -0.82 (d, *J* = 78.3 Hz, 2H of BH_4). ^{13}C{^{1}H}-NMR (125.8 MHz; C_6D_6; δ, ppm): 17.1 (br s); 28.2 (d, *J* = 23.6 Hz); 50.9; 72.5; 108.3 (m); 115.7 (m); 126.3 (m); 143.6 (d, *J* = 35.5 Hz); 149.7; 166.1 (m). ^{31}P{^{1}H}-NMR (202.5 MHz; C_6D_6; *δ*, ppm): 205.42 (s, O*P*^{i}Pr$_2$). ^{11}B{^{1}H}-NMR (160.5 MHz; C_6D_6; δ, ppm): -36.5 (br s, BH_4).

(^{iPr}POCN^{Me2})Ni(OAc) (17-Me$_2$)

A solution of **8-Me$_2$** (153.8 mg, 0.380 mmol) in THF was added at room temperature to a suspension of AgOAc (63.4 mg, 0.380 mmol) in THF. The reaction mixture was left with stirring overnight. Next day, the solvent was removed in vacuum and residue was extracted with toluene. Removal of all volatiles under reduced pressure gave a yellow solid (103.5 mg, 71%). ^{1}H-NMR (500 MHz; C_6D_6; δ, ppm): 6.92 (t, *J* = 7.6 Hz, 1H aromatic), 6.62 (d, *J* = 7.9 Hz, 1H aromatic), 6.40 (d, *J* = 7.3 Hz, 1H aromatic), 3.26 (s, 2H, NCH_2), 2.58 (m, *J* = 13.9 Hz, 7.0 Hz, 2H, 2 CH of ^{i}Pr$_2$P), 2.28 (s, 6H, 2 CH_3 of NMe_2), 2.10 (s, 3H, CH_3 of OAc), 1.53 (d, *J* = 6.6 Hz, 3H, CH_3 of ^{i}Pr$_2$P), 1.50 (d, *J* = 7.2 Hz, 3H, CH_3 of ^{i}Pr$_2$P), 1.27 (d, *J* = 7.1 Hz, 3H, CH_3 of ^{i}Pr$_2$P), 1.24 (d, *J* = 7.0 Hz, 3H, CH_3 of ^{i}Pr$_2$P). ^{13}C{^{1}H}-NMR (125.8 MHz; C_6D_6; δ, ppm): 16.9 (d, *J* = 3.0 Hz); 18.7 (d, *J* = 6.0 Hz); 23.7; 29.1 (d, *J* = 23.9 Hz); 47.56; 47.58; 71.2 (d, *J* = 2.2 Hz); 107.9 (d, *J* = 11.4 Hz); 115.0 (d, *J* = 2.1 Hz); 126.6; 138.3 (d, *J* = 34.5 Hz); 150.6; 167.0 (d, *J* = 10.3 Hz); 175.4. ^{31}P{^{1}H}-NMR (202.5 MHz; C_6D_6; *δ*, ppm): 192.7 (s, O*P*^{i}Pr$_2$). Elemental Analysis (%): calcd for $C_{17}H_{28}NNiO_3P$ (384.08): C 53.16, H 7.35, N 3.65; found: C 53.31, H 7.95, N 3.16.

(^{iPr}POCN^{Me2})Ni(OTf) (18-Me$_2$)

A solution of **8-Me$_2$** (150.0 mg, 0.370 mmol) in toluene was added at room temperature to a suspension of AgOTf (114.2 mg, 0.440 mmol) in toluene. The reaction mixture was left at room temperature with stirring overnight. Next day, the mixture was filtered, all volatiles were removed under reduced pressure and the residue was dried in vacuum to give a yellow powder (147.5 mg, 84%). ^{1}H-NMR (500 MHz; C_6D_6; δ, ppm): 6.79 (t, 1H aromatic), 6.42 (d, *J* = 3.8 Hz, 1H aromatic), 6.21 (d, *J* = 4.2 Hz, 1H aromatic), 2.97 (s, 2H, NCH_2), 2.37 (m, *J* = 6.6 Hz, 2H, 2CH of ^{i}Pr$_2$P), 2.19 (s, 6H, 2CH_3 of NMe_2), 1.52-1.41 (dd, 6H, 2CH_3 of ^{i}Pr$_2$P), 1.09-0.99 (dd, 6H, 2CH_3 of ^{i}Pr$_2$P). ^{13}C{^{1}H}-NMR (125.8 MHz; C_6D_6; δ, ppm): 16.7 (d, *J* = 3.1 Hz); 18.0 (d, *J* = 5.9 Hz); 28.3 (d, *J* = 22.4 Hz); 47.85; 47.86; 70.4 (d, *J* = 2.4 Hz); 108.9 (d, *J* = 12.1 Hz); 116.0 (d, *J* = 2.1 Hz); 131.3

(d, J = 33.1 Hz); 151.1; 167.2 (d, J = 9.2 Hz); other resonances are onscured by the resonance of C_6D_6. $^{31}P\{^1H\}$-NMR (202.5 MHz; C_6D_6; δ, ppm): 199.6 (s, OP^iPr$_2$). ^{19}F-NMR (470.6 MHz; C_6D_6; δ, ppm): -77.58 (s). Elemental Analysis (%): calcd for $C_{16}H_{26}F_3NNiO_4PS$ (474.10): C 40.53, H 5.32, N 2.95; found: C 41.12, H 5.48, N 2.53.

(^{iPr}POCN^{Me2})Ni(ONO$_2$) (19-Me$_2$)

$AgNO_3$ (26.6 mg, 0.156 mmol) suspension in THF was added to a solution of **8-Me$_2$** (53.3 mg, 0.132 mmol) in THF and the reaction mixture was left to stir for 4 days at room temperature. Upon completion, the solvent was removed in vacuum, and the residue was extracted with toluene, after which volatiles were evaporated. The product was dried to give a yellow powder (38.8 mg, 76%). ^1H-NMR (500 MHz; C_6D_6; δ, ppm): 6.84 (t, J = 6.6 Hz, 1H, C_6H_3), 6.49 (d, J = 7.3 Hz, 1H, C_6H_3), 6.29 (d, J = 6.8 Hz, 1H, C_6H_3), 3.08 (br s, 2H, NCH_2), 2.13 (br s, 2 CH_3 of NMe_2), 1.88 (m, 2H, 2 CH of ^{i}Pr$_2$P), 1.22-1.29 (m, 6H, 2 CH_3 of ^{i}Pr$_2$P), 1.07 – 1.13 (m, 6H, 2 CH_3 of ^{i}Pr$_2$P). $^{13}C\{^1H\}$-NMR (125.8 MHz; C_6D_6; δ, ppm): 16.5; 16.9 (d, J = 5.7 Hz); 28.1 (d, J = 22.2 Hz); 45.6; 70.8; 108.6 (d, J = 12.4 Hz); 116.0; 129.3; 1234.9 (d, J = 33.8 Hz); 151.0; 167.2 (d, J = 9.5 Hz). $^{31}P\{^1H\}$-NMR (202.5 MHz; C_6D_6; δ, ppm): 195.5 (s, OP^iPr$_2$).

(^{iPr}POCN^{Me2})Ni(SPh) (20-Me$_2$)

To a suspension of NaH (35.6 mg, 1.482 mmol) in THF, HSPh (126.8 μL, 1.235 mmol) was added at 0 °C, and the resulting reaction mixture was stirred for 1 hour (30 mins in cooling bath at 0 °C then 30 mins outside of the bath at room temperature). To a resulted mixture a solution of **8-Me$_2$** (100.0 mg, 0.247 mmol) in THF was added at room temperature. The color immediately changed form yellow to orange and the mixture was refluxed for 24 hours. All volatiles were evaporated and the residue was extracted with toluene through a pad of silica gel. The solvent was removed under reduced pressure and the residue was recrystallized from Et_2O at -30 °C to give an orange powder (89.5 mg, 83%). ^1H NMR (500 MHz, δ, ppm): 1.15 (dd, J = 14.5, 7.0 Hz, 6H, 2 CH_3 of ^{i}Pr$_2$P); 1.34 (dd, J = 17.2, 7.2 Hz, 6H, 2 CH_3 of ^{i}Pr$_2$P); 2.19 – 2.06 (m, 2H, 2 CH of ^{i}Pr$_2$P); 2.39 (s, 6H, 2 CH_3 of NMe_2), 3.34 (s, 2H, NCH_2), 6.49 (d, J = 7.4 Hz, 1H, C_6H_3), 6.71 (d, J = 7.9 Hz, 1H, C_6H_3), 6.93-6.99 (m, 2H, 1H of C_6H_3 and *p*-H of SPh), 7.12 (t, J = 7.6 Hz, 2H, *m*-H of SPh), 8.15 (d, J = 7.4 Hz, 2H, *o*-H of SPh). $^{13}C\{^1H\}$-NMR (125.8 MHz; C_6D_6; δ, ppm): 17.0; 18.1; 28.3 (d, J = 25.3 Hz); 48.4; 73.1; 108.2 (d, J = 12.9 Hz); 115.6; 121.7; 133.7; 146.1 (d, J = 31.3 Hz); 149.1; 151.0; 165.6 (d, J = 10.6 Hz); other ^{13}C resonances are obscured by the resonance of C_6D_6. $^{31}P\{^1H\}$-NMR (202.5 MHz; C_6D_6; δ, ppm): 195.03 (s, OP^iPr$_2$).

General procedure for catalytic deoxygenative hydroboration of carboxamides

0.124 mmol of the amide substrate were added at room temperature to a solution of a nickel pre-catalyst (5 mol%) in 0.6 ml of C_6D_6 in an NMR tube. This was followed by room temperature addition of 89.8 µl (0.619 mmol; 5 equivalents to the amide substrate) of HBPin. The NMR tube was sealed, connected to the Schlenk line and was placed in oil bath for 24 hours at appropriate temperature (60, 80 or 110 °C). At the beginning of the reaction vigorous gas release was observed and the pressure in NMR tube was released a few times through the Schlenk line bubler. After 24 hours the reaction mixture was analyzed by ^{1}H-NMR using 0.2 equivalents (4.2 mg, 0.025 mmol) of 1,3,5-trimethoxybenzene as internal standard. The yields of the produced amine or N-borylamine products were calculated based on the integration of the resonance of these products against the internal standard.

NMR spectra of $PhCH_2N(BPin)_2$ [96] and $PhCH_2N(Me)BPin$ [84] are consistent with those previously described in the literature. PrN(Ph)BPin: ^{1}H NMR (500 MHz, δ, ppm): 0.82 (t, *J* = 7.4 Hz, 3H, CH_3); 1.08 (s, 12H, BPin); 1.47-1.58 (m, 2H, CH_2); 3.56 (t, *J* = 7.2 Hz, 2H, CH_2); 6.89 (t, *J* = 7.3 Hz, 1H, *p*-H, NPh); 7.17-7.24 (m, 2H, *m*-H, NPh); 7.42-7.45 (m, 2H, *o*-H, NPh).

NMR scale reaction of benzamide with HBPin

(A): HBPin (107.8 µl, 0.743 mmol; 5 equivalents) was added *via* syringe at room temperature to a suspension of benzamide (18.0 mg, 0.149 mmol) in 0.6 ml of C_6D_6 in an NMR tube. Formation of gas was observed and the NMR tube was connected to the Schlenk line and depressurized. After that the sample was left for 20 hours at room temperature and the reaction was monitored by NMR showing after 20 hours full conversion of benzamide and formation of a mixture of PhC(O)N(H)BPin (64%), an *O*-addict $PhC(O)NH_2$•HBPin (26%) [85] and PhC(H)=NBPin (9%).

(B): HBPin (90.0 µl, 0.62 mmol; 5 equivalents) was added *via* syringe at room temperature to a suspension of benzamide (15.0 mg, 0.124 mmol) in 0.6 ml of C_6D_6 in an NMR tube. The NMR tube was sealed, connected to the Schlenk line and was placed in the (80 °C) oil bath for 24 hours. Vigorous release of H_2 gas was observed at the beginning of the reaction and the NMR tube was depressurized a few times using the Schlenk line. NMR analysis after 24 hours of heating at 80 °C showed full conversion of benzamide and formation of a mixture of PhC(O)N(H)BPin (88%), PhC(H)=NBPin (11%) and $PhCH_2N(BPin)_2$ (<1%) [96].

PhC(O)N(H)BPin: ^{1}H NMR (500 MHz, δ, ppm) 1.07 (s, 12H, BPin); 6.47 (br s, 1H, NH); 6.96 (t, *J* = 7.6 Hz, 2H, *m*-H of C_6H_5); 7.05 (t, *J* = 8.0 Hz, 1H, *p*-H of C_6H_5); 7.57 (d, *J* = 7.8 Hz, 2H, *o*-H of C_6H_5). **PhC(H)=NBPin** was assigned based on characteristic imine resonance at 10.37 ppm in the ^{1}H-NMR spectrum

NMR scale reaction of *N*-phenylbenzamide with HBPin

HBPin (69.9 µl, 0.482 mmol; 5 equivalents) was added *via* syringe at room temperature to a suspension of *N*-phenylbenzamide (19.0 mg, 0.096 mmol) in 0.6 ml of C_6D_6 in an NMR tube. The NMR tube was sealed, connected to the Schlenk line and was placed in the (80 °C) oil bath for 24 hours. No gas release was observed. NMR analysis after 24 hours of heating at 80 °C showed no reaction between *N*-phenylbenzamide and HBPin.

X-Ray diffraction analysis

Suitable single crystals were mounted on a glass microloop covered with perfluoroether oil (Paratone® N). Crystallographic data were collected on Bruker APEX-II CCD diffractometer equipped with an Oxford Cryosystems lowtemperature device operating at 150.0(1) K. Generic φ and ω scans (MoKα, λ = 0.71073 Å) were used for the data measurement. The diffraction patterns were indexed, and the unit cells refined with SAINT (Bruker, V.8.34A, after 2013) software. Data reduction, scaling and absorption correction were performed with SAINT and SADABS software (Bruker, 8.34A after 2013). A multi-scan absorption correction was applied within SADABS-2014/4 (Bruker, 2014/4). Space group determination was based upon analysis of systematic absences, E statistics, and successful refinement of all structures. The structures were solved by ShelXT (Sheldrick, 2015) structure solution program with Intrinsic phasing algorithm and refined with Least squares method by minimization of Σw(F0 2 -Fc 2) 2. SHELXL weighting scheme was used under 2018/3 version of ShelXL (Sheldrick, 2015). Structure solution, refinement and CIF compilation was performed within Olex2SyS software (Dolomanov, 2009). All non-hydrogen atoms were refined anisotropically. The positions of the hydrogen atoms were calculated geometrically and refined using the riding model. Neutral atom scattering factors for all atoms were taken from the International Tables for Crystallography.

Crystallographic parameters for (^{iPr}POCN^{Me2})Ni(η^2-BH_4) (16-Me_2)

The sample is represented by two molecules co-crystallized. The refinement of Br and BH_4 occupancies led to the non-integer number for B, Br and H.

```
Bond precision:        C-C = 0.0020 A                Wavelength=0.71073
Cell:        a=9.3802(11)      b=9.4495(11)      c=10.9044(13)
             alpha=66.939(4)   beta=78.797(4)    gamma=75.715(4)
Temperature: 150 K
                     Calculated                          Reported
Volume               856.63(18)                          856.63(18)
Space group          P -1                                P -1
Hall group           -P 1                                -P 1
Moiety formula       C15 H28.35 B0.84 Br0.16 N Ni O P    C15 H28.36 B0.84 Br0.16 N Ni O P
Sum formula          C15 H28.35 B0.84 Br0.16 N Ni O P    C15 H28.36 B0.84 Br0.16 N Ni O P
Mr                   350.36                              350.29
Dx,g cm-3            1.358                               1.358
Z                    2                                   2
Mu (mm-1)            1.597                               1.594
F000                 372.4                               372.0
F000'                373.26
h,k,lmax             12,12,14                            12,12,14
Nref                 4364                                4327
Tmin,Tmax            0.631,0.877                         0.480,0.746
Tmin'                0.619
Correction method= # Reported T Limits: Tmin=0.480 Tmax=0.746
AbsCorr = MULTI-SCAN
Data completeness= 0.992           Theta(max)= 28.557
R(reflections)= 0.0278( 4017)         wR2(reflections)= 0.0710( 4327)
S = 1.048               Npar= 213
```

5 Conclusion and future perspectives

This study has presented comparative analysis of catalytic activity in deoxygenative hydroboration of amides to the corresponding amines using a series of imino- and aminophosphinite POCN pincer complexes of nickel (II). The alkyl and alkoxy complexes of the general formulae (POCN)NiR (where R = Alk, OAlk) were found to be the most active pre-catalysts for hydroboration of primary and secondary amides. The reactions proceeded at 80 °C, presenting rare examples of deoxygenative reduction catalysts operating under mild conditions (<100 °C). In contrast, oppositely to the generally accepted trend of the reactivity of amides (primary < secondary < tertiary), tertiary amides turned out to be noncompatible with the developed pre-catalysts, presumably due to the steric hindrance in these substrates or due to the difference in the mechanisms for hydroboration of tertiary *vs.* secondary and primary amides. Thus, we proposed a mechanism according to which reductive hydroboration proceeds *via* activation of Ni pre-catalyst, forming catalytically active nickel hydride species. This was additionally confirmed by the stoichiometric reactivity of the alkoxy nickel complexes with HBPin generating thermally unstable Ni(II) hydride species. Our mechanistic studies also suggested that hydroboration of primary and secondary amides proceeds with an intermediacy of the imine species, $R^1C(H)=NR^2$ (where R^2 = BPin or hydrocarbyl, respectively), which undergo addition of HBPin to generate the N-borylamine products. Formation of the imine intermediates is not possible for tertiary amide substates, which could be a reason for the observed low or no reactivity of tertiary amides in Ni-catalyzed hydroboration reactions.

Figure 5. (POCN)NiOPh (A) and (POCOP)NiH (B) pincer complexes

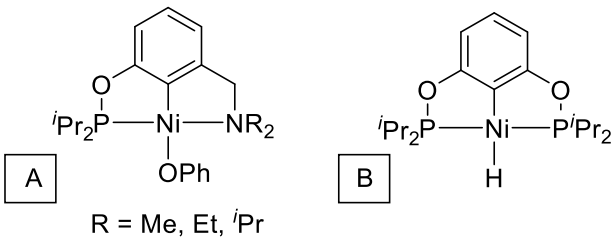

Despite the observed high activity of the alkoxy complexes (POCN)Ni(O^{t}Bu) in hydroboration reactions, they turned out to have limited thermal stability, presumably due to the presence of destabilizing dπ–pπ interactions in the Ni-O^{t}Bu moiety. Thus, to improve the stability of such nickel pre-catalysts our future work will concentrate on preparation of analogous aryloxy derivatives (Figure 5A), which are believed to possess higher stability due to the presence of less electron-rich oxygen center compared to alkoxy compounds. Once these complexes are prepared,

our investigations will be directed towards expansion of the amides substrate scope in deoxygenative hydroboration reactions.

Finally, since the control experiments showed the formation of catalytically active nickel(II) hydride species, we will investigate whether previously reported bis(phosphinite) POCOP pincer nickel hydride complexes (akin to those depicted in Figure 5B) can be employed as the catalysts for deoxygenatve hydroboration of amides to amines.

References

1. Smith, M. *Organic Synthesis*, 4th ed.; Academic Press: London, UK, 2017.
2. Lawrence, S. A. *Amines: Synthesis, Properties and Applications;* Cambridge University Press: Cambridge, UK, 2004.
3. Eller, K.; Henkes, E.; Rossbacher, R.; Höke, H. *Amines, Aliphatic*. In *Ullmann's Encyclopedia of Industrial Chemistry*; Wiley-VCH: Weinheim, Germany, 2005.
4. Andersson, P. G.; Munslow, I. J. *Modern Reduction Methods*; Wiley-VCH: Weinheim, Germany, 2008.
5. Seyden-Penne, J. *Reductions by the Alumino- and Boro-hydrides in Organic Synthesis*; VCH: New York, 1991.
6. Magro, A. A. N.; Eastham, G. R.; Cole-Hamilton, D. J. The Synthesis of Amines by the Homogeneous Hydrogenation of Secondary and Primary Amides. *Chem. Commun.* **2007**, 3154–3156.
7. Coetzee, J.; Dodds, D. L.; Klankermayer, J.; Brosinski, S.; Leitner, W.; Slawin, A. M. Z.; Cole-Hamilton, D. J. Homogeneous Catalytic Hydrogenation of Amides to Amines. *Chem. Eur. J.* **2013**, *19*, 11039–11050.
8. Meuresch, M.; Westhues, S.; Leitner, W.; Klankermayer, J. Tailor−Made Ruthenium−Triphos Catalysts for the Selective Homogeneous Hydrogenation of Lactams. *Angew. Chem. Int. Ed.* **2016**, *55*, 1392–1395.
9. Khalimon, A. Y.; Gudun, K. A.; Hayrapetyan, D. Base Metal Catalysts for Deoxygenative Reduction of Amides to Amines. *Catalysts* **2019**, *9*, 490.
10. Larock, R. C. *Comprehensive Organic Transformations: A Guide to Functional Group Preparation*; Wiley-VCH: New York, USA, 1989.
11. Ricci, A. *Amino Group Chemistry. From Synthesis to the Life Sciences*; Ricci, A., Ed.; Wiley-VCH: Weinheim, Germany, 2008.
12. Li, B., Sortais, J.-B.; Darcel, C. Amine synthesis via transition metal homogeneous catalysed hydrosilylation. *RSC Advances* **2016**, *6*, 57603–57625.
13. Miecznikowski, J. R.; Crabtree, R. H. Transfer hydrogenation reduction of ketones, aldehydes and imines using chelated iridium(III) N-heterocyclic biscarbene complexes. *Polyhedron* **2004**, *23*, 2857-2872.
14. Nurseiit, A., Janabel, J., Gudun, K. A., Kassymbek, A., Segizbayev, M., Seilkhanov, T. M.; Khalimon, A.Y. Bench-Stable Cobalt Pre-Catalysts for Mild Hydrosilative Reduction of Tertiary Amides to Amines and Beyond. *ChemCatChem* **2018**, *11*, 790-798.

15. Cabrita, I.; Fernandes, A. C. A novel efficient and chemoselective method for the reduction of nitriles using the system silane/oxo-rhenium complexes. *Tetrahedron*, **2011**, *67*, 8183-8186.
16. Formenti, D.; Ferretti, F.; Scharnagl, F. K.; Beller, M. Reduction of Nitro Compounds Using 3d-Non-Noble Metal Catalysts. *Chem. Rev*. **2019**, *119*, 2611–2680.
17. Ogo, S.; Uehara, K.; Abura, T.; Fukuzumi, S. pH-dependent chemoselective synthesis of amino acids reductive amination of -keto acids with ammonia catalyzed by acid-stable iridium hydride complexes in water. *J. Am. Chem. Soc.* **2004**, *126*, 3020-3021.
18. Cabrero-Antonino, J. R.; Alberico, E.; Junge, K.; Junge, H.; Beller, M. Towards a General Ruthenium-Catalyzed Hydrogenation of Secondary and Tertiary Amides to Amines. *Chem. Sci.* **2016**, *7*, 3432–3442.
19. Yuan, M.-L.; Xie, J.-H.; Zhou, Q.-L. Boron Lewis Acid Promoted Ruthenium−Catalyzed Hydrogenation of Amides: An Efficient Approach to Secondary Amines. *ChemCatChem* **2016**, *8*, 3036–3040.
20. Matsubara, K.; Iura, T.; Maki, T.; Nagashima, H. A Triruthenium Carbonyl Cluster Bearing a Bridging Acenaphthylene Ligand: An Efficient Catalyst for Reduction of Esters, Carboxylic Acids, and Amides by Trialkylsilanes. *J. Org. Chem.* **2001**, *67*, 4985–4988.
21. Motoyama, Y.; Mitsui, K.; Ishida, T.; Nagashima, H. Self-Encapsulation of Homogeneous Catalyst Species into Polymer Gel Leading to a Facile and Efficient Separation System of Amine Products in the Ru-Catalyzed Reduction of Carboxamides with Polymethylhydrosiloxane (PMHS). *J. Am. Chem. Soc.* **2005**, *127*, 13150–13151.
22. Sasakuma, H.; Motoyama, Y.; Nagashima, H. Functional group-selective poisoning of molecular catalysts: a ruthenium cluster-catalysed highly amide-selective silane reduction that does not affect ketones or esters. *Chem. Commun*. **2007**, 4916–4918.
23. Hanada, S.; Ishida, T.; Motoyama, Y.; Nagashima, H. The Ruthenium-Catalyzed Reduction and Reductive N-Alkylation of Secondary Amides with Hydrosilanes: Practical Synthesis of Secondary and Tertiary Amines by Judicious Choice of Hydrosilanes. *J. Org. Chem.* **2007**, *72*, 7551–7559.
24. Li, B.; Sortais, J.-B.; Darcel, C. Unexpected selectivity in ruthenium-catalyzed hydrosilylation of primary amides: synthesis of secondary amines. *Chem. Commun.* **2013**, *49*, 3691–3693.
25. Kuwano, R.; Takahashi, M.; Ito, Y. Reduction of Amides to Amines via Catalytic Hydrosilylation by a Rhodium Complex. *Tetrahedron Lett.* **1998**, *39*, 1017–1020.
26. Bornschein, C.; Lennox, A. J. J.; Werkmeister, S.; Junge, K.; Beller, M. A Mild and Selective Reduction of β-Lactams: Rh-Catalyzed Hydrosilylation towards Important Pharmacological Building Blocks. *Eur. J. Org. Chem.* **2015**, 1915–1919.

27. Das, S.; Li, Y.; Bornschein, C.; Pisiewicz, S.; Kiersch, K.; Michalik, D.; Gallou, F.; Junge, K.; Beller, M. Selective Rhodium-Catalyzed Reduction of Tertiary Amides in Amino Acid Esters and Peptides. *Angew. Chem. Int. Ed.* **2015**, *54*, 12389–12393.
28. Yuan, M.-L.; Xie, J.-H.; Zhu, S.-F.; Zhou, Q.-L. Deoxygenative Hydrogenation of Amides Catalyzed by a Well−Defined Iridium Pincer Complex. *ACS Catal*. **2016**, *6*, 3665–3669.
29. Park, S.; Brookhart, M. Development and Mechanistic Investigation of a Highly Efficient Iridium(V) Silyl Complex for the Reduction of Tertiary Amides to Amines. *J. Am. Chem. Soc.* **2012**, *134*, 640–653.
30. Cheng, C.; Brookhart, M. Iridium-Catalyzed Reduction of Secondary Amides to Secondary Amines and Imines by Diethylsilane. *J. Am. Chem. Soc*. **2012**, *134*, 11304–11307.
31. Motoyama, Y.; Aoki, M.; Takaoka, N.; Aoto, R.; Nagashima, H. Highly efficient synthesis of aldenamines from carboxamides by iridium-catalyzed silane-reduction/dehydration under mild conditions. *Chem. Commun*. **2009**, 1574–1576.
32. Tahara, A.; Miyamoto, Y.; Aoto, R.; Shigeta, K.; Une, Y.; Sunada, Y.; Motoyama, Y.; Nagashima, H. Catalyst Design of Vaska-Type Iridium Complexes for Highly Efficient Synthesis of π–Conjugated Enamines. *Organometallics* **2015**, *34*, 4895–4907.
33. Guzmán, J.; Bernal, A. M.; Garcia-Orduna, P.; Lahoz, F. J.; Oro, L. A.; Fernández-Alvarez, F.J. Selective reduction of formamides to O-silylated hemiaminals or methylamines with $HSiMe_2Ph$ catalyzed by iridium complexes. *Dalton Trans.* **2019**, *48*, 4255–4262.
34. Hanada, S.; Motoyama, Y.; Nagashima, H. Dual Si–H effects in platinum-catalyzed silane reduction of carboxamides leading to a practical synthetic process of tertiary-amines involving self-encapsulation of the catalyst species into the insoluble silicone resin formed. *Tetrahedron Lett.* **2006**, *47*, 6173–6177.
35. Hanada, S.; Tsutsumi, E.; Motoyama, Y.; Nagashima, H. Practical Access to Amines by Platinum-Catalyzed Reduction of Carboxamides with Hydrosilanes: Synergy of Dual Si-H Groups Leads to High Efficiency and Selectivity. *J. Am. Chem. Soc.* **2009**, *131*, 15032–15040.
36. Pisiewicz, S.; Junge, K.; Beller, M. Mild Hydrosilylation of Amides by Platinum N-Heterocyclic Carbene Catalysts. *Eur. J. Inorg. Chem.* **2014**, 2345–2349.
37. Chirik, P. J. *Catalysis without Precious Metals*; Ballock, R. M., Ed.; Wiley-VCH: Weinheim, Germany, 2008.
38. Kelly, C. M.; McDonald, R.; Sydora, O. L.; Stradiotto, M.; Turculet, L. A Manganese Pre-Catalyst: Mild Reduction of Amides, Ketones, Aldehydes, and Esters. *Angew. Chem. Int. Ed.* **2017**, *56*, 15901–15904.
39. Junge, K.; Schröder, K.; Beller, M. Homogeneous catalysis using iron complexes: recent developments in selective reductions. *Chem. Commun.* **2011**, *47*, 4849-4859.

40. Yang, X.; Wang, C. Manganese-Catalyzed Hydrosilylation Reactions. *Chem. Asian J.* **2018**, *13*, 2307–2315.

41. Arora, V.; Narjinari, H.; Nandi, P. G.; Kumar, A. Recent advances in pincer-nickel catalyzed reactions. *Dalton Trans.* **2021**, *50*, 3394-3428

42. Junge, K.; Papa, V.; Beller, M. Cobalt-Pincer Complexes in Catalysis, *Chem. Eur. J.* **2019**, *25*, 122-143.

43. Volkov, A.; Tinnis, F.; Slagbrand, T.; Trillo, P.; Adolfsson, H. Chemoselective reduction of carboxamides. *Chem. Soc. Rev.* **2016**, *45*, 6685–6697.

44. Marciniec, B.; Gulinski, J.; Urbaniak, W.; Kornetka, Z.W. *Comprehensive Handbook on Hydrosilylation*; Marciniec, B., Ed.; Pergamon Press: Oxford, UK, 1992.

45. Papa, V.; Cabrero-Antonino, J. R.; Spannenberg, A.; Junge, K.; Beller, M. Homogeneous cobalt-catalyzed deoxygenative hydrogenation of amides to amines. *Catal. Sci. Technol.* **2020**, *10,* 6116-6128

46. Simmons, B. J.; Hoffmann, M.; Hwang, J.; Jackl, M. K.; Garg, N. K. Nickel-catalyzed reduction of secondary and tertiary amides. *Org. Lett.* **2017**, *19*, 1910–1913

47. Selvakumar, K.; Rangareddy, K.; Harrod, J. F. The titanocene-catalyzed reduction of acetamides to tertiary amines by $PhMeSiH_2$. *Can. J. Chem.* **2004**, *82*, 1244–1248.

48. Laval, S.; Dayoub, W.; Pehlivan, L.; Métay, E.; Favre-Réguillon, A.; Delbrayelle, D.; Mignani, G.; Lemaire, M. Hydrosiloxane–$Ti(O^iPr)_4$: an efficient system for the reduction of primary amides into primary amines as their hydrochloride salts. *Tetrahedron Lett.* **2011**, *52*, 4072–4075.

49. Fernandes, A. C.; Romao, C. C. Reduction of amides with silanes catalyzed by MoO_2Cl_2. *J. Mol. Catal. A Chem.* **2007**, *272*, 60–63.

50. Volkov, A.; Tinnis, F.; Slagbrand, T.; Pershagen, I.; Adolfsson, H. $Mo(CO)_6$ catalysed chemoselective hydrosilylation of α,β-unsaturated amides for the formation of allylamines. *Chem. Commun.* **2014**, *50*, 14508–14511.

51. Das, S.; Join, B.; Junge, K.; Beller, M. A general and selective copper-catalyzed reduction of secondary amides. *Chem. Commun.* **2012**, *48*, 2683–2685

52. Calas, R. Thirty years in organosilicon chemistry. *J. Organomet. Chem.* **1980**, *200*, 11–36.

53. Das, S.; Addis, D.; Zhou, S.; Junge, K.; Beller, M. Zinc-Catalyzed Reduction of Amides: Unprecedented Selectivity and Functional Group Tolerance. *J. Am. Chem. Soc.* **2010**, *132*, 1770–1771.

54. Das, S.; Addis, D.; Junge, K.; Beller, M. Zinc-Catalyzed Chemoselective Reduction of Tertiary and Secondary Amides to Amines. *Chem. Eur. J.* **2011**, *17*, 12186–12192.

55. Kovalenko, O. O.; Volkov, A.; Adolfsson, H. Mild and Selective Et_2Zn-Catalyzed Reduction of Tertiary Amides under Hydrosilylation Conditions. *Org. Lett.* **2015**, *17*, 446–449.

56. Adkins, H.; Wojcik, B. Hydrogenation of Amides to Amines. *J. Am. Chem. Soc.* **1934**, *56*, 247.

57. Beamson, G.; Papworth, A.J.; Philipps, C.; Smith, A. M.; Whyman, R. Selective Hydrogenation of Amides Using bimetallic Ru/Re and Rh/Re Catalysts. *J. Catal.* **2011**, *278*, 228–238.

58. Wojcik, B.; Adkins, H. Catalytic Hydrogenation of Amides to Amines. *J. Am. Chem. Soc.* **1934**, *56*, 2419–2424.

59. Stein, M.; Breit, B. Catalytic Hydrogenation of Amides to Amines under Mild Conditions. *Angew. Chem. Int. Ed.* **2013**, *52*, 2231–2234.

60. Toyao, T.; Siddiki, S. M. A. H.; Morita, Y.; Kamachi, T.; Touchy, A. S.; Onodera, W.; Kon, K.; Furukawa, S.; Ariga, H.; Asakura, K.; Yoshizawa, K.; Shimizu, K.-I. Rhenium-Loaded TiO_2: A Highly Versatile and Chemoselective Catalyst for the Hydrogenation of Carboxylic Acid Derivatives and the N-Methylation of Amines Using H_2 and CO_2. *Chem. Eur. J.* **2017**, *23*, 14848–14859.

61. Lampland, N. L.; Hovey, M.; Mukherjee, D.; Sadow, A. D. Magnesium-Catalyzed Mild Reduction of Tertiary and Secondary Amides to Amines. *ACS Catal.* **2015**, *5*, 4219–4226.

62. Mukherjee, D.; Shirase, S.; Spaniol, T. P.; Mashima, K.; Okuda, J. Magnesium hydridotriphenylborate $[Mg(thf)_6][HBPh_3]_2$: A versatile hydroboration catalyst. *Chem. Commun.* **2016**, *52*, 13155–13158.

63. Barger, C. J.; Dicken, R. D.; Weidner, V. L.; Motta, A.; Lohr, T. L; Marks, T. J. $La[N(SiMe_3)_2]_3$-Catalyzed Deoxygenative Reduction of Amides with Pinacolborane. Scope and Mechanism. *J. Am. Chem. Soc.*, **2020**, *142*, 8019-8028

64. Gudun, K. A.; Segizbayev, M.; Adamov, A.; Plessow, P. N.; Lyssenko, K. A.; Balanay, M. P.; Khalimon, A. Y. POCN Ni(II) pincer complexes: synthesis, characterization and evaluation of catalytic hydrosilylation and hydroboration activities. *Dalton Trans.* **2019**, *48*, 1732–1746.

65. Morales-Morales, D.; Jensen, C. *The Chemistry of Pincer Compounds,* Elsevier, Amsterdam, 2007.

66. Stein, M.; Breit, B. Catalytic Hydrogenation of Amides to Amines under Mild Conditions. *Angew. Chem. Int. Ed.* **2013**, *52*, 2231–2234.

67. Beamson, G.; Papworth, A. J.; Philipps, C.; Smith, A. W.; Whyman, R. Selective Hydrogenation of Amides using Ruthenium/Molybdenum Catalysts. *Adv. Synth. Catal*. **2010**, *352*, 869–883.

68. Coetzee, J.; Manyar, H. G.; Hardacre, C.; Cole-Hamilton, D. J. The First Continuous Flow Hydrogenation of Amides to Amines. *ChemCatChem* **2013**, *5*, 2843–2847.

69. Zhou, S.; Junge, K.; Addis, D.; Das, S.; Beller, M. A Convenient and General Iron-Catalyzed Reduction of Amides to Amines. *Angew. Chem. Int. Ed.* **2009**, *48*, 9507–9510.

70. Sunada, Y.; Kawakami, H.; Imaoka, T.; Motoyama, Y.; Nagashima, H. Hydrosilane Reduction of Tertiary Carboxamides by Iron Carbonyl Catalysts. *Angew. Chem. Int. Ed.* **2009**, *48*, 9511–9514.

71. Tsutsumi, H.; Sunada, Y.; Nagashima, H. New catalyst systems for iron-catalyzed hydrosilane reduction of carboxamides. *Chem. Commun*. **2011**, *47*, 6581–6583.

72. Bézier, D.; Venkanna, G. T.; Sortais, J.-B.; Darcel, C. Well-Defined Cyclopentadienyl NHC Iron Complex as the Catalyst for Efficient Hydrosilylation of Amides to Amines and Nitriles. *ChemCatChem* **2011**, *3*, 1747–1750.

73. Volkov, A.; Buitrago, E.; Adolfsson, H. Direct Hydrosilylation of Tertiary Amides to Amines by an In Situ Formed Iron/N-Heterocyclic Carbene Catalyst. *Eur. J. Org. Chem.* **2013**, *11*, 2066–2070.

74. Blom, B.; Tan, G.; Enthaler, S.; Inoue, S.; Epping, J. D.; Driess, M. Bis-N-Heterocyclic Carbene (NHC) Stabilized η^6-arene Iron(0) Complexes: Synthesis, Structure, Reactivity, and Catalytic Activity. *J. Am. Chem. Soc.* **2013**, *135*, 18108–18120.

75. Macaulay, C. M.; Ogawa, T.; McDonald, R.; Sydora, O. L.; Stradiotto, M.; Turculet, L. A comparative analysis of hydrosilative amide reduction catalyzed by first-row transition metal (Mn, Fe, Co and Ni) N-phosphinoamidinate complexes. *Dalton Trans.* **2019**, *48*, 9581-9587

76. Das, S.; Wendt, B.; Möller, K.; Junge, K.; Beller, M. Two Iron Catalysts are Better than One: A General and Convenient Reduction of Aromatic and Aliphatic Primary Amides. *Angew. Chem. Int. Ed.* **2012**, *51*, 1662–1666.

77. Dombray, T.; Helleu, C.; Darcel, C.; Sortais, J.-B. Cobalt Carbonyl-Based Catalyst for Hydrosilylation of Carboxamides. *Adv. Synth. Catal.* **2013**, *355*, 3358–3362.

78. Mamillapalli, N. C.; Sekar, G. Chemoselective reduction of a-keto amides using nickel catalysts. *Chem. Commun.* **2014**, *50*, 7881–7884.

79. Simmons, B. J.; Hoffmann, M.; Hwang, J.; Jackl, M. K.; Garg, N. K. Nickel-Catalyzed Reduction of Secondary and Tertiary Amides. *Org. Lett.* **2017**, *19*, 1910–1913.

80. Panda, T. K. K.; Das, S.; Karmakar, H.; Bhattacharjee, J. Aluminium complex as an efficient catalyst for chemo-selective reduction of amides to amines. *Dalton Trans.* **2019**, *48*, 11978

81. Zhang, G.; Wu, J.; Zheng, S.; Neary, M. C.; Mao, J.; Flores; M.; Dub, P. A. Redox Non-Innocent Ligand Supported Vanadium Catalysts for the Chemoselective Reduction of C=X (X = O, N) Functionalities. *J. Am. Chem. Soc.* **2019**, *141*, 15230−15239

82. Bhunia, M.; Sahoo, S. R.; Das, A.; Ahmed, J.; Prasannan, S.; Mandal, K. Transition metal-free catalytic reduction of primary amides using an abnormal NHC based potassium complex: integrating nucleophilicity with Lewis acidic activation. *Chem. Sci.* **2020**, *11*, 1848

83. Ye, P.; Shao, Y.; Ye, X.; Zhang, F.; Li, R.; Sun, J.; Xu, B.; Chen, J. Homoleptic Bis(trimethylsilyl)amides of Yttrium Complexes Catalyzed Hydroboration Reduction of Amides to Amines. *Org. Lett.* **2020**, *22*, 1306-1310

84. Tamang, S. R.; Singh, A.; Bedi, D.; Bazkiaei, A. R.; Warner, A. A.; Glogau, K.; McDonald C.; Unruh, D. K.; Findlater, M. Polynuclear lanthanide–diketonato clusters for the catalytic hydroboration of carboxamides and esters. *Nat. Catal.* **2020**, *3*, 154–162.

85. Saha, S.; Eisen M. S. Mild catalytic deoxygenation of amides promoted by thorium metallocene. *Dalton Trans.* **2020**, *49*, 12835-12841

86. Mougang-Soumé, B.; Belanger-Gariépy, F.; Zargarian, D. Synthesis, characterization, and oxidation of new $POCN_{imine}$-type pincer complexes of nickel. *Organometallics* **2014**, *33*, 5990-6002

87. Pandarus, V.; Zargarian D. New pincer-type diphosphinito (POCOP) complexes of nickel. *Organometallics* **2007**, *26*, 4321-4334

88. Eberhardt, N. A.; Guan, H. Nickel hydride complexes. *Chem. Rev.* **2016**, *116*, 8373–8426

89. Hao, J.; Mougang-Soume, B.; Vabre, B.; Zargarian, D. On the Stability of a $POC_{sp3}OP$-Type Pincer Ligand in Nickel(II) Complexes. *Angew. Chem. Int. Ed.* **2014**, *53*, 3218-3222

90. Vabre, B.; Petiot, P.; Declercq, R.; Zargarian, D. Fluoro and Trifluoromethyl Derivatives of POCOP-Type Pincer Complexes of Nickel: Preparation and Reactivities in S_N2 Fluorination and Direct Benzylation of Unactivated Arenes. *Organometallics* **2014**, *33*, 5173−5184

91. Spasyuk, D. M.; Zargarian, D.; van der Est, A. New POCN-type pincer complexes of Ni(II) and Ni(III). *Organometallics* **2009**, *28*, 6531–6540

92. Smith, J. B.; Miller, A. J. M. Connecting Neutral and Cationic Pathways in Nickel-Catalyzed Insertion of Benzaldehyde into a C−H bond of Acetonitrile. *Organometallics* **2015**, *34*, 4669–4677

93. Fulmer, G. R.; Miller, A. J. M.; Sherden, N. H.; Gottlieb, H. E.; Nudelman, A.; Stoltz, B. M.; Bercaw J. E.; Goldberg. K. I. NMR Chemical shifts of trace impurities: common laboratory solvents, organics, and gases in deuterated solvents relevant to the organometallic chemist. *Organometallics* **2010**, *29*, 2176–2179

94. Liu, T.; Meng, W.; Ma, Q.-Q.; Zhang, J.; Li, H.; Li, S.; Zhao, Q.; Chen, X. Hydroboration of CO_2 catalyzed by bis(phosphinite) pincer ligated nickel thiolate complexes. *Dalton Trans.* **2017**, *46*, 4504-4509

95. Khake, S. M.; Soni, V.; Gonnade, R. G.; Punji, B. Design and development of POCN-pincer palladium catalysts for C–H bond arylation of azoles with aryl iodides. *Dalton Trans.* **2014**,*43*, 16084-16096

96. Gudun, K. A.; Slamova, A.; Hayrapetyan, D.; Khalimon, A. Y. Efficient Co-catalyzed Double Hydroboration of Nitriles: Application to One-Pot Conversion of Nitriles to Aldimines. *Chem. Eur.J.* **2020**, *26,* 4963-4968